

HIGH DENSITY SURFACE ELECTROMYOGRAPHY FOR THE ASSESSMENT OF
PELVIC FLOOR DYSFUNCTION

by
Nicholas Conner Dias

A dissertation submitted to the Department of Biomedical Engineering
College of Engineering
in partial fulfillment of the requirements for the degree of

DOCTOR OF PHILOSOPHY

in Biomedical Engineering

Chair of Committee: Yingchun Zhang, Ph. D

Committee Member: Nuri Ince, Ph. D

Committee Member: H. Henry Lai, M.D

Committee Member: Mario Romero-Ortega, Ph. D

Committee Member: Jinsook Roh, Ph. D

University of Houston
December 2020

Acknowledgements

There are many people to which I owe my thanks during my graduate career. First and foremost, I need to express my gratitude to my Ph.D advisor, Dr. Yingchun Zhang. From my first day in the lab as an undergraduate researcher, to the end of my Ph.D study, Dr. Zhang has provided me the tools, knowledge, and most importantly, the encouragement to keep searching for answers to pressing questions. Additionally, I would like to thank Dr. Metin Akay for your advice and enthusiasm for research, which facilitated my early interest in biomedical engineering.

Clinical research requires close collaboration with physicians and clinical care providers, and I am grateful for having worked with many amazing clinical professionals. Specifically, I would like to thank Dr. Rose Khavari and Dr. Timothy Boone at Houston Methodist Hospital, for insightful consultations, which provided impetus for the early stages of my investigations. I would like to thank Dr. Christopher Smith at Baylor College of Medicine for lending his expertise in Botulinum toxin treatment modalities, and his assistance in my studies. I have the utmost gratitude for the entire research team at Washington University School of Medicine, Dr. Henry Lai, Dr. Theresa Spitznagle, Karla Bergeron, and Alex Klim, and, not only for your astute research discussion and support in my studies, but for making me feel at home in St. Louis during my many visits. Finally, I would like to thank Dr. Charles Popeney, for lending your valued expertise in pudendal nerve stimulation, and our many discussions on chronic pelvic pain, and pudendal neuropathy.

Thank you to the Society of Urodynamics, Female Pelvic Medicine, and Urogenital Reconstruction and National Institutes of Health for providing funding support for my research.

Next, I need to thank all my lab mates throughout the last 5 years. Specifically, thank you to Yun, Chuan, Yang, Feng, Thinh, Tom, and Eric for always being there to listen to my ideas with an open mind. I would like to thank my friends for your support during my graduate career, all of you had made my graduate studies much easier.

Finally, I must express my love and gratitude to my family, who provided encouragement and support during all stages of my academic study.

Abstract

This dissertation aims to develop a reliable, non-invasive technique for assessing PFM overactivity and determining patient-specific innervation zone (IZ) distributions. Existing techniques for evaluating PFM activity include magnetic resonance imaging, ultrasound, and digital palpation. All the previous techniques provide qualitative information about the length and pressure generated by the PFMs, but do not provide any information about the neuromuscular activity or the IZ. Digital palpation is completely subjective and relies on the examiner's experience. High density surface EMG provides a non-invasive, quantitative technique to assess muscle activity, yet has seldom been applied to the PFMs. In this dissertation, I aim to develop techniques to 1) map PFM hypertonicity at rest, and 2) help personalize treatment by guiding therapeutic neurotoxin towards the IZ. The goal of my PhD study is to noninvasively, objectively and quantitatively assess the neuromuscular activity related to PFM dysfunction using a novel intravaginal high-density surface EMG probe. Surface interference EMG and decomposed MUAP information were used to elucidate PFM overactivity and define PFM IZ distributions. Specifically, in collaboration with Baylor College of Medicine I:

- Mapped hypertonicity severity in women with and without confirmed PFM hypertonicity,
- Developed a novel IZ mapping technique that can guide the location and dosage of BoNT towards the hypertonic muscle.

In collaboration with Washington University School of Medicine I:

- Determined a significant increase in normalized intravaginal EMG at rest in women with IC/BPS ($p < 0.002$).
- Mapped patient specific IZ's in thirty women
- Mapped hypertonicity severity in women with IC/BPS and healthy controls.

The enhanced spatiotemporal information afforded by intravaginal HD-sEMG greatly enhances the ability to assess PFM activity in women. In this dissertation, I developed a novel hypertonicity mapping technique, and for the first time, showed spatial distribution of PFM hypertonicity in women with IC/BPS. Further, I developed a novel PFM IZ mapping technique, which can be used in the clinic to personalize the treatment of PFM hypertonicity. Finally, the developed techniques can be adapted to assess PFM activity in many pelvic floor dysfunctions, including stress urinary incontinence, fecal incontinence, and pudendal neuropathy.

Table of Contents

<i>Acknowledgements</i>	<i>ii</i>
<i>Abstract</i>	<i>iv</i>
<i>List of Tables</i>	<i>ix</i>
<i>List of Figures</i>	<i>x</i>
<i>Nomenclature</i>	<i>xii</i>
<i>Chapter 1 Background and Introduction</i>	<i>1</i>
The Pelvic Floor	1
Pelvic Floor Dysfunction	4
Stress Urinary Incontinence	4
Fecal Incontinence	4
Pudendal Neuralgia	6
Pelvic Floor Hypertonicity	7
Chronic Pelvic Pain	7
IC/BPS	7
Endometriosis	8
Inflammatory bowel disease	8
Vulvodynia	8
Neurophysiology Underlying Muscle Tone	9
Pelvic Floor Hypertonicity	10
Current Clinical Evaluation Techniques	13
Neuromuscular Junction	16
Electromyographic techniques	17
Single Fiber Electromyography	17
Intramuscular Needle Electromyography	18
Conventional Surface Electromyography	18
High-Density Surface Electromyography	19
Innervation Zone localization	20
Treatment	25
Conservative care	25
Pudendal Neuralgia	26
Botulinum toxin injections	27
Hypothesis and Specific Aims	31

Outline of Chapters	32
<i>Chapter 2 Assessment of Pelvic Floor Overactivity in Women with IC/BPS and Healthy Controls</i>	33
Introduction	33
Materials and Methods	36
Reliability	40
Statistical analysis	40
Results	41
Pelvic floor exam	41
Intravaginal High definition surface EMG	43
Discussion	51
Conclusions	59
<i>Chapter 3 Assessing Pelvic Floor overactivity in Women with IC/BPS to guide BoNT injection</i>	60
Introduction	60
Materials and Methods	62
Participants	62
Study Protocol	63
Signal processing	64
Statistical analysis	66
Results	67
Discussion	72
Conclusion	77
<i>Chapter 4 Assessment of PFM myofascial trigger points using HD-sEMG</i>	78
Introduction	78
Materials and Methods	80
Results and Statistical Analysis	81
Discussion	82
Conclusions	83
<i>Chapter 5 Non-invasive and Quantitative Assessment of the Number of Functioning Motor Units in the Puborectalis Muscle</i>	85
Introduction	85
Material and Methods	86
Participants	86
Signal Acquisition	87
Signal Analysis	88

Results	89
Discussion	91
Motor Unit Number Estimation	91
Limitations	93
Conclusions	94
<i>Chapter 6 Conclusions and Future Directions</i>	95
Guidance of Physical Therapy	95
Injection therapy	98
Summary	100
<i>References</i>	101
<i>Appendix 1. Publication list.</i>	127
<i>Appendix 2. Conference Proceedings list.</i>	128

List of Tables

<i>Table 2-1 Summarized patient demographics and pelvic exam findings. (*p<0.05, **p<0.01) †one control and one IC/BPS did not respond to the query about current medications.....</i>	<i>41</i>
<i>Table 2-2 Summary of EMG Findings for all features †Mann-Whitney U test used for non-normally distributed distributions.....</i>	<i>43</i>
<i>Table 2-3 Summary of reliability coefficients for each feature.....</i>	<i>51</i>
<i>Table 3-1: Digital VAS pain scores and hypertonicity assessment (+/-) for all subjects upon palpitation.....</i>	<i>68</i>

List of Figures

Figure 1.1 (A) 3D model of the pelvic floor muscles (B) pelvic floor muscles with pelvic organs, Figure reproduced from (7).....	2
Figure 1.2 The innervation of the PFM. Figure reproduced from (10).....	3
Figure 1.3 Flowchart outlining the proposed factors and hypothesis that contribute to pelvic floor hypertonicity/overactivity, and the interaction between hypertonicity and symptoms of CPP. Figure adapted from (82).	13
Figure 1.4 Example of innervation zone detection from a linear electrode array from the Biceps Bracii. Reproduced from (130).....	21
Figure 1.5 Example of a 2D mapping of a MUAP IZ from a single motor unit. . Reproduced from (130).....	22
Figure 1.6 representative bipolar mapping of the highlighted row of channels Figure reproduced from (118)	24
Figure 1.7 Illustration of the alpha gamma co-activation responsible for muscle tone, and the innervation zone detection and circumferential bipolar recording setup.....	25
Figure 1.8 Summary of CMAP reduction after BoNT injection in the control group (CG) and guided injection group (EG).....	30
Figure 2.1 Summary figure of intravaginal HD-sEMG collection. A) HD-sEMG probe, B) 64-channel electrode grid with RMS mapping overlaid, C) Raw differential EMG signals for all 64 channels, D) 64-channel MUAP template after decomposition and spike-triggered averaging.....	38
Figure 2.2 Detailed outline of testing protocol. Figure reproduced from (177).....	40
Figure 2.3 Comparison of resting RMS amplitude for both groups, and filtered EMG traces from one control and IC/BPS subject.....	45
Figure 2.4 Comparison of RMS ratio spatial map intensities between Control and IC/BPS groups.....	46
Figure 2.5 64-channel resting RMS ratio mappings for all subjects. Note: 64-channel mappings were interpolated by a factor of 2, white dots mark the IZ location. Figure reproduced from (177)	46
Figure 2.6 Resting and Contraction EMG features for diagnostic groups during both sessions. RMS ratio represents the average intensity of each subjects RMS ratio mapping.....	47
Figure 2.7 Effect of resting PFM alignment on RMS ratios.....	48
Figure 2.8 Linear relationships between average RMS ratio map intensity and Symptom, Problem, and Pain Scores	48
Figure 2.9 Relationship between sub-channel RMS ratio and average MUAP firing rate in women with IC/BPS (orange) and healthy controls (magenta).....	49
Figure 2.10 Receiver operating characteristic curves for all EMG features in Session 1 (above) and Session 2 (below).....	50
Figure 3.1 Top) Filtered HD-sEMG signals from one subject, Bottom) 64-channel motor unit action potential mapping overlaid on hypertonicity mapping result for one subject. Red box marks the IZ location. Figure reproduced from (193)	66
Figure 3.2 Summary of hypertonicity mapping results. Figure reproduced from (193) ...	67
Figure 3.3 Summary of hypertonicity index and repeatability results. Figure reproduced from (193)	69
Figure 3.4 Summary of proposed IZ injection guidance technique. Figure reproduced from (193)	71

<i>Figure 3.5 Left) Relationship between average hypertonicity index and baseline pain. Right) Relationship between average hypertonicity index and cumulative pain upon palpation. Figure reproduced from (193)</i>	<i>71</i>
<i>Figure 4.1 RMS ratios for participants with and without myofascial trigger points.</i>	<i>81</i>
<i>Figure 4.2 Location of myofascial trigger points (red box) overlaid on RMS mappings from Chronic Pelvic Pain Patients.</i>	<i>82</i>
<i>Figure 5.1 Procedural flowchart for PFM MUNE</i>	<i>90</i>
<i>Figure 6.1 Pilot results from two women with CPP and PFM tenderness.....</i>	<i>97</i>
<i>Figure 6.2 Summary of proposed IZ injection guidance technique. Figure reproduced from (193)</i>	<i>99</i>

Nomenclature

PFM – Pelvic floor muscle

PRM – Puborectalis muscle

PCM – Pubococcygeus muscle

ICM – Illieococcygeus muscle

OI – Obturator internus

PM – Perineal Membrane

EMG – Electromyography

iEMG – intramuscular EMG

sEMG – surface EMG

HD-sEMG – High density surface EMG

IZ – innervation zone

MU – Motor unit

MUAP – Motor Unit Action Potential

BoNT – Botulinum neurotoxin

NMJ – Neuromuscular Junction

Ach – Acetylcholine

AchR – Acetylcholine receptor

MUNE – Motor Unit Number Estimation

CMAP – Compound muscle action potential

SMUP – Single motor unit potential

HI – Hypertonicity Index

NPS – Numerical Pain Scale

ICSI/ICPI – Interstitial Cystitis Symptom/Problem Index

BPI – Brief pain inventory

Chapter 1 Background and Introduction

The Pelvic Floor

The Pelvic Floor muscles (PFM) are skeletal muscles that are comprised of two major layers. The first, most superficial layer, is composed of the bulbospongiosus and ischiocavernosus muscles (1). The bulbospongiosus muscle provides some support for the pelvic organs, but its main function is related to support of sexual function and micturition. Specifically, the bulbospongiosus maintains erection and facilitates ejaculation in men (2), and supports the perineal body in women (3). The ischiocavernosus muscle, similarly, supports erection in men, and contracts the vaginal wall during orgasm in women. Contrarily, the deep PFM, comprised of the levator ani, iliococcygeus, and coccygeus muscles, are integrally important in managing support of the pelvic organs, and as a result, the maintenance of urinary and fecal continence (4). The levator ani can further be divided into the puborectalis and pubococcygeus muscles. The levator ani muscles have been shown to contribute the most to the support of the pelvic organs (5). The pubococcygeus has its origin in the pubic symphysis and inserts into the anterior sacrococcygeal ligament (6). The puborectalis shares its origin with the pubococcygeus at the pubic symphysis but terminates at a “sling” behind the rectum. Figure 1.1 shows the female pelvic musculature (A) and relevant viscera (B), where PRM is the puborectalis muscle, PCM is pubococcygeus, PM is perineal membrane, ICM is iliococcygeus.

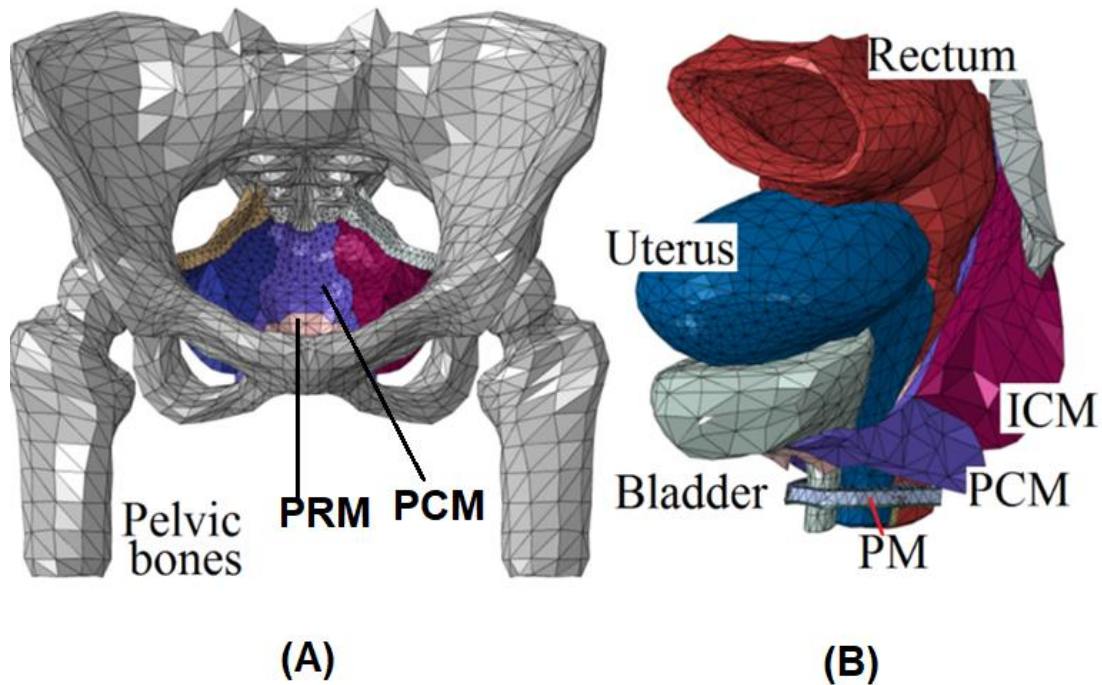


Figure 1.1 (A) 3D model of the pelvic floor muscles (B) pelvic floor muscles with pelvic organs, Figure reproduced from (7).

Other important pelvic muscles that do not contribute to the anatomy to the PFM, but are integral to the maintenance of continence include the external anal sphincter and external urinary sphincter, both of which are circular muscles surrounding the anal canal and urethra, respectively.

The PFM are innervated by branches of the sacral nerves S2-S4 (8). The S2-S4 nerve roots pass through the piriformis, past the ischial spine, to enter Alcock's canal (9). From there, the nerve roots split into the inferior rectal (anal) nerve, pudendal nerve, and dorsal nerve of the Penis/Clitoris (10). The S3-S4 sacral spinal nerve passes under the piriformis, past the ischial spine to innervate the pelvic musculature. The external anal sphincter, external urinary sphincter, and partially the puborectalis are innervated by the pudendal nerve (10). The

pubococcygeus and iliococcygeus are innervated by sacral spinal nerve S4, and the inferior rectal branch of the pudendal nerve (10).

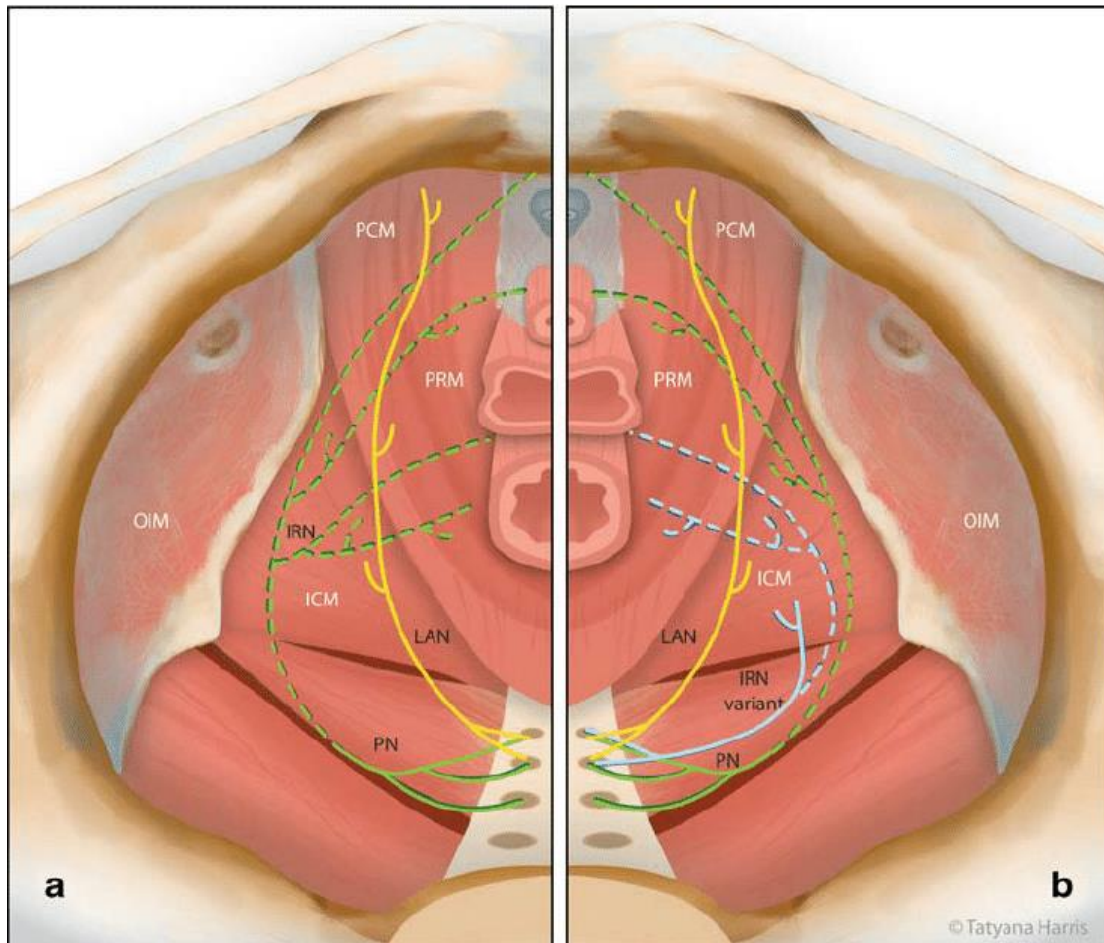


Figure 1.2 The innervation of the PFMs. Figure reproduced from (10).

The innervation of the PFMs has been controversial. Figure 1.2 illustrates the innervation of the PFMs, and shows varied innervation of the PFMs, where a) shows a classical distribution, and b) shows a variant distribution. Early electrophysiological studies by Snooks et al. (11) suggested that the PFMs are not innervated by the pudendal nerve, but rather innervated directly by S3 and S4 spinal roots. Later studies have evidenced a dual innervation of the PFM by the S3 and S4 spinal roots, as well as the pudendal nerve (12).

Pelvic Floor Dysfunction

Stress Urinary Incontinence

The PFM differs from most skeletal muscles in that it is constantly exhibiting tonic motor unit activity at rest (8). The PFMs provide constant support to the pelvic organs, thereby requiring constant muscle tone to maintain this support. The most common forms of pelvic floor dysfunction (PFD) occur when the PFMs become weakened at rest, or their ability to react to events of increased abdominal pressure are diminished (13). In the “hammock hypothesis” theory, the levator ani plays a significant role in maintaining urinary continence (14). During an IAP increase, the levator ani contractions help the urinary sphincters close the urethra by contractile force and maintain an angle between the urethral opening and the bladder neck. PFM weakness or trauma can lead to excessive urethral excursion, measured as the urethral angle change during Valsalva (15). Excessive urethral excursion has been associated with stress urinary incontinence. PFM weakness can result from obstetric trauma, neuropathic disorders, spinal cord injury, and healthy aging, and as such, stress urinary incontinence is the most common form of PFD, with the highest prevalence estimates suggesting that up to 35% of women in the USA suffer from stress urinary incontinence (16). EMG has been used to reveal delays in muscle response to increased intra-abdominal pressure in women with stress urinary incontinence, signifying motor control deficits in these patients (17).

Fecal Incontinence

Anorectal disorders, such as idiopathic fecal incontinence (FI), are frequently encountered in the aging population and reported in up to 19% of individuals aged 65 years and older, causing a devastating impact on their quality of life (18). The

external anal sphincter (EAS), which plays an important role in maintaining anorectal function through contributing to the resting anal tone and participating in voluntary contraction, can be affected by aging. Multiple sophisticated studies have reported structural/mechanical changes in the EAS associated with aging in asymptomatic women and patients (19-22), while the mechanism by which aging affects EAS function remains unclear. A second major risk factor for fecal incontinence is vaginal child delivery. During vaginal delivery, pelvic nerves and muscles are exposed to mechanical stretch and compression, and compromised blood flow by maternal expulsive efforts (23, 24). This process can introduce severe injuries to the external anal sphincter, pelvic floor muscles, and their innervating nerves (25, 26), especially in cases such as large birthweight, prolonged second stage of labor and use of instrumentation (27-29). Furthermore, the puborectalis muscle plays an integral role in the maintenance of fecal incontinence. The U-shaped puborectalis muscle maintains the resting anorectal angle, aiding the EAS in maintaining fecal continence. In fact, in patients with severe sphincter laxity, maintenance of fecal continence can be achieved by repairing the anorectal angle with a synthetic puborectal sling (30).

The decline in the strength of a muscle can often be attributed to a number of alterations affecting the musculoskeletal and/or the nervous systems (31), including reduced cortical and spinal excitability (32-35), altered motor unit discharge properties (36-39), reduced motor unit size and number (40-43), reduced muscle mass (44), and changes in the muscle's contractile properties (45, 46), all of which may play a role in the occurrence of idiopathic stress urinary and

fecal incontinence. Each of these factors can be assessed with sophisticated electromyographic signal processing protocols and recording techniques.

Pudendal Neuralgia

Pudendal neuralgia is a severely painful, sometimes debilitating neuropathic condition affecting the dermatome of the pudendal nerve (47). This leads to neuropathic pain in the clitoris, vulva, perineum, and rectum that is exacerbated by sitting (48). Patients often exhibit hyperalgesia, allodynia, and paresthesia across the dermatome of the pudendal nerve. Injury can take place throughout the nerve's course including denervation at the neuromuscular junction, stretching of the nerve, and compression of the nerve inside the pudendal canal (49). Compressive effects lead to loss of conduction, which is associated with the generation of paresthesia caused by ectopic impulses. Risk factors for pelvic floor injury during childbirth include forceps delivery, episiotomy, increased fetal size, and prolonged second-stage labor (23). Studies employing rabbit models have shown that permanent nerve conduction failure can occur in peripheral nerves if strain exceeds 15% of its original length (50). Using this standard, a simulation study quantified the stretch of four pudendal nerve branches during childbirth, demonstrating that the inferior rectal and perianal nerve branch innervating the anal sphincter underwent maximum strain values above 33%, suggesting the possibility for severe nerve damage caused by vaginal child delivery (51). Electromyographic techniques have been employed to directly measure changes in the conduction velocity of the pudendal nerve, which can serve as a direct measure of nerve health (52). Future studies may aim to employ electromyography to study changes in innervation induced by labor or other nerve trauma.

Pelvic Floor Hypertonicity

Another form of PFD occurs when the PFM become overactive at rest, termed PFM hypertonicity (13). PFH sufferers are unable to void properly, resulting in increased visceral pain, leading to a positive feedback loop where guarding mechanisms and intravesical pain begin to perpetuate the PFM hypertonicity. This condition is explained in the below section entitled “**Pelvic Floor Hypertonicity.**”

Chronic Pelvic Pain

Chronic pelvic pain (CPP), defined as persistent pain in the lower abdomen or the pelvis without an obvious on-going disease process (53). Owing to its multifactorial etiology, risk factors for CPP have been hard to assess. CPP is twice as prevalent in women, when compared to men (54-56). Race has been associated with a decreased risk of CPP in non-Caucasian women when compared to Caucasian women (57, 58). Many conditions have been found to underlie the CPP population, including interstitial cystitis/bladder pain syndrome (IC/BPS), Endometriosis, Inflammatory bowel disease, and a history of sexual or physical abuse. Complicating the diagnosis and treatment of CPP is the coexistence of many of these disorders. If all pain source are not initially identified, the initial course of treatments may not be curative.

IC/BPS

IC/BPS contributes to a substantial portion of CPP sufferers. In IC/BPS, patients become hypersensitive to bladder filling, resulting in “severe pain in the absence of any infection or any other identifiable causes” (59, 60). Bladder hyperalgesia

may present in concert with the presence of inflamed lesions on the bladder mucosa, called Hunner lesions. Recent studies have shown that IC/BPS patients with and without Hunner lesions may represent specific phenotypic clusters of patients (61). In addition to bladder hyperalgesia, visceroviscero convergence may refer pain to adjacent organs, potentially expressing as vaginal pain or reducing uterine contractile activity (62, 63). A significant portion of IC/BPS patients also present with pelvic floor muscle instability and hypertonicity (64).

Endometriosis

Endometriosis is a painful disorder characterized by the growth of endometrial tissue outside of the uterus. Pain associated with endometriosis increases during menstruation but is not altered by bladder filling or emptying. Up to 33% of CPP sufferers are comorbid for endometriosis (65). In addition to pain symptoms, a certain percentage of late stage endometriosis patients suffer from infertility (66).

Inflammatory bowel disease

Inflammatory bowel disease (IBD) involves the chronic inflammation of the intestinal tract. Inflammatory cytokines related to IBD explain the existence of pain in 70% of IBD sufferers (67). In animal models, experimental gastrointestinal inflammation led to increased excitability of convergent dorsal root ganglion neurons receiving afferent input from the bladder and colon, potentially revealing a mechanism for pelvic organ cross sensitization (68).

Vulvodynia

Vulvodynia is defined as the existence of chronic pain near the opening of the vagina. Vulvodynia can be either provoked (PVD) or generalized (GVD) (69). The

underlying etiology of vulvodynia is poorly understood, with many competing theories as to its pathogenesis. Generally there is an identifiable trigger or injury to the vulva, such as childbirth, that precedes vulvodynia (70). This initial insult to the vulva leads to noxious afferents and wind-up of the dorsal horn, leading to peripheral and central sensitization (71). Vulvodynia is often also secondary to another CPP disorder, such as IC/BPS (72). Vulvodynia negatively impacts sexual function and quality of life, due to an increase in catastrophizing thoughts related to pain during intercourse (73).

Neurophysiology Underlying Muscle Tone

Muscle tone is defined as the resting tension of muscle tissue, as described by its deformative properties and resistance to changes in length or stretch (74). As shown in Figure 1.7, in its simplest sense, the circuit responsible for the maintenance of muscle tone is composed of α -motor neurons, γ -motor neurons, type Ia afferent fibers from mechanoreceptors in the muscle spindle, and type Ib afferent fibers from the Golgi tendon organ (not shown), and type II afferent fibers (75). Muscle tone is maintained by the co-activation of the α -motor neurons and γ -motor neurons in the stretch reflex. In short, constant steady state stimulus of intrafusal muscle fibers is maintained by γ -motor neuron excitation. This excitation keeps the muscle spindle taut and stimulates Ia sensory fibers, leading to the activation of α -motor neurons (75). The α -motor neuron stimulation then modulates contraction of the extrafusal muscle fibers, leading to muscle shortening. Proper α - γ coactivation is vital to the sensitivity of the muscle to length

changes, forming the basis for muscle tone maintenance. As such, proper α - γ coactivation of the is integral to the maintenance of muscle tone (75).

A common cause of muscle tone disorders is an insult to the upper motor neuron. In patients with an upper motor neuron syndrome (UMNS), velocity dependent muscle spasticity may result from altered sensory processing from Ia and II afferents (76). It is not likely that abnormal muscle tone resulting from a UMNS is related to γ motor dysfunction, as stroke patients are able to activate the fusimotor system during voluntary contraction (consisting of γ motor neurons and β motor neurons) (77).

Hypertonicity of the pelvic floor, however, is often not due to an upper motor neuron lesion, but rather secondary to a chronic pelvic pain syndrome. It has been reported that increased muscle tone is present in conjunction with anxiety (78), potentially providing an explanation for some of the increased muscle tone present in CPP sufferers. Theories which attempt to explain the emergence of PFM overactivity and hypertonicity in women with CPP are discussed in the following section.

Pelvic Floor Hypertonicity

Pelvic floor hypertonicity (PFH), characterized by an increase in the tonic activity of a pelvic floor muscle, is a symptom related to myofascial pain that presents in up to 85% of patients with interstitial cystitis/bladder pain syndrome (IC/BPS) (79), up to 90% of vulvodynia (80), as well as a substantial portion of irritable bowel syndrome (IBS) and endometriosis patients (81, 82). The etiology of PFH is unclear but has been associated with direct muscle injuries such as

obstetric trauma, instrumented delivery or pelvic surgery, as well as overuse injuries, that can occur due to IBS, obstructive defecation or anxiety.

PFH can be segmented into two main subgroups, non-neurogenic hypertonicity and neurogenic hypertonicity (83). In PFH sufferers with non-neurogenic hypertonicity, tissue properties in the PFM have become altered. Specifically, the resting filamentary tension from stable cross-links inside the cellular structure of the muscle filament (84). Further, passive stiffness contributed by muscle connective tissue may influence the resting tone of the pelvic floor muscles (84). Neither the resting filamentary tension nor muscle connective tissue properties will influence the electrical activity of the resting PFM (85).

In sufferers with neurogenic hypertonicity, peripheral and central sensitization result in “visceromuscular hyperalgesia,” in which pain felt in the primary pain generator (bladder in IC/BPS) is referred to the pelvic floor muscles (86). One theory supporting the emergence of muscle hypertonicity in response to referred muscle pain is the Johansson/Sojka hypothesis, in which spasm induces muscle ischemia and pain, followed by a consequential release of neuromuscular transmitters and inflammatory mediators. Inflammatory mediators then induce afferent (group III and IV) hyperexcitability (87, 88). The group III and IV afferent firings then induce γ motor neuron firing, leading to muscle instability, stretch sensitivity, and increased tone via α -motor neuron excitation (87, 88). Once the muscles become hypertonic, conditions conducive to the development of myofascial trigger points are present in the muscle (89). It should be noted that recent findings show induced muscle pain did not induce γ -motor neuron

hyperexcitability in awake human subjects, so future studies may investigate the validity of the Johansson/Sojka hypothesis in chronic pain sufferers (90).

An important component in pain induced PFM dysfunction is the psychological component. Sexual abuse has been shown to significantly associate with chronic pelvic pain (91). Traumatic events have been shown to induce neuroendocrine changes, leading to the development of behavioral changes which may manifest as neurologic such as anxiety and depression (92), and somatic symptoms (93). Women with vaginal and pelvic floor muscle spasm (vaginismus) are shown to report higher levels of generalized anxiety, suggesting that anxiety predisposes some women to develop vaginismus (94). Once vaginismus develops, penetration becomes extremely painful, sexual function decreases and occasionally results in complete sexual aversion (95). Furthermore, fear of pain can contribute to additional muscle hypertonicity.

In a similar vein, CPP has been shown to significantly associate with painful sexual intercourse (dyspareunia), with 75% of CPP sufferers reporting dyspareunia (79). C-Fiber activation from noxious bladder afferents leads to dorsal horn windup and altered pain processing. This induced vulvodynia then prompts anticipatory PFM contractions in advance to vaginal penetration (96). This symptom phenotype fits the fear-avoidance model of pain (97), in which maladaptation to painful experiences result in chronic pain, contributing to withdrawal from otherwise “normal” activities. In CPP sufferers, this is often withdrawal from partner intimacy and sexual dysfunction (97). *Figure 1.3* summarizes how a combination of the above factors can lead to PFH, and how

PFH can be the primary or secondary generator of CPP and multiple voiding, sexual and defecatory disorders, and a major contributor to the perpetuation of pain symptoms even after the elimination of original cause (98).

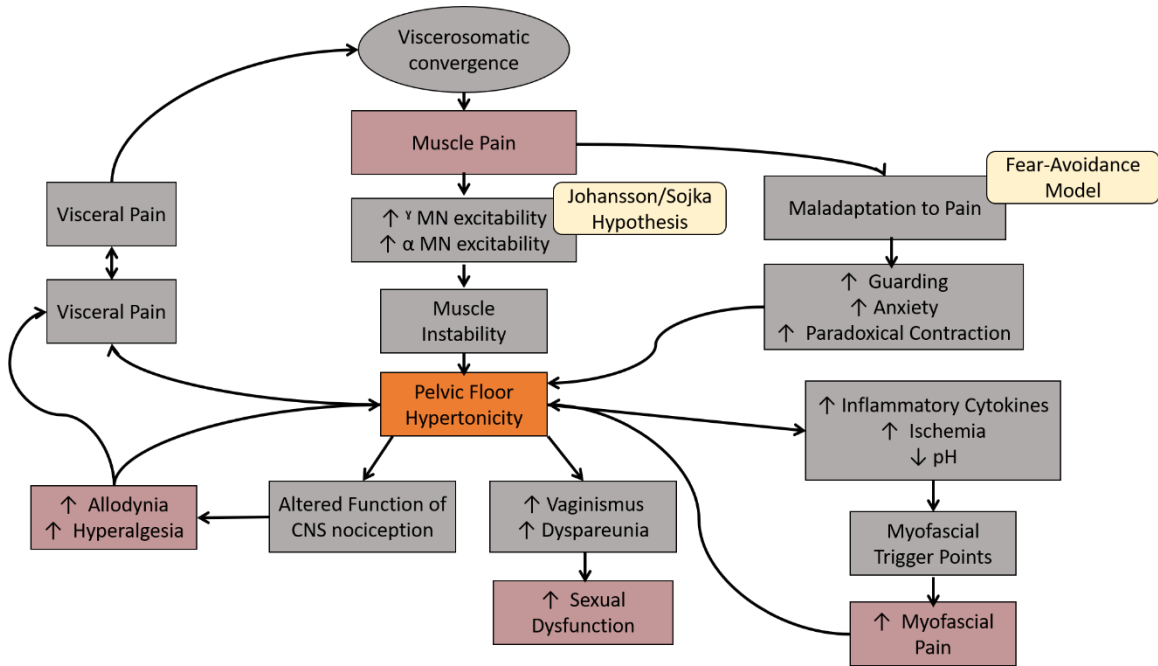


Figure 1.3 Flowchart outlining the proposed factors and hypothesis that contribute to pelvic floor hypertonicity/overactivity, and the interaction between hypertonicity and symptoms of CPP. Figure adapted from (82).

Current Clinical Evaluation Techniques

Pelvic floor pain and hypertonicity is intrinsically a multifactorial dysfunction that is attributed to a wide variety of musculoskeletal factors. Using digital palpation, Tu et. al found that women with chronic pelvic pain disorders exhibited significantly increased PFM tone and inability to relax the PFM (99). PFM weakness has also been shown to associate with PFM pain, with the possible etiology of a weak PFM being unable to support the saddle area, potentially the posterior femoral cutaneous nerve (100). In addition to short, tight, painful pelvic floor muscles, Haugstad et. al proposed a posture and gait based paradigm for

explaining the presence of CPP, and found that women with CPP demonstrated a specific pattern of posture and pain (101). In a later study, the same group demonstrated that movement impairments of the trunk were also demonstrated by women with CPP (102). Unfortunately, no technology is currently available for quantitatively and objectively assessing these etiologic factors associated with pelvic floor pain, which, otherwise, would advance the understanding of the underlying mechanisms and allow for phenotyping patients for appropriate intervention personalization. The assessment of musculoskeletal function in women with pelvic floor pain commonly is achieved with digital palpation (103), intra-vaginal manometry (104), and surface EMG (105).

Digital palpation of the pelvic musculature is carried out intra-vaginally and intra-rectally. During a digital pelvic exam, an examiner measures the length of the PFM, pain upon digital palpation, presence of myofascial trigger points, and muscle tone. As such, digital palpation relies on the examiner's subjective opinion on the presence of an abnormality. Tu et. al found that women with chronic pelvic pain disorders exhibited significantly increased PFM pain upon palpation (99). Digital palpation, as a purely subjective assessment technique, has shown to be poorly reliable in detecting increased muscle tone (106).

Imaging techniques have shown some utility in detecting PFM hypertonicity in women with CPP. Using magnetic resonance imaging, Ackerman et. al showed that, on average, 15 women with CPP demonstrated significantly shorter puborectalis muscles than 15 healthy control women, which is indicative of PFM hypertonicity (107). In addition to diagnostic utility, imaging techniques have been

used to aid in the treatment of CPP and PFM hypertonicity. Nesbitt-Hawes et al. developed a novel 4-dimensional ultrasound guidance technique for guiding injections towards a target muscle. Using this technique, they showed accurate muscle infiltration and fluid expansion after a median of 1 injection attempts (108).

Intravaginal manometry uses an air-filled balloon to measure the pressure inside the vaginal lumen. Pressure measurements are made at rest, and during voluntary PFM contraction. Naess and Bo found that women with provoked vestibulodynia demonstrated significantly increased intravaginal pressure at rest, that was reduced to a normal range after three maximum voluntary contractions of the PFMs (109). Nesbitt-Hawes et. al utilized intravaginal manometry as an outcome measure to assess reductions in PFM hypertonicity after pelvic intramuscular injections of botulinum toxin (BoNT) (110). Despite the use of manometry in research studies, absence of validated reference ranges limits the clinical utility of intravaginal manometry.

Conventional surface EMG technology is incapable of comprehensively assessing the neuromuscular function of the PFM because of the complicated pelvic anatomy (111). Commonly, patch electrodes may be placed over the perineum or near the external anal sphincter to measure myoelectric activity produced by the superficial pelvic floor muscles, however, this provides no myoelectric information from the deep pelvic floor muscles. Several studies have utilized conventional surface EMG probes to quantify muscle activity in people with chronic pelvic pain with varied results. Hetrick et al. demonstrated that men with CPP has significantly increased resting EMG potentials, when compared to

controls (10.4 ± 3.12 vs 6.4 ± 0.96) (112). Similarly, Loving et. al used a conventional surface EMG probe to demonstrate that women with CPP presented with significantly higher resting EMG when compared to women without CPP (Median[IQR] $1.9[1.2-3]$ vs. $0.9[0.9-2]$) (113). Engman et. al, however, found no significant difference in resting EMG potentials between women with partial vaginismus and asymptomatic controls (4.55 ± 2.04 vs 4.35 ± 2.65) (114).

These varied findings may be partially attributed to shortcomings in the design of commercially available intravaginal sEMG probes. A reliable technique to quantitatively assess mechanistic musculoskeletal alterations of muscles in a comprehensive muscle network will be able to phenotype CPP patients for appropriate physical therapy protocol but is currently lacking.

Neuromuscular Junction

The axon of an alpha motor neuron forms a synapse with an innervating muscle fiber at the neuromuscular junction (NMJ). When an action potential reaches the NMJ, the release of Acetylcholine (ACh) is triggered. ACh then diffuses across the synaptic cleft to bind with Acetylcholine receptors (AChR). The ACh then binds to nicotinic acetylcholine receptors (nAChR) which are ligand-gated ion channels. Upon binding, the ligand gated ion channels open and allow sodium to influx, generating an action potential inside the muscle fiber (115). This muscle fiber action potential then propagates in opposite directions down the muscle fibers towards the tendons. It is propagation of the sum of all muscle fibers innervated by a single motor neuron that can be detected by multichannel EMG to localize the innervation zone.

Early studies have employed cholinesterase staining to elucidate the locations of the muscle where neuromuscular junctions are most densely distributed. Erna Christensen illustrated the distribution of motor endplates in sixteen muscles from stillborn infants and found that the location of densely distributed motor endplates varied by muscle type, however, they were commonly located near the muscle belly with some exceptions (116). Later, Pierce et al. used a similar end plate staining technique to characterize motor end plate distributions in the pelvic floor muscles of the female squirrel monkey. They found that the motor endplates in the pubocaudalis and coccygeus muscles were distributed medially across the muscle in a straight line, whereas a U-shaped distribution was present in the iliocaudalis muscle (117). Cholinesterase staining techniques are useful in determining neuromuscular junction and motor end plate distributions in *ex vivo* tissue preparations, however, they are clearly not applicable to developing *in vivo*, personalized innervation distributions.

Although these histochemical studies have shown a medial distribution of motor end plates in the coccygeus and pubocaudalis muscles, it has been shown that injury to the innervation of the PFMs occurs during childbirth, and even healthy aging (51, 118). Therefore, it is necessary to develop an *in vivo* phenotyping tool to produce patient specific innervation zone distributions.

Electromyographic techniques

Single Fiber Electromyography

Single-fiber EMG measures the action potentials from individual muscle fibers but is a complex measurement technique that requires specialized

equipment and a highly trained operator. Furthermore, the uptake area of a single fiber electrode is approximately $300\ \mu\text{m}$ (119), allowing for a highly selective recording to be made. This allows for muscle denervation and reinnervation to be measured by calculating the density of individual muscle fibers innervated by a motor unit, where an increase in fiber density for a particular motor unit is representative of post-denervation reinnervation (120).

Intramuscular Needle Electromyography

Concentric needle EMG are commonly used in the clinic, due to its ease of use and high selectivity. With an uptake area of approximately $1000\text{-}2000\ \mu\text{m}$, (121) concentric needle EMG allows for the direct measurements of motor unit action potentials (MUAP), representing the sum of all muscle fiber potentials innervated by the same motor neuron. Concentric needle EMG is used in the clinic for the diagnosis of neurogenic and myopathic disorders via analysis of fibrillations, MUAP morphology, and MUAP firing characteristics.

Conventional Surface Electromyography

Surface Electromyography measures a surface interference pattern (SIP) representing the summation of MUAP trains that occur beneath the electrode of interest. Cancellation of motor unit action potential signals occurs due to recording of a large selection of motor units through the skin and fat tissue, which limits the direct interpretation MUAP morphology or spikes recorded from conventional surface EMG (122), thereby limiting its diagnostic ability. Regardless, conventional surface EMG has proven useful in kinesiological posture and gait analysis, and for the differentiation of dystonias (123). In the pelvic space, conventional surface EMG has been widely used as an assessment tool for resting and contraction

activity of the PFM. The Glazer EMG protocol was developed to comprehensively assess the phasic, tonic, endurance contractions of the pelvic floor, which are all informative in measuring the ability of the PFM to contract voluntarily. This is useful in assessing the strength of the PFMs but does not provide much help in the diagnosis or assessment of PFM overactivity. A recent comprehensive review of clinically available intravaginal EMG probes demonstrated a lack of channel quantity in most, possibly predisposing these probes to recording cross-talk from neighboring muscles (111).

High-Density Surface Electromyography

High-Density Surface Electromyography (HD-sEMG) provides abundant spatio-temporal information regarding target muscles. This detailed information allows for the non-invasive assessment of motor unit properties including innervation zones, firing rate, and amplitude. This has allowed for a variety of techniques to be developed that have furthered the non-invasive assessment of muscle activity. The first of which is the assessment of conduction velocity (124), which is a measure of how fast a MUAP propagates along a muscle fiber. Later advances in signal processing developed algorithms to decompose multi-channel SIP signals into constitutive motor unit spike trains.

The first decomposition algorithm was reported by Mambrino and De Luca et. al, in which a template matching technique was developed and tested on simulated and real EMG signals, demonstrating the first competent multichannel EMG decomposition (125). Holobar and Zazula later developed a blind source separation (BSS) technique for decomposing HD-sEMG signals via deconvolution,

named convolution kernel compensation (CKC) (126). Ning et al. improved upon the CKC algorithm by including an initialization step in which initial points are clustered using k-means (127), resulting in improved decomposition yield.

The K-means modified CKC algorithm was employed to decompose the HD-sEMG signals acquired in this dissertation, and readers interested in the details of the algorithm are urged to read reference (127). Briefly, a time instant n_0 with several simultaneously active MUs was selected based on the global activity index. Then, firing instants generated by MUs which are simultaneously active at n_0 are collected. The K-means clustering method was utilized to cluster these collected firing instants into groups corresponding to different MUs. The group with the largest number of firing instants is used to construct the initial MUAP pulse train via the linear minimum mean square error method (128). Finally, a modified multi-step iterative convolution kernel compensation (CKC) method (126) was employed to update the estimated MUAP pulse trains to improve the decomposition accuracy. MUAP pulse trains with a pulse-to-noise ratio greater than 30 were accepted (129).

Regardless of the method used to decompose the signal, decomposition allows for the spatial distribution of muscle activity single motor units can be elucidated via spike triggered averaging based on spike timings from a specific motor unit, and their innervation zones elucidated.

Innervation Zone localization

This section outlines introduces innervation zone localization techniques, and is adapted from (130). The innervation zone (IZ) is a term used in the EMG

literature that indicates the physical territory of densely distributed neuromuscular junctions to a motor unit (MU) (131). Elucidation the of global IZ distribution can aid in the diagnosis and treatment of neuromuscular dysfunction (132-135).

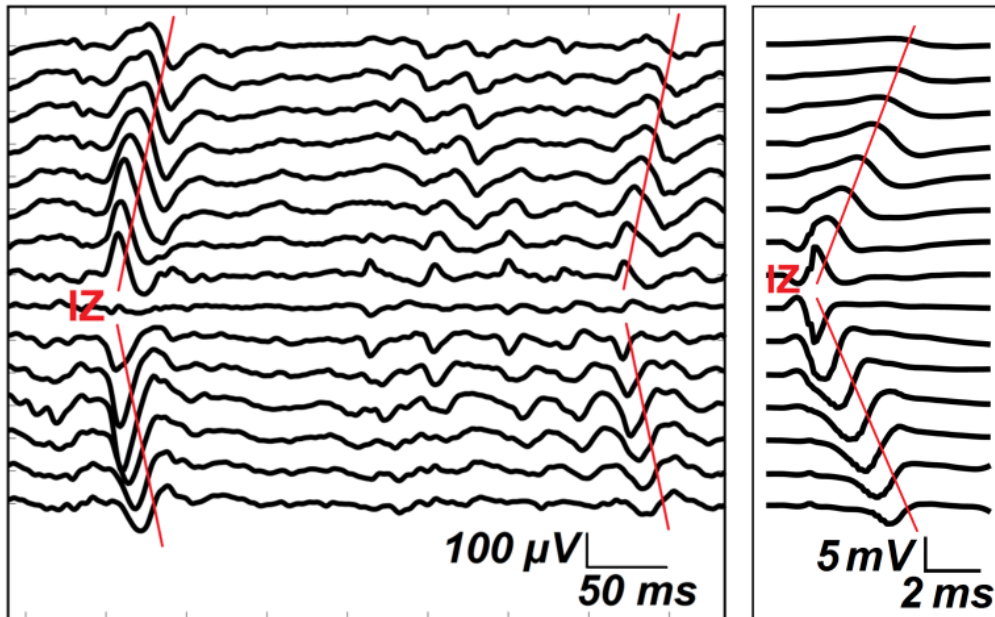
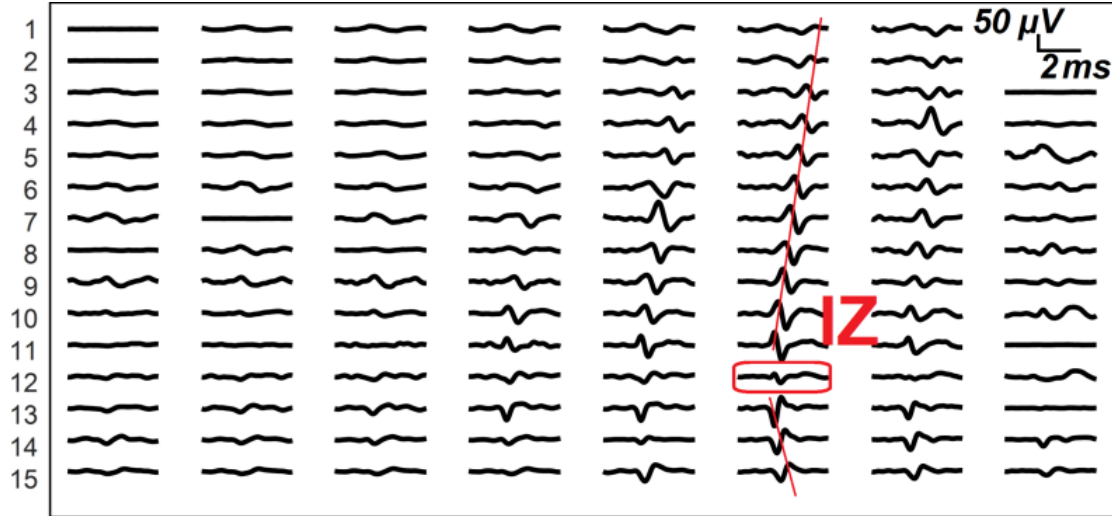


Figure 1.4 Example of innervation zone detection from a linear electrode array from the Biceps Bracii. Reproduced from (130).

The basis for IZ localization is provided by the propagation of MUAPs away from the neuromuscular junction towards the origin and insertion of the muscle (131). HD-sEMG has been used to capture this MUAP propagation by spacing sEMG sensors parallel to the muscle fiber direction. The IZ can then be identified merely as the point of signal symmetry by a human observer (136). Figure 1.4 shows an

example of IZs visually identified from biceps brachii recordings using a linear array.



*Figure 1.5 Example of a 2D mapping of a MUAP IZ from a single motor unit. .
Reproduced from (130).*

HD-sEMG allows for the entire global IZ distribution to be assessed and enables the implementation of advanced IZ detection methods. Decomposed MUAP spike trains can be spike-trigger averaged to produce a two-dimensional (2D) sEMG grid visualizing the IZ distribution over the skin, as shown in Figure 1.5 from Biceps Brachii recordings. Three-dimensional (3D) source imaging techniques, which are employed in brain imaging studies, have been utilized to extend the dimensionality of IZ detection in muscles. Extending IZ detection into 3-dimensions allows for the depth of the IZ inside the muscle to be localized, which is integral to the reliable detection of the IZ in anatomically thick muscles like the Biceps Brachii or Rectus Femoris.

Most studies on the IZ focus on the limb and trunk muscles, however, several studies have aimed at elucidating the innervation zone distributions of the

pelvic muscles. The first study to examine the IZs in the pelvic muscles was by Enck et. al, in which a circular linear array mounted on an intrarectal probe was employed to elucidate external anal sphincter innervation zones in 15 healthy males, and 37 healthy females. Innervation zones were visually identified as a phase inversion between neighboring channels in circumferentially calculated bipolar surface recordings (137). In a later study, Cescon et al. further assessed pelvic innervation zones intra-rectally with a glove mounted linear array (138). This study revealed uni-laterally propagating IZs in the puborectalis muscle, propagating towards the puborectalis sling, from the ventral direction (138). This finding suggests a more ventral recording location, like the intravaginal surface, would provide a better site for the localization of the IZs, providing the basis for the intravaginal IZ recording location used in this dissertation.

Peng et al. later defined a comprehensive distribution of PFM IZ's using two 64-channel intravaginal and intrarectal probes in healthy women (133). I later extended this work to study changes in innervation zone innervation during aging, and found the emergence of an innervation asymmetry in older women (118), using the spatio-temporal mappings of motor unit action potentials to localize the IZ, as shown in Figure 1.6.

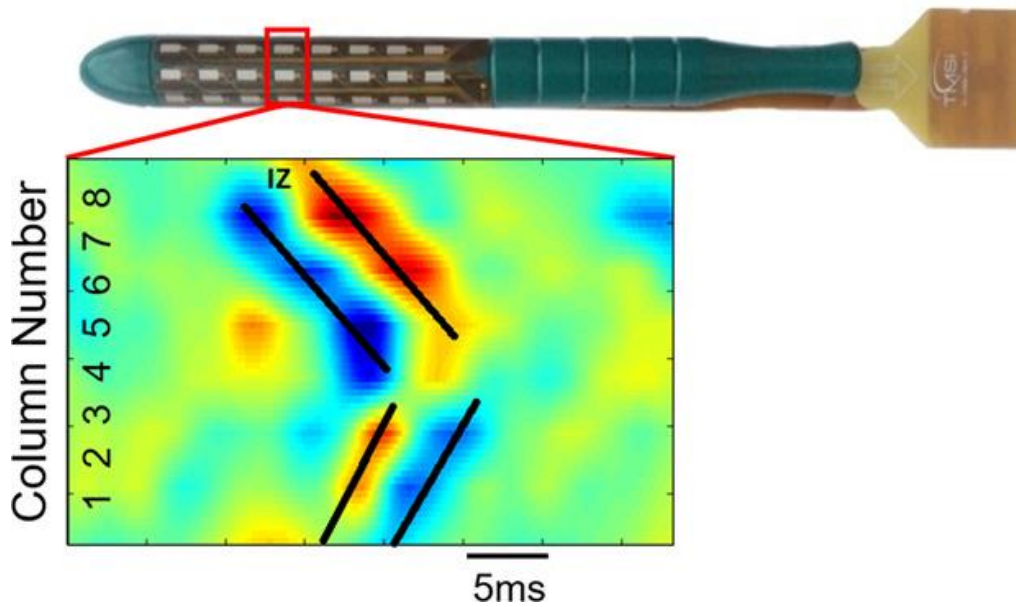


*Figure 1.6 representative bipolar mapping of the highlighted row of channels
Figure reproduced from (118)*

In this dissertation, I will be using a combination of the 2-Dimensional IZ detections method shown in Figure 1.5 and Figure 1.6, adapted to suit the cylindrical intravaginal probe, as shown in Figure 1.7. For IZ localization to be successful, the bipolar channel configuration with respect to the muscle fiber direction must be discerned. Concurrent magnetic resonance imaging (MRI) with intravaginal HD-sEMG probe insertion was accomplished by Voorham-van der Zalm et al., and coronal pelvic scans revealed that muscle fibers of the levator ani muscle complex were largely perpendicular to the vaginal wall (139). Further, PFM diffusion tensor tractography studies reported by Zijta et. al demonstrated that muscle fibers from the Pubovisceral (Levator ani) muscle would pass parallel to the circumferential direction of the intravaginal probe (140), informing the decision to employ a circumferential bipolar configuration for IZ detection.

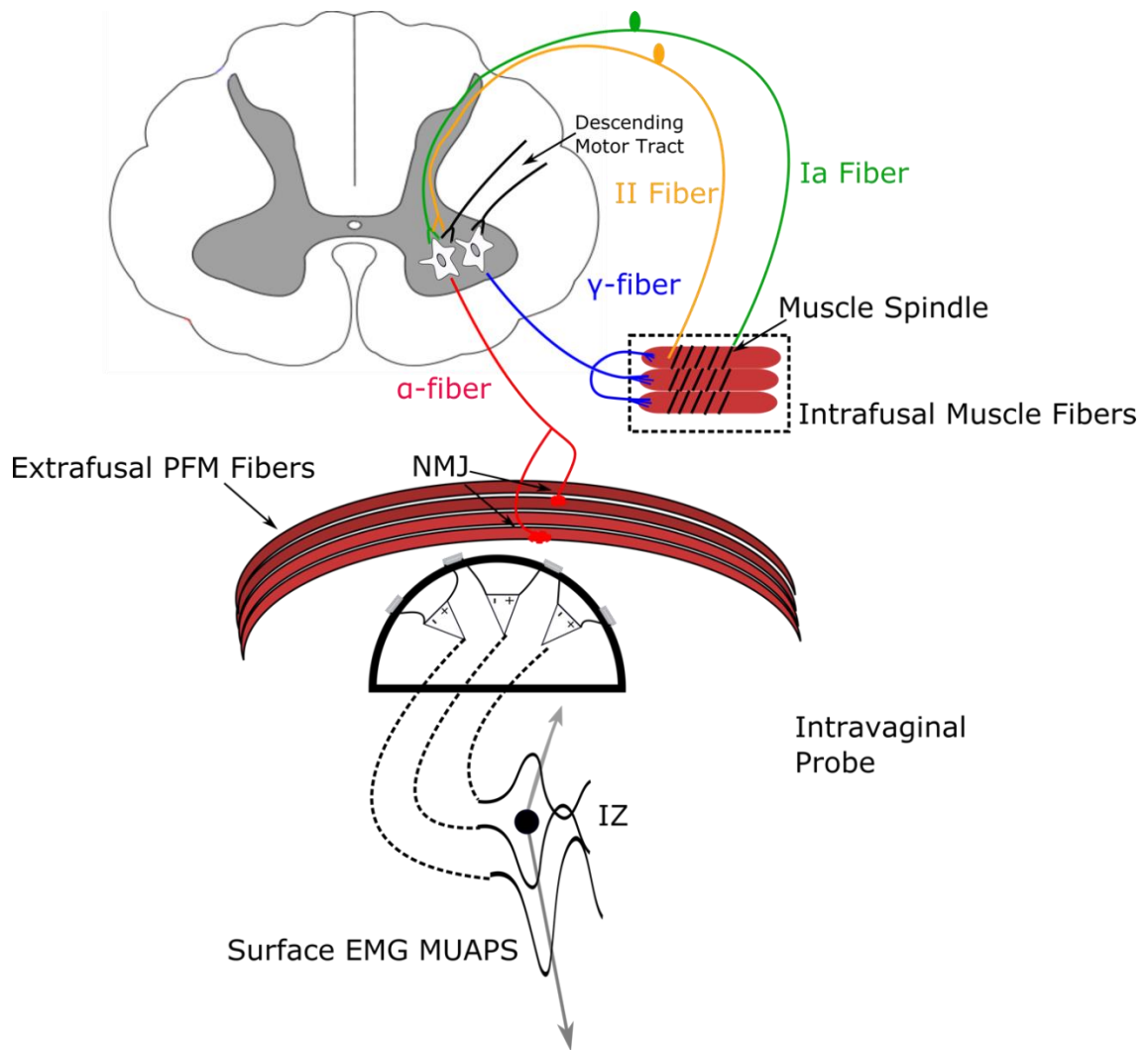


Figure 1.7 Illustration of the alpha gamma co-activation responsible for muscle tone, and the innervation zone detection and circumferential bipolar recording setup.

Treatment

Conservative care

Clinical management of PFH involves the retraining and rehabilitation of the dysfunctional muscles, often through behavioral and physical therapy, oral medications, neuromodulation and trigger point injections (98). Despite these methods, the management of PFH remains challenging and sometimes inefficient due to its multifactorial nature (141). Treatment for pelvic floor pain is largely

dependent on the attributed conditions underlying the pain. Commonly, 1st line treatment includes behavioral modification, stress reduction, and education about CPP and pelvic muscle pain, followed by myofascial physical therapy as 2nd line.

The current gold-standard for conservative CPP management is myofascial physical therapy. A recent landmark RCT of 81 women with IC/BPS and concomitant pelvic floor tenderness showed a 59% global response assessment rate to a 10-week myofascial physical therapy protocol (142). Despite being proven to be an effective treatment for pelvic floor pain in women with IC/BPS, 41% of women still did not respond to treatment, possibly due to heterogeneous symptom etiology. Myofascial physical therapy treats the muscle directly via manual manipulation of hyper-contracted muscles and trigger points, release of connective tissue restrictions, and retraining of weak PFMs where necessary (142).

Alternative therapy techniques, like movement physical therapy, aim to treat gait and posture abnormalities that could lead to pelvic floor muscle pain (101). The current 'trial and error' approach in CPP treatments results in increased healthcare costs and frustration for patients, necessitating careful patient phenotyping and treatment personalization to optimize treatment. A quantitative evaluation technique may provide a phenotyping tool to aid in this optimization of conservative care options.

Pudendal Neuralgia

Due to the wide range of factors contributing to pudendal neuralgia, treatment varies for each patient (143). Treatment of pudendal neuralgia starts with conservative options as simple as avoiding activities that cause the pain. High-

risk patients such as gymnasts and cyclists should decrease or cease such activities. Many patients are responsive to physical therapy. A more aggressive treatment for entrapment neuralgia is the pudendal nerve block. A guided pudendal nerve block can both diagnose and treat pudendal neuralgia. If the pain is relieved after the block, the pain is directly related to the pudendal nerve (144). Pudendal nerve block is successful when there is a temporary elimination of pain. The most aggressive form of treatment is surgical. The nerve is manually decompressed by a surgeon.

Botulinum toxin injections

Currently, botulinum neurotoxin (BoNT) is receiving growing interest in relieving PFH and myofascial pain, with superior performance compared to conventional injection therapies (145, 146). BoNT has proven to be effective in treating multiple conditions including blepharospasm, spasticity, and myofascial pain (147); and is specifically useful in managing a number of pelvic disorders including detrusor overactivity (urge incontinence), CPP, detrusor sphincter dyssynergia, vaginismus, obstructed defecation, and voiding dysfunction (148). Symptom relief from BoNT injections are attributed to the blockage of acetylcholine neurotransmitters release at the neuromuscular junction (NMJ) that are involved in muscle contraction, nociceptive signaling (149), and central sensitization (150).

Despite its proven potency and relative safety in the management of hypertonicity, BoNT therapy is expensive and can cause dose-dependent adverse effects. Fortuna et. al demonstrated a 95% loss of muscle strength in rabbits injected with BoNT in the quadriceps femoris. Furthermore, they demonstrated up

to an 80% loss of contractile tissue via fat substitution (151). In addition to a loss of muscle strength and contractile tissue, they observed similar, albeit smaller strength reductions in off-target muscles. Mancini et al. varied dosage strength in lower limb spasticity patients, and patients reported pain at the injection site at lower dosage. When dosages were increased, patients reported flu-like symptoms and general weakness (152). At the highest end of dosages, Borodic et al. found in rabbit studies, very high dosages (12 U/kg), the BoNT will saturate the injection site, leading to diffusion and possibly predisposition for systemic toxicity (153). Furthermore, Greene et. al reported the development of drug resistance in 4.3% of torticollis patients receiving BoNT for management of muscle spasticity (154). When looking specifically at the PFMs, high dosages have been associated with increased rates of pelvic disorders such as urinary incontinence, urinary retention, worsening constipation and fecal incontinence (155, 156).

Moreover, considerable variation of treatment outcome has been reported. Abbott et al. reported significant reductions in PFM spasm in women receiving intra-PFM BoNT injections, when compared to placebo (104). Morrissey et al. examined the utility of intramuscular EMG guidance for localizing PFM overactivity, and the guidance of BoNT injections towards these overactive regions, and demonstrated significant reductions in patient reported outcomes, as well as PFM pressure at rest (155). Adelwolo et al. studied outcomes of intra-PFM BoNT injections in women with a short, tightened PFM, and found that 79.3% of patients reported improvement in pain (156). Dessie et al. studied the effects of intra-myofascial trigger point injections in the PFM using a double blind

randomized control trial, and found that BoNT injections targeted towards myofascial trigger points did not significantly improve pain symptoms associated with CPP(157). These issues may be attributed to the varied dosages and non-targeted injections (158). These complications and variable treatment efficacy have reinforced the necessity of precise and reliable injection techniques to minimize the required dose of toxin and therapy cost, while maintaining stable, optimized treatment effectiveness (158).

Currently, the clinical injection of BoNT requires the manual palpation of the pelvic muscles and/or the trigger points, defined by small 3 to 6 mm nodules within a taut band that reproduces the pain and referral pattern (98, 104, 159). Instrumented guidance employing ultrasonography or electromyography (EMG) has also been reported to improve injection efficacy; yet these studies suffered from small sample size and the absence of control injections (155, 160). Ultrasonography can recognize the muscle territory and differentiate adjacent structures; however, it does not provide any further information to identify the NMJ location, often indicated by the innervation zone (IZ). EMG can be employed to ensure injection to the IZ proximity (161), and injection guidance techniques are commonly based on intramuscular EMG recordings under voluntary contraction or electrical stimulation (162, 163). However, intramuscular EMG is limited by its invasive nature and a lack of adequate spatial coverage for proper global IZ estimation. Surface EMG is the only non-invasive method to define muscle innervation; however, it has seldom been employed to characterize the IZ distribution of pelvic floor muscles (PFMs), possibly due to the complex pelvic

anatomy, making the multi-channel surface access difficult. As BoNT acts at the NMJ, it is reasonable to assume injections directed to the NMJ or IZ will optimize its therapeutic performance. Studies have demonstrated that increasing the injection distance by 1 cm from the IZs reduced the effect of BoNT by 46% (164).

Our recent Phase 4 clinical trial assessed a novel IZ localization technique in stroke survivors, and IZ targeted BoNT injections resulted in significantly increased reductions in compound muscle action potential (CMAP) amplitude, and clinical spasticity scores. Figure 1.8 shows mean CMAP for the guided and non-guided injection groups, where the left shows the absolute CMAP amplitude before injection, at maximum efficacy (2nd visit), and after washout (3rd visit), and right shows the relative reduction in CMAP amplitude before the first and second visits.

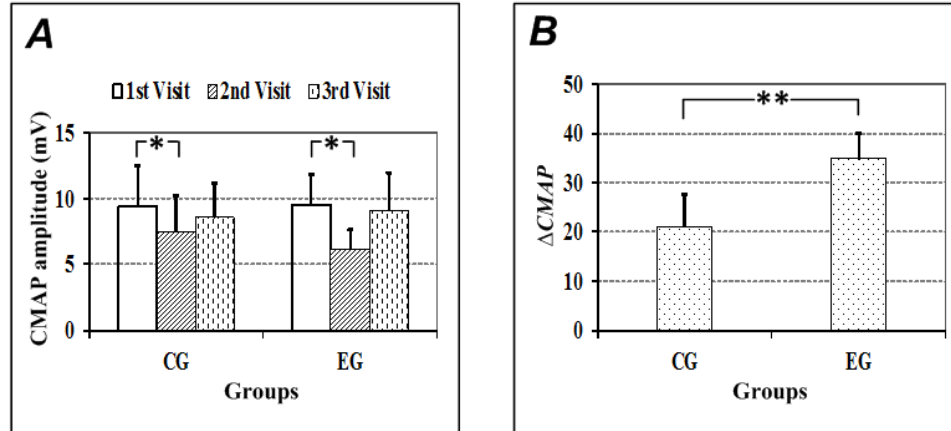


Figure 1.8 Summary of CMAP reduction after BoNT injection in the control group (CG) and guided injection group (EG).

IZ distributions, however, vary between muscles and individuals (165). Therefore, a strategy for reliable and precise IZ detection, specifically for the pelvic

muscles, is necessary for establishing targeted-injection therapies for optimal treatment.

Hypothesis and Specific Aims

Based on the research and technological gaps presented above, the topics discussed in this dissertation aim to provide novel electrophysiological tools to aid in the diagnosis and treatment of CPP, specifically those related to pelvic floor hypertonicity. The central hypothesis of this dissertation is that intravaginal high-density surface electromyography can noninvasively assess the neuromuscular activity related to PFM dysfunction using a novel intravaginal HD-sEMG probe.

The first aim of my dissertation is to develop a patient-specific PFM hypertonicity severity mapping technique to characterize the PFM hypertonicity severity pattern for each individual patient with IC/BPS from their specific HD-sEMG signals recorded from the hypertonic PFMs at rest with intra-vaginal EMG probes. This aim will test the sub-hypothesis that the pattern of the PFM hypertonicity severity mappings vary among patients to with IC/BPS, and the patient-specific phenotypes of the PFM hypertonicity severity map can be characterized from intra-vaginal HD surface EMG recordings.

The second aim of my dissertation is to develop a patient-specific PFM innervation zone (IZ) mapping technique to map the distribution of PFM IZs for each patient with IC/BPS from their specific HD surface EMG signals recorded during voluntary contractions with intra-vaginal HD surface EMG probes. This aim will test the sub-hypothesis that the locations of PFM IZs can be determined from

HD surface EMG recordings by the phase reversion of the propagation of EMG signals along muscle fibers.

Outline of Chapters

The first chapter introduces the PFMs, CPP, and diagnostic tools used to assess the PFMs. The second chapter of this dissertation discuss the efforts to use HD-sEMG to assess and localize pelvic floor hypertonicity in a cohort of women with IC/BPS, and healthy controls. Chapter 3 develops a patient specific PFM IZ mapping technique for the personalization of PFM BoNT injections in a small cohort of women with IC/BPS. Next, the ability of HD-sEMG to localize myofascial trigger points are discussed in Chapter 4. Finally, the first effort to quantify the number of functioning motor units in the puborectalis muscle is described in Chapter 5. Chapter 6 summarizes the dissertation and suggests future research applying the developed tools for 1) targeted IZ injections of Botox, and 2) personalized physical therapy.

Chapter 2 Assessment of Pelvic Floor Overactivity in Women with IC/BPS and Healthy Controls

Introduction

Pelvic floor hypertonicity (PFH), characterized by an increase in the tonic activity of a pelvic floor muscle (PFM), is present in up to 85% of patients with interstitial cystitis/bladder pain syndrome (IC/BPS) (79). The etiology of PFH is unclear but has been associated with the release of neuromuscular transmitters, peripheral and central sensitization, and myofascial pain (166). PFH may perpetuate discomfort even after the original cause of the pain is eliminated (98). Multiple studies have shown that interventions for PFM impairments including injections (167), pudendal nerve blocks (48), neuromodulation (168) and myofascial massage (142) relieve pain; however, the underlying therapeutic mechanism remains poorly understood. Consequently, it is clinically important to objectively and quantitatively assess pelvic floor dysfunction in IC/BPS to better understand the etiology of PFH and ensure complete symptom resolution. Unfortunately, little effort has been made to assess the contribution of PFM innervation to PFH, possibly because of a lack of competent tools for PFM neuromuscular assessment.

Imaging modalities such as ultrasound and MRI can detect anatomical abnormalities but cannot assess the functional status and innervation of muscles, which may be critical in the presence of pain syndromes. Pain arising from PFMs with myofascial trigger points is believed to result from an excessive release of

acetylcholine from neuromuscular junctions (NMJs) after chronic muscle hypercontraction (169). Intramuscular EMG can detect abnormally increased neuromuscular activity, but it is painful, and spatially limited to a small uptake area of the needle electrode (170). Digital palpation relies on the examiner's subjective opinion on the presence of an abnormality, and is poorly reliable (106). The clinical utility of intravaginal manometry is limited by the absence of validated reference ranges, and results can be confounded by passive muscle resistance and increased intra-abdominal pressure. Conventional intravaginal surface EMG records neuromuscular activity of the pelvic floor muscles, but current clinically available EMG probes are susceptible to cross-talk from neighboring muscles, due to a lack of channel resolution (111). A reliable method to quantify and integrate muscle activity from the entire pelvic floor, trunk, and leg muscles is necessary to non-invasively phenotype pelvic floor pain patients. Objective and quantitative measures of PFM function in IC/BPS patients are lacking, which would otherwise help elucidate the contribution of pelvic floor dysfunction to the pathophysiology of IC/BPS and how IC/BPS affects the PFM.

Electromyography (EMG) measures the electrical potential produced by motor unit firings of a contracting muscle. EMG has been used to assess the neuromuscular activity of the painful pelvic floor. Many studies have employed conventional surface and intramuscular EMG to quantify myoelectric output at rest in women with pelvic pain with varied results. Obtaining EMG from the deep PFMs presents unique challenges. Trans-perineal surface EMG is convenient to use but suffers from severe cross-talk from neighboring muscles due to the non-specificity

of the electrodes. Intra-vaginal EMG probes have been employed to directly measure neuromuscular global activity from the PFMs from two to four electrodes but lack electrode density to localize EMG activity to regions of the PFMs (111). High-density surface EMG (HD-sEMG) utilizes an array of electrodes to detect neuromuscular information from the entire PFM, allowing for a more comprehensive view of the neuromuscular activity, as shown in Figure 2.1B (133). The reliability of intravaginal high-density surface EMG has been reported to be good to excellent in healthy controls using both conventional and high-density intravaginal probes (139, 171). To our knowledge, no studies have examined repeated measures of intravaginal EMG in women with IC/BPS and pelvic floor tenderness.

To bridge this knowledge gap, and to objectively phenotype IC/BPS patients in terms of their pelvic floor function, we have recently developed a novel intravaginal high-density surface electromyography (HD-sEMG) technique to acquire abundant spatiotemporal PFM activity information via a vaginal probe covered with a 64-channel array of circular electrodes (Figure 2.1A) (133). The high spatiotemporal resolution may allow for an objective and quantitative assessment of the neuromuscular function of PFM. This study represents the first effort to

- 1) Objectively and quantitatively assess the hypertonicity severity of different PFMs,
- 2) Map their NMJs, indicated by innervation zones (IZs)

- 3) Quantify the alterations of PFMs in women with IC/BPS and compare the results to controls using the novel intravaginal HD-sEMG technique.

Materials and Methods

Women diagnosed with IC/BPS (n=15) and female healthy controls (n=15) were recruited to participate at Washington University School of Medicine between March 2018 and November 2019. Demographic information is summarized in Table 2-1. Inclusion criteria for the IC/BPS group: the participant must have a prior diagnosis of IC/BPS (AUA/SUFU Guideline) (172), with pain in the bladder region that increases with bladder filling or improves upon micturition, and PFM pain upon palpation during the exam. Controls cannot have a diagnosis of IC/BPS or PFM pain on exam. All participants must be above 18 years of age. The experimental protocol was approved by Washington University School of Medicine and University of Houston institutional review boards. Subjects were excluded if they were unable to consent, pregnant, had concurrent IC/BPS and endometriosis, had a history of vaginal surgery, cystoplasty, cystectomy, or were later found not to meet the inclusion criteria.

After giving informed consent, participants completed the IC Symptom Index, IC Problem Index, and Brief Pain Inventory questionnaires, and were then placed in the dorsal lithotomy position for a standardized pelvic exam with the physical therapy expert sequenced as follows. Exams were completed with the examiner's left hand. First, muscle length was determined (100, 173). During placement of the examining digit in the vagina, the midpoint of the most superficial aspect of the anterior of the PFM was identified. The depth of palpation was noted

for the both sides of the PFM. A shortened PFM was determined if the muscle was felt initially at the depth of the examiner's distal interphalangeal joint. Normal length was determined at a depth of palpation of the proximal interphalangeal joint and lengthened was determined at the depth of the metacarpo-phalangeal joint (100, 173). Due to hand position during the exam, palpation of the left PFM was used for analysis. Pain to palpation was determined for each of the muscle groups (obturator internus, coccygeus, anterior, and posterior levator ani muscles) and was graded on a 0-10 scale (174). Presence and location of myofascial trigger points, defined as a taut muscle band or nodule felt upon palpation, in each muscle were noted as present or absent. Active trigger points, defined as painful or causing referred pain, as well as inactive trigger points, defined as non-painful were noted. Inactive trigger points are found in a percentage of individuals who are not otherwise presenting with a pain syndrome (175). Finally, the ability of each subject to contract and lift the muscle, relax post contraction and then lower the PFM was recorded.

HD-sEMG signals were band-pass filtered between 10 Hz and 500 Hz via a second-order Butterworth filter. Mains interference was attenuated with a 60 Hz Butterworth notch filter. Differential EMG signals were obtained by circumferentially subtracting signals from neighboring channels, the resulting signals were segmented into trials based on the study paradigm described in Figure 2.2, and the root mean square (RMS) values were calculated channel-wise in half-second intervals for each resting trial and all intervals were averaged. The resting RMS ratio was calculated channel-wise for each trial by normalizing the

averaged resting RMS values to the peak RMS reached during the corresponding MVC trial. An increased average RMS ratio would then represent increased resting EMG amplitude, increased spatial region of resting EMG, or decreased peak amplitude during MVC, or a combination of each factor. Signal processing was accomplished in MATLAB R2019b (Mathworks, Natick, USA).

Filtered HD-sEMG signals acquired during rest and MVC were decomposed into motor unit action potentials (MUAP) using the k-means clustering convolution kernel compensation algorithm (176). The IZ of each motor unit (MU), which indicates the NMJ, can be identified from a bipolar map of the decomposed 64-channel MUAPs by visualizing the phase reversion of the propagating signals along muscle fibers(133, 137), as illustrated in Figure 1.7, and shown in Figure 2.1.

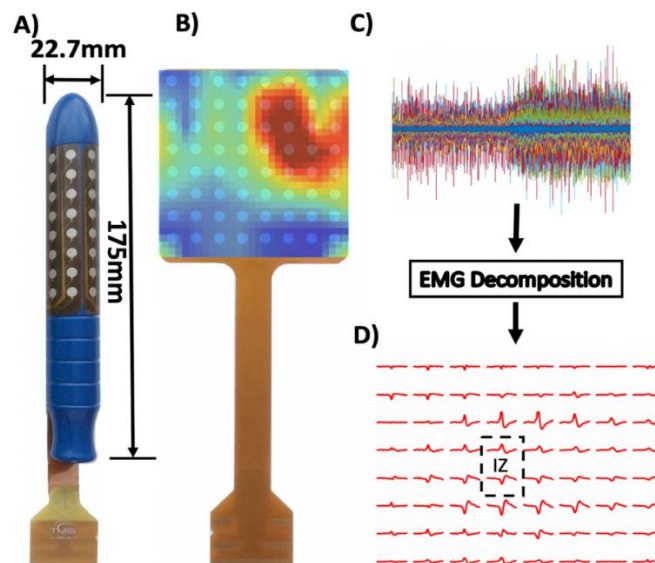


Figure 2.1 Summary figure of intravaginal HD-sEMG collection. A) HD-sEMG probe, B) 64-channel electrode grid with RMS mapping overlaid, C) Raw

differential EMG signals for all 64 channels, D) 64-channel MUAP template after decomposition and spike-triggered averaging

HD-sEMG acquisition commenced after the first pelvic assessment utilizing the 64-channel intravaginal HD-sEMG probe (Figure 2.1). The intravaginal HD-sEMG probe was designed at UH with a plastic vaginal probe covered by an 8x8 surface electrode grid and manufactured by TMSi (TMSi, Enschede, Netherlands) as shown in Figure 2.1B. The HD-sEMG probe was lubricated with conductive gel and introduced into the vaginal space by the study urologist. Care was taken to standardize probe orientation between subjects by aligning the electrode gap along the probe's dorsal surface. A ground electrode was attached to the wrist, and an adhesive reference electrode was attached to the thigh. HD-sEMG signals were recorded at 2048Hz with a Refa-136 amplifier (TMSi, Enschede, Netherlands), shown in Figure 2.1C. A 60-second resting period was allowed for electrode-mucosa contact stabilization. Once stabilization was assured, an additional 10-second resting period was allowed (resting trial 1) followed by a 10-second maximum voluntary contraction (MVC). The resting and MVC trials were repeated alternately to give a total of 3 trials for each in Session 1, as shown in Figure 2.2. The probe was removed, followed by a 10-minute break. The process was then repeated in Session 2.

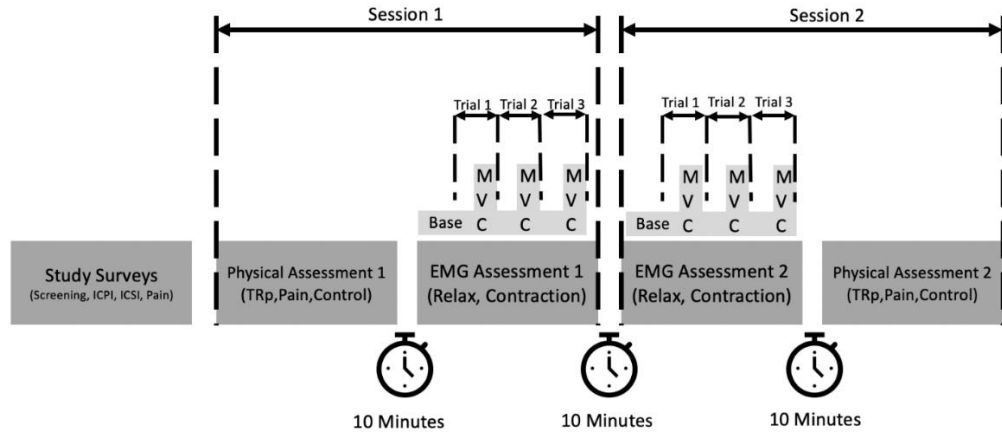


Figure 2.2 Detailed outline of testing protocol. Figure reproduced from (177)

Reliability

Reliability for continuous variables (RMS Ratio, Contraction RMS, Rest RMS, Peak RMS) were calculated with via ICC(2,1), a two-way random effects, absolute agreement model as defined in Bartko et. al (178), and is expressed as (1)

$$\frac{MS_p - MS_e}{MS_p + (k-1)MS_e + \frac{k}{n}(MS_s - MS_e)} \quad (1)$$

Where n is the number of subjects, k is number of sessions, MS_e is the mean squared error, MS_p is the mean square of persons, MS_s is the mean square of sessions.

Statistical analysis

Statistical analysis was carried out using SciPy(179) and Statsmodels packages for Python 3. Due to the low sample size of this study, categorical variables were compared via a Fisher Exact test. Distributional form was determined via a Shapiro-Wilk test, and appropriate statistical tests were used when distributions were found to be non-normal. Continuous variables were

compared via two-tailed Student's t-tests, and Mann-Whitney U-tests (where noted). Linear relationships were assessed with Ordinary Least Squares regression and Spearman's Rho. Receiver operating characteristic curves (ROC) were constructed using the roc_curve() function in the scikit-learn Python package, area under the ROC curve was calculated in the same package using the roc_auc_score() function. Statistical significance was accepted at $p < 0.05$. Error bars represent 95% confidence interval.

Results

Pelvic floor exam

As expected, women with IC/BPS reported higher IC Symptom Index, IC Problem Index, and numeric ratings of pain compared to controls (Student's t-test, $p < 0.001$, see Table 2-1).

Table 2-1 Summarized patient demographics and pelvic exam findings. ($p < 0.05$, ** $p < 0.01$) †one control and one IC/BPS did not respond to the query about current medications.*

	IC/BPS (n=15)	Control (n=15)
Patient Demographics		
Mean±SD (Range)		
Age	39.9±15.1 (20-65.2)	39.7±14.2 (23.1-70.9)
BMI	27.5±7.4 (17.6-46.2)	31.5±11.3 (19.2-62.7)
IC Symptom Index**	9.93±4.36 (4-18)	1.93±2.37 (0-7)
IC Problem Index**	8.4±3.6 (3-15)	0.33±1.04 (0-4)
Numeric rating of Pain (0-10)**	5.93±2.4 (1-9)	0.0±0.0 (0-0)
Pelvic Exam Findings		

Table 2-1 Continued

% with Shortened PFM**	80% (12/15)	13.3% (2/15)
% Able to Lower PFM	40% (6/15)	73.3% (11/15)
% Able to Relax PFM	80% (12/15)	100% (15/15)
% with myofascial trigger points**	86.7% (13/15)	13.3% (2/15)
Current Treatment †		
No Treatment	21.4% (3/14)	92.8% (13/14)
InterStim	7.1% (1/14)	0% (0/14)
Pentosan Polysulfate	7.1% (1/14)	0% (0/14)
Phenazopyridine	21.4% (3/14)	0% (0/14)
Natural Supplements	14.2% (2/14)	0% (0/14)
NSAIDs	14.2% (2/14)	7.1% (1/14)
Opioids	14.2% (2/14)	0% (0/14)
Topical Analgesic	7.1% (1/14)	0% (0/14)
Antihistamine	14.2% (2/14)	0% (0/14)
Heat/Cold Therapy	14.2% (2/14)	0% (0/14)
Bladder Relaxant	7.1% (1/14)	0% (0/14)
Antibiotics	7.1% (1/14)	0% (0/14)

All women with IC/BPS reported pelvic floor tenderness in at least 1 muscle upon palpation, while no controls reported tenderness. Myofascial trigger points were present in thirteen of fifteen women with IC/BPS (86.7%) and two of fifteen controls (13.3%) (Fisher's Exact test, $p < 0.01$).

PFM control was assessed during the digital pelvic exam. Twelve of fifteen women with IC/BPS (80%) demonstrated shortened PFM alignment at rest

compared to two of fifteen controls (13.3%) (Fisher’s exact test, $p<0.01$). Twelve (80%) IC/BPS and all (100%) controls could relax the PFM (Fisher’s exact test, $p=0.224$). Six (40%) IC/BPS and eleven (73.3%) controls could lower the PFM (Fisher’s exact test, $p=0.139$).

Table 2-2 Summary of EMG Findings for all features †Mann-Whitney U test used for non-normally distributed distributions.

Session 1		μ	σ	Median	IQR	Shapiro - Wilk p-value	Comparison p-value†
RMS Ratio	Control	0.099	0.041	0.104	[0.074-0.118]	0.935	0.002*
	IC/BPS	0.155	0.048	0.167	[0.119-0.184]	0.471	
Mean Resting RMS	Control	6.531	4.311	5.41	[4.24-6.24]	<1e-5	0.034*
	IC/BPS	8.338	4.901	6.7	[5.84-8.65]	0.004	
Mean Contraction RMS	Control	15.954	7.388	15.02	[10.46-18.28]	0.069	0.901
	IC/BPS	14.668	5.954	13.09	[11.13-15.77]	0.007	
Peak Contraction RMS	Control	70.717	32.168	69.01	[44.89-81.06]	0.176	0.263
	IC/BPS	60.021	35.936	45.51	[36.94-76.37]	0.004	
Session 2		μ	σ	Median	IQR	Shapiro - Wilk p	Comparison p-value†
RMS Ratio	Control	0.109	0.049	0.107	[0.074-0.138]	0.967	0.099
	IC/BPS	0.14	0.05	0.131	[0.109-0.164]	0.829	
Mean Resting RMS	Control	6.092	4.478	4.6	[3.80-6.21]	<0.001	0.074
	IC/BPS	7.365	4.14	6.3	[5.03-7.89]	0.002	
Mean Contraction RMS	Control	14.439	7.434	12.08	[9.76-15.40]	0.004	0.361
	IC/BPS	15.57	6.938	14.51	[11.47-15.86]	0.023	
Peak Contraction RMS	Control	71.005	53.2	54.37	[44.46-65.77]	0.002	0.431
	IC/BPS	55.649	32.102	47.29	[43.11-57.57]	<0.001	

Intravaginal High definition surface EMG

HD-sEMG signals were successfully acquired from all participants. In session 1, the average intensity of the resting RMS ratio mappings were found to be significantly higher in the IC/BPS group compared to controls (Mean±STD: 0.155 ± 0.048 vs. 0.099 ± 0.041 , $p=0.0019$ via Student’s t-test), suggesting that women in the IC/BPS group had either increased resting EMG, spatially broad

region of increased resting EMG, decreased peak amplitude during MVC, or a combination of these factors, as shown in Figure 2.4. The spatial intensity of the resting RMS ratios for all participants in session 1 is presented in Figure 2.5.

Average resting RMS amplitude was found to be significantly increased in the IC/BPS group (Median(IQR): 6.71 (5.84-8.65) vs. 5.42(4.24-6.24) $p = 0.0344$, via Mann-Whitney U-Test), as shown in Figure 2.3 yet no significant difference was observed in average contraction RMS amplitude (13.10(11.14-15.77) vs. 15.02(10.46-18.28) $p = 0.91$), via Mann-Whitney U-test).

Resting RMS amplitude was compared between groups using mixed ANOVA, and post-hoc analysis via pairwise Mann Whitney U-tests and Wilcoxon signed rank tests. Resting RMS amplitude was found to be significantly increased in the IC/BPS group ($p=0.034$, via Mann Whitney U-test) during session 1, but not during session 2 ($p=0.074$, via Mann Whitney U-test) when compared to the control group. A significant decrease was present between session 1 or 2 for the IC/BPS group, via Wilcoxon signed rank test, but not for controls ($p=0.148$ for Control, $p=0.007$ for IC/BPS, via Wilcoxon signed rank test). There was no significant difference between session 1 and 2 for the average intensity of RMS ratio mappings in either group.

No significant differences between diagnostic group, or repeated measures were found for mean RMS during contraction, or peak RMS reached during contraction via mixed ANOVA and post-hoc comparison with pairwise Mann Whitney U-tests and Wilcoxon signed rank tests.

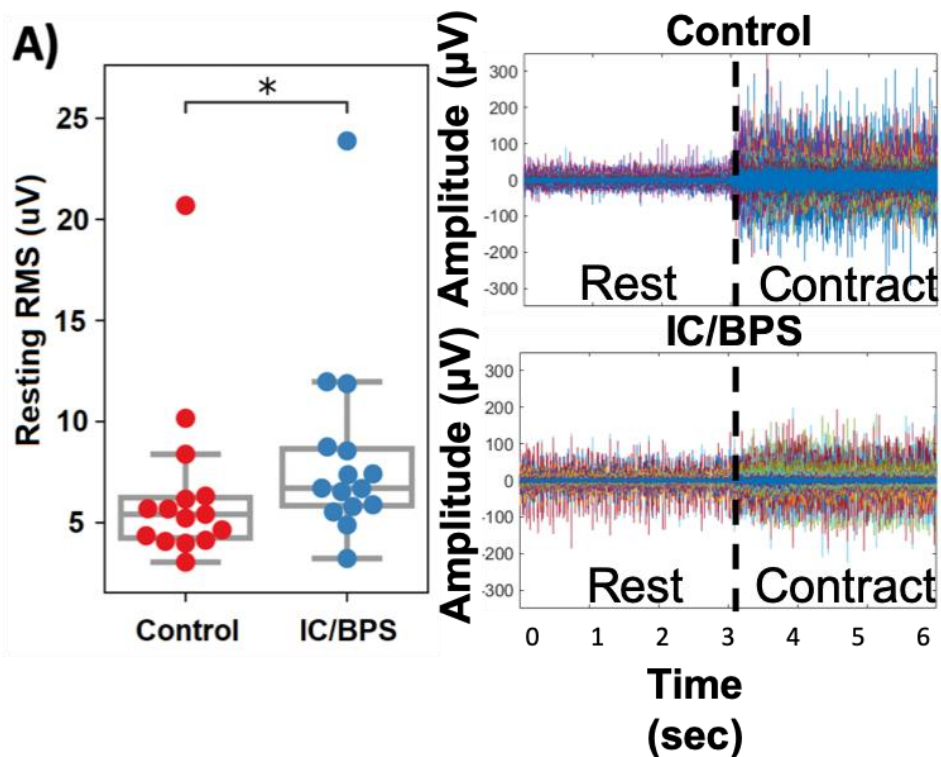


Figure 2.3 Comparison of resting RMS amplitude for both groups, and filtered EMG traces from one control and IC/BPS subject.

Reliability was assessed with ICC(2,1), and results for each diagnostic group are shown in Table 2-3.

Using the guidelines proposed by Portney et. al (180), mean resting RMS showed excellent reliability for the IC/BPS and Control groups (ICC=0.94,0.97, respectively, ICC(2,1)), good reliability for contraction RMS (ICC=0.77,0.84, ICC(2,1)), and fair to good reliability for RMS Ratios (ICC=0.67,0.77, ICC(2,1)).

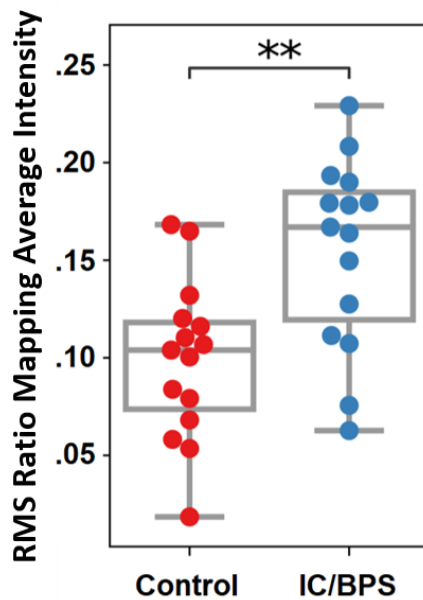


Figure 2.4 Comparison of RMS ratio spatial map intensities between Control and IC/BPS groups.

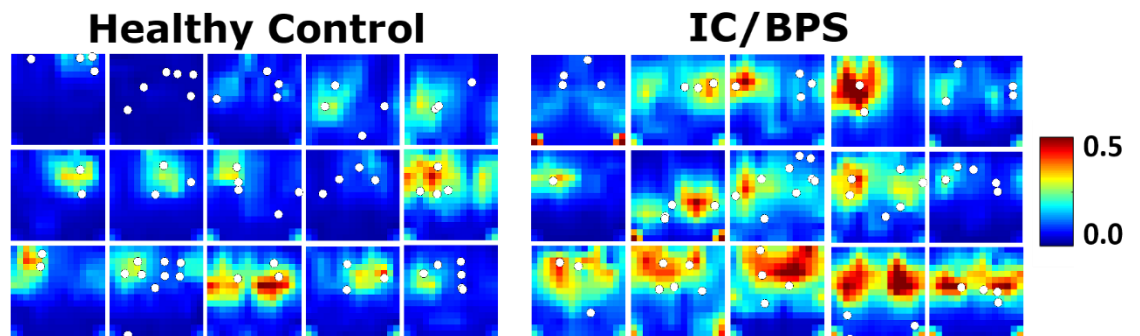


Figure 2.5 64-channel resting RMS ratio mappings for all subjects. Note: 64-channel mappings were interpolated by a factor of 2, white dots mark the IZ location. Figure reproduced from (177)

Table 2.2 and Figure 2.6 summarizes EMG features for both diagnostic groups. EMG RMS at rest was found to be 6.53 ± 4.31 and 8.34 ± 4.90 for the control and IC/BPS groups, respectively for session 1, 6.09 ± 4.47 and 7.36 ± 4.14 for session 2. During MVC, RMS on average increased to 15.95 ± 7.38 and 14.67 ± 5.95 for the control and IC/BPS groups for session 1, 14.44 ± 7.43 and 15.57 ± 6.94 during

session 2. Peak RMS reached for the control and IC/BPS groups were 70.72 ± 32.16 and 60.02 ± 35.94 , respectively during session 1, 71.01 ± 53.19 and 55.65 ± 32.10 during session 2.

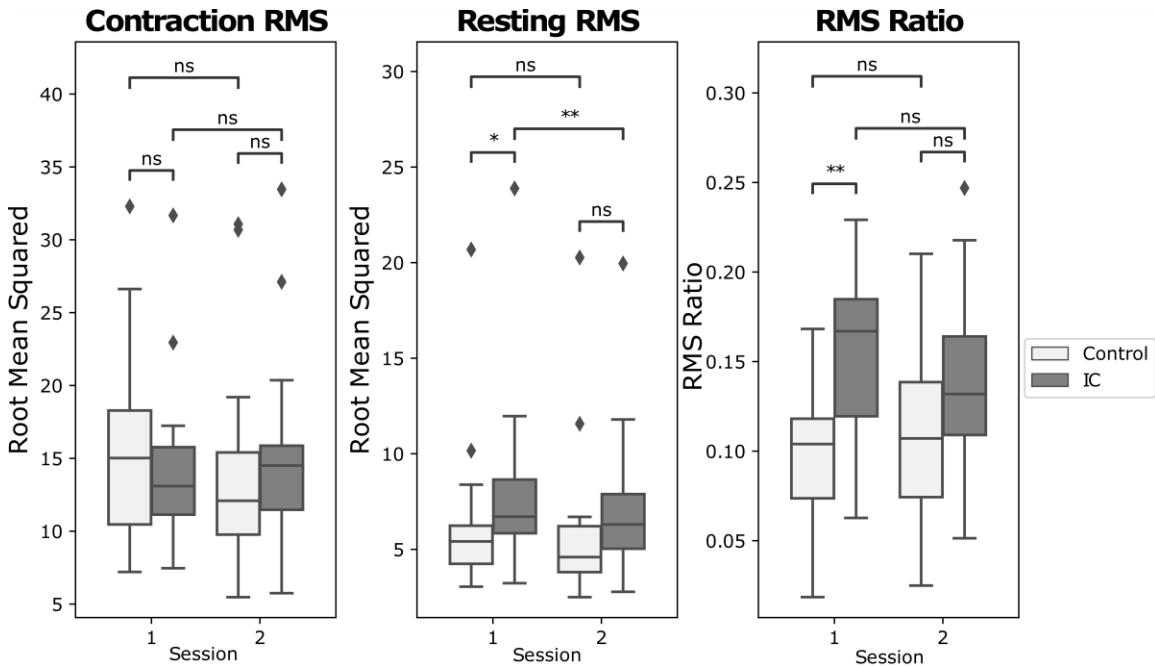


Figure 2.6 Resting and Contraction EMG features for diagnostic groups during both sessions. RMS ratio represents the average intensity of each subjects RMS ratio mapping.

As shown in Figure 2.7, resting RMS ratio was compared between PFM evaluation groups. Women from both diagnosis groups with normal, shortened, or lengthened PFMs were grouped, and a significantly increased resting RMS ratio mapping intensity was found in women with shortened PFMs (0.155 ± 0.046 vs. 0.107 ± 0.040 , $p=0.0058$, *Student's t-test*). There was no difference in resting RMS ratio mapping intensity between women who could not lower their PFM and those who could (0.134 ± 0.049 vs 0.121 ± 0.054 , $p>0.5$, *Student's t-test*). Women who could not relax their PFM showed significantly increased resting RMS ratio map

intensity compared to women who could (0.188 ± 0.017 vs 0.120 ± 0.050 , $p=0.028$, Student's *t*-test).

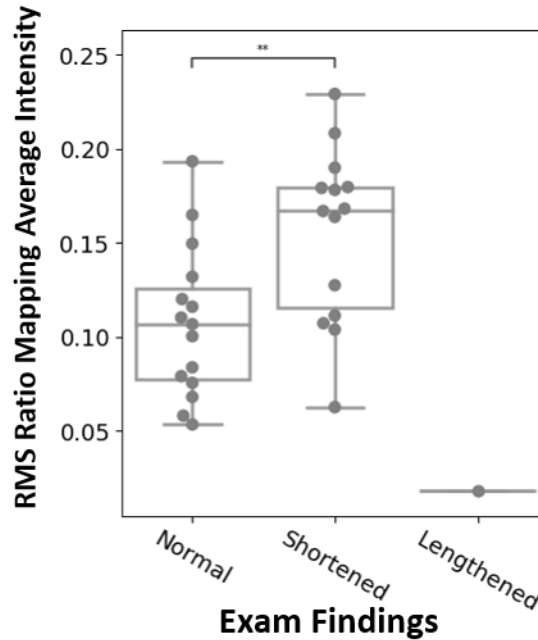


Figure 2.7 Effect of resting PFM alignment on RMS ratios

The relationship between resting RMS ratio and self-reported clinical scores including IC Symptom Index, IC Problem Index, and 0-10 pain scores, were assessed as shown in Figure 2.8. A significant linear relationship was found between the resting RMS ratio and the separate self-reported clinical scores ($r_s=0.523$, $p=0.003$), ($r_s=0.521$, $p=0.003$), ($r_s=0.60$, $p<0.001$), in all cases.

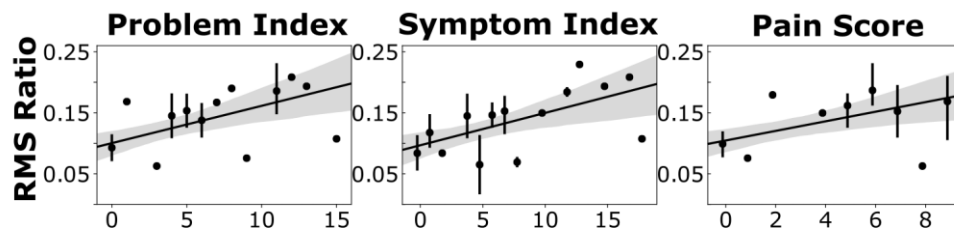


Figure 2.8 Linear relationships between average RMS ratio map intensity and Symptom, Problem, and Pain Scores

MUAP Firing rates were averaged for each subject during rest and contraction, and the channel where the largest monopolar MUAP amplitude was located for each MUAP. The resting RMS ratio was then logged for this corresponding channel. The average MUAP for each subject during rest and contraction was plotted against the resting sub-channel RMS ratio, as shown in Figure 2.9. A significant negative relationship ($p < 0.03$) was found between both features in IC/BPS, but not healthy controls.

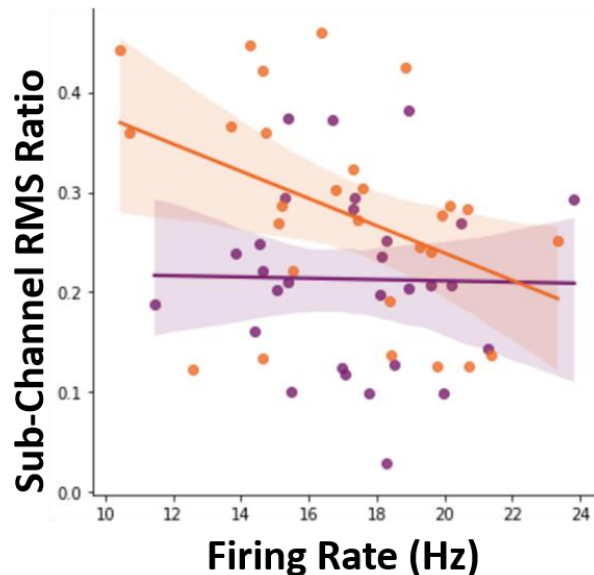


Figure 2.9 Relationship between sub-channel RMS ratio and average MUAP firing rate in women with IC/BPS (orange) and healthy controls (magenta).

A receiver operating characteristic curve (ROC curve) was constructed to assess the sensitivity and specificity of each feature for both sessions, as shown in Figure 2.10. Area under the ROC curve (AUC) depicts the ability of each feature to correctly classify patients into diagnostic groups based on a specific EMG feature. The RMS ratio showed good classification performance in session 1 (AUC=0.81), but poor performance in session 2 (AUC=0.67). Resting RMS

amplitudes showed acceptable performance in session 1 (AUC=0.73), but not in session 2 (AUC=0.69). Average contraction RMS and Peak RMS reached during contraction showed poor performance in both sessions (AUC = 0.51,0.60 and AUC=0.52,0.59, respectively).

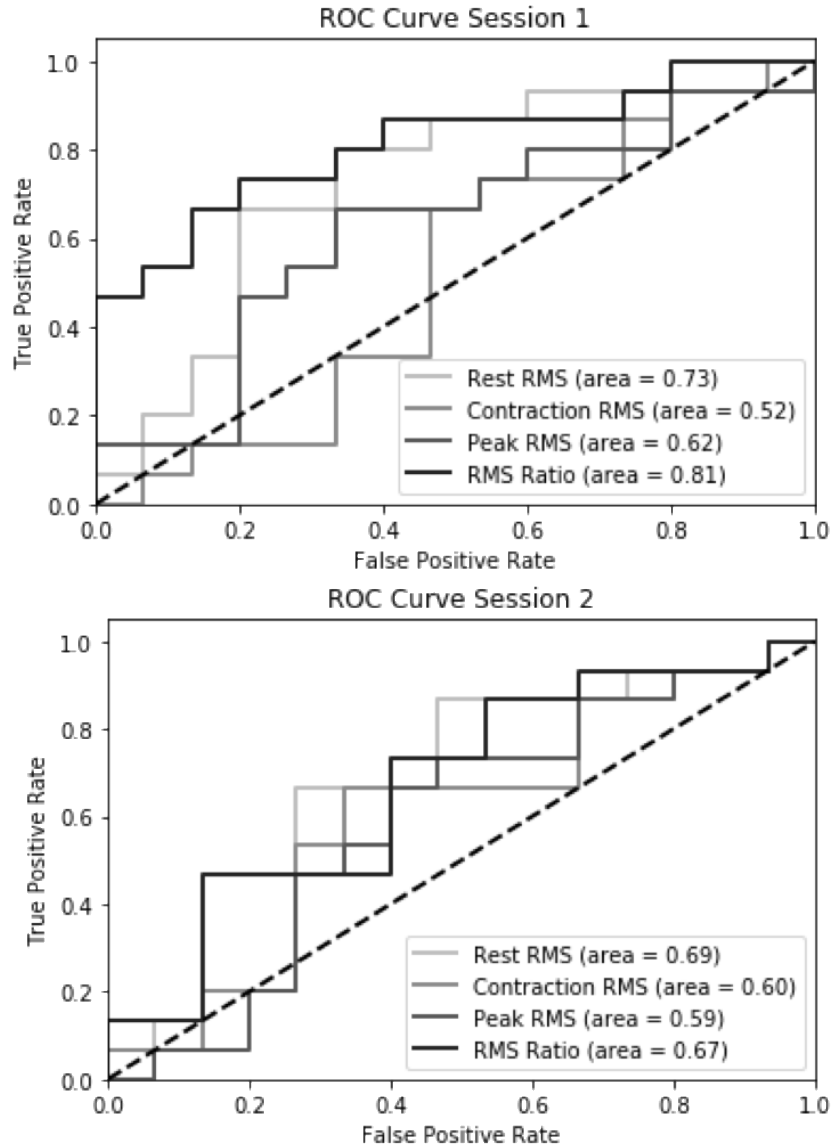


Figure 2.10 Receiver operating characteristic curves for all EMG features in Session 1 (above) and Session 2 (below).

Table 2-3 Summary of reliability coefficients for each feature.

EMG FINDINGS		
		ICC
RMS ratio	Control	0.77
	IC/BPS	0.67
Resting RMS	Control	0.97
	IC/BPS	0.94
Contraction RMS	Control	0.84
	IC/BPS	0.77
Peak contraction RMS	Control	0.71
	IC/BPS	0.89
		ICC
Number of banding and nodules	Control	0.65
	IC/BPS	0.59
Cumulative pain upon palpation	Control	N/A
	IC/BPS	0.89

Discussion

This study is the first to objectively and quantitatively assess the neuromuscular function of the PFMs in IC/BPS using an intravaginal HD-sEMG technique.

Pelvic floor hypertonicity (PFH) presents in up to 85% of patients with interstitial cystitis/bladder pain syndrome (IC/BPS) (79), up to 90% of patients with vulvodynia (80), and a percentage of endometriosis patients (82). In this project, we focused on PFM hypertonicity in women with IC/BPS by having objective HD-sEMG and subjective pelvic floor exam data. Future studies may aim to assess these findings in a wider variety of pelvic floor pain patients.

Conventional surface EMG has been used to quantify myoelectric output at rest in women with pelvic pain with varied observations (85). Loving *et al.* used a standard resolution surface EMG probe to demonstrate that women with IC/BPS presented with significantly increased EMG activity at rest when compared to controls (113). In contrast, Engman *et al.* were unable to find a significant difference in resting sEMG between women with vestibulodynia and controls (114). In this study, we showed that women with IC/BPS had significantly increased EMG at rest when normalized against peak RMS amplitude. The variable results in past studies can be possibly explained by signal crosstalk and/or specificity challenges due to insufficient spatiotemporal information in conventional EMG.

In this study, we show that women with IC/BPS demonstrate significantly increased EMG at rest, and when normalized with respect to peak RMS amplitude during the first session. Resting RMS ratio was the most suitable feature to discern IC/BPS from controls in Session 1, and an AUC of 0.81 was observed via ROC curve analysis. This suggests that the RMS ratio is a better feature to aid the diagnosis of hypertonic pelvic floor disorders in women with IC/BPS when compared to absolute resting RMS (AUC = 0.73), contraction RMS (AUC = 0.52), or peak RMS (AUC = 0.62).

Interestingly, we also notice a slight decrease in the average intensity of the RMS ratio mappings during the second session. Concordantly we observed a significant decrease in the average resting RMS in IC/BPS patients from session 1 to 2. The diagnostic ability of the average intensity of the RMS ratio maps as indicated by AUC values, as well as the average RMS during rest decreased from

session 1 to 2. It is possible that these decreases represent a mild therapeutic effect of three sustained PFM MVCs or are an effect of anticipatory contraction in response to catastrophizing the initial probe insertion in the IC/BPS group. In the second case, it may be that the probe insertion was found to not aggravate the PFM myalgia, so the patients do not contract their PFMs in anticipation of pain. This finding is similar to that reported by Naess and Bo, who found that only three MVCs were required to significantly reduce resting PFM EMG activity in thirty-five women with provoked vestibulodynia, but not in healthy controls (109). A follow up study with a larger sample, possible with concurrent real time imaging of the PFMs will help determine the origin of this slight decrease in PFM EMG.

Many studies have explored the reliability of various pelvic floor muscle evaluation techniques. Kavvadias et al. showed that, although the reliability digital pelvic exam based measures of contractile strength was good to excellent in the posterior levator ani, piriformis, and presence of contraction, palpation was poorly reliable in discerning PFM tone (ICC=0.10-0.13) (181). This finding suggests that a more reliable technique is necessary for the objective measurement of PFM tone. Manometry has been shown to be a reliable measure of PFM tone (concordance correlation coefficient =0.95) (182), but only allows for the presence or absence of abnormal tone to be detected, and gives no information about the origin of an abnormality. On the other hand, HD-sEMG has the unique ability to allow for the decomposition of EMG signals into individual motor unit components, allowing for information regarding the neural drive and innervation to the PFMs to be studied (118, 133, 177). Auchincloss and McLean compared the reliability of two

conventional intravaginal EMG probes (two channel) and showed fair to high between trial reliability (0.58-0.98), but poor between-day reliability (ICC=0.08-0.84). Van der Zalm et. al used a high-density (24 channel) EMG probe to assess the PFMs of women and men with and without various pelvic ailments and showed fair-to- excellent reliability (ICC=0.53-0.91), however it wasn't clear if their study design included removal and reinsertion of the probe between recording sessions. We saw similarly high reliability using our 64-channel HD-sEMG probe (ICC=0.67-0.97), with probe removal and reinsertion. Reliability was reduced in the IC/BPS group, likely due to the intrinsic muscle changes present in the IC/BPS population.

Resting EMG RMS showed the highest reliability in both sessions in Control and IC/BPS (ICC=0.97, 0.94 respectively), and was slightly higher than the contraction-based features, or normalized EMG, for both groups. This may be attributed to the lack of a volitional component to the resting measurements, rather, the patient simply rests while EMG is measured from the PFMs. This finding contrasts with Grape et. al, who found higher test-retest reliability measures in peak contraction amplitude and average contraction amplitude compared to baseline measurements (171).

Our study was limited by the lack of a between-day comparison. All test-retest measurements were made after removing the probes for 10 minutes, which can account for differences in electrode-mucosa contact, but not environmental or hormonal factors on PFM EMG activity. Future studies should examine the between-day reliability of intra-vaginal HD-sEMG, to see if the additional channel

density improves upon the poor between-day reliability reported by Auchincloss and McLean (183).

A recent comprehensive review by Keshwani and McClean investigated commercially available intravaginal sEMG probes, and found that most of these probes only offer one to four electrodes, leaving them susceptible to cross-talk (111). The intravaginal HD-sEMG probe employed in this study offered a novel solution to this issue by offering 64 evenly spaced electrodes in an 8 by 8 grid, allowing for a true differential setup which can localize increased muscle activity at rest, and provide high-resolution and patient-specific spatial mappings, as shown in Figure 2.5, which conventional surface EMG probes cannot produce. We observed unique hypertonicity distribution patterns in women with IC/BPS, indicating that hypertonic EMG signals originating from different PFMs are patient-specific, while the mapping results from healthy controls mostly showed uniformly low intensity across channels, indicating an absence of PFM hypertonicity.

Previous MRI studies have revealed significantly shorter levator muscles at rest in women with IC/BPS compared to healthy controls (107). Our study also observed that significantly higher percentage of women (80% vs 13.3%) with IC/BPS had shortened PFMs at rest. Women with shortened PFM at rest demonstrated significantly higher resting EMG ratios, as shown in Figure 2.7. This finding suggests that the shortened PFM is partially “active” in origin, and it requires further effort to elucidate the contributions of “active” and “passive” hypertonicity components in women with IC/BPS. Furthermore, three women could not relax their PFMs, and demonstrated significantly higher resting RMS ratios,

suggesting sensitivity to non-relaxing PFM, however this finding should be confirmed with a larger sample size.

A strong linear relationship between IC Symptom Index, IC Problem Index, patient-reported pain and average intensity of the RMS ratio mappings was found, as shown in Figure 2.8. This finding suggests that patients with more severe pain and urinary symptoms also had PFMs with the highest resting tone, reduced contraction capacity, or a combination of both. Hypertonicity may contribute to the urgency symptoms captured by the IC symptom index. In the case of a hypertonic pelvic floor, intravesical pressures will be increased, producing an increased urge to void.

A significant negative linear relationship was present between MUAP Firing Rate during rest and contraction, and sub-channel RMS ratios in women with IC/BPS, but not controls. It has been shown that average MUAP Firing Rates are decreased in fatigued muscles (184), when taken in combination with the RMS ratio findings, it is possible that the state of hypercontraction resulting in increased average RMS ratios in a given muscle leads towards muscle fatigue, manifesting as reduced MUAP firing rates. Alternatively, the muscle pain itself may be driving the reduction in MUAP firings detected near hypertonic zones. Tucker et al. demonstrated that experimentally induced muscle pain can significantly reduce the MUAP firing rates of newly recruited motor units (185). Taken in this context, it may be possible that lower firing motor units are recruited in patients with severe symptoms potentially to adapt to the pain and limit further aggravation of the painful/hyperactive muscle.

Intravaginal HD-sEMG has the unique ability to localize IZs in the PFM. We were successful in localizing IZs in all subjects tested, and a unique IZ distribution was present across all subjects, as shown in Figure 2.5. OnabotulinumtoxinA (BoNT, Botox) is receiving growing interest in relieving PFH and myofascial pain (145). However, considerable outcome variation has been reported (155, 156). Critical to maximizing the efficacy of BoNT is injection to the IZ (164). The presented technique can be potentially applied to improve the treatment efficacy, and reduce the treatment variation and cost, with an IZ-targeted PFM BoNT injection.

Muscle length changes are a critical component of the cluster of impairments associated with myofascial pain. The method for determining length of the PFM has not been well studied. Thus, one limitation of the current study is that length of the entire PFM was assessed based on a clinical test of the depth of palpation of the PFM. Future studies may aim to compare intravaginal HD-sEMG findings with an imaging-based examination of the length of the PFM to better identify morphological changes that occur due to hypertonicity.

An important factor not captured by the present study is the lack of parity information from the present cohort. The pelvic floor muscles and innervating nerves undergo significant morphological and ischemic distress during childbirth, which likely insults the otherwise healthy innervation of the PFM. Future studies may employ intravaginal HD-sEMG to study changes in the innervation to the PFM.

The location of muscle spasm or hypertonicity was not assessed for each individual pelvic floor muscle component, largely because studies have shown measures of muscle tone using digital palpation to have poor reliability (181), likely because these measures are purely subjective. Instead, we used a less subjective measure based on the alignment of the pelvic floor muscles with predefined markers along the length of the examiner's finger (100).

We made muscle level comparisons between the presence of trigger points in each muscle and EMG signatures present near those muscles and found little to no agreement between EMG and the trigger point exam. It is likely that surface EMG is unable to detect trigger points, or that trigger points are electrically silent (83). We do not believe this is a significant limitation, as myofascial trigger point targeted Botox injections were shown to be no better than saline in a recent RCT (157). Botox acts at the neuromuscular junction, and the innervation zone is where neuromuscular junctions are most densely distributed. Theoretically innervation zone targeted (rather than trigger point targeted) injections should improve treatment outcomes in the pelvic floor muscles, which has yet to be studied. Furthermore, the location of trigger points and innervation zones were found to differ in the trapezius muscle (186), as well as the current manuscript, so the therapeutic effect of trigger point injections may be improved on by instead targeting the innervation zone.

Finally, although not explored in this manuscript, potential applications of this technology are varied. By providing pelvic muscle IZ distribution information and suppressing pelvic muscle crosstalk, IZ imaging technique may provide critical

information for phenotyping axonal or central neurodegeneration, monitoring neuromuscular remodeling, and guiding the precision injection of BoNT for optimal treatment outcome. Further extensions of this technique can provide depth information based on the morphology of the decomposed MUAPs,(187) and upon construction of an anatomical model of the pelvis, a more localized estimate of the IZ location can be elucidated. (130, 188, 189)

Conclusions

The presented HD-sEMG technique provides a method to non-invasively quantify and localize electrical output from the PFMs and found that women with IC/BPS had significantly higher normalized EMG at rest compared to controls. The HD-sEMG technique allows for spatial mappings depicting the electrical output from the muscle at rest, unveiling unique hypertonicity distribution patterns in women with IC/BPS. Furthermore, the high spatiotemporal resolution provided by the 64-channel electrode grid allows for the decomposition of EMG signals, permitting the localization of IZs.

Chapter 3 Assessing Pelvic Floor overactivity in Women with IC/BPS to guide BoNT injection

Introduction

Pelvic floor hypertonicity (PFH) is characterized by an increase in resting pelvic floor muscle tone resulting from either increased contractile activity (neurogenic hypertonicity) and/or passive stiffness (non-neurogenic hypertonicity) (83). PFH presents in up to 87% of women with interstitial cystitis or bladder pain syndrome (IC/BPS) (79). The etiology of PFH in IC/BPS patients is postulated to be that silent afferents within the bladder become activated and this results in a constant barrage of noxious stimuli that can then result in wind-up of the dorsal horn. This leads to the development of an abnormal viceromuscular reflex that triggers muscular hyperalgesia and allodynia. These neuromuscular changes result in hypertonicity (166). PFH is often identified through digital pelvic palpation, which largely depends on the examiner's subjective perception of an abnormality, and therefore results can vary between examiners. Currently, there lacks a proper objective technique that is clinically accepted for diagnosing PFH.

Furthermore, approximately 30% of patients fail conservative therapy (190) and require more aggressive treatment. Botulinum neurotoxin (BoNT) has recently received growing interest in the management of pelvic pain secondary to PFH,(156) with a well-evidenced therapeutic benefit (110). BoNT relaxes the pelvic floor muscles (PFM) and nociceptive signaling by blocking the release of acetylcholine at neuromuscular junctions. The injection location modulates the efficacy of BoNT. The therapeutic effect of BoNT is suppressed by approximately

half when injected 1 cm away from the innervation zone (IZ) (164). The IZ represents the location where the alpha-motor neuron forms synapses with target muscle fibers and neuromuscular junctions are distributed densely (186). To reach an ideal therapeutic effect, some practitioners may inject a higher dosage of BoNT; however, BoNT may induce dose-dependent side effects such as urinary and fecal incontinence.

The current clinical standard for BoNT injection involves the manual digital palpation of a hypertonic muscle, followed by an injection towards the palpating finger (191). This injection protocol, like the assessment of PFH itself, is subjective and inaccurate, and may not provide a consistent therapeutic effect due to non-targeted injections.

There is no existing technique that can guide the injection of BoNT to the IZ in the PFMs. Endovaginal ultrasound provides anatomical information but does not specify myoelectric information. A 4D ultrasound technique was recently developed to provide visual feedback to the operator, greatly improving the precision and repeatability of the injection (108). Ultrasound, however, is unable to localize the IZ or determine which muscle is overactive, permitting potential improvements to the injection process. Intramuscular electromyography (iEMG) has been employed to localize hypertonicity for BoNT injection; (155) however, iEMG is limited by its invasive nature, poor spatial resolution, and is incapable of characterizing the IZ distribution. A competent and objective tool is necessary for the reliable diagnosis and treatment of PFH.

High-density surface electromyography (HD-sEMG) allows for the non-invasive quantification of global muscle activity, as opposed to local activity assessed by iEMG. The motor unit action potential (MUAP) initiates at the IZ and propagates along muscle fibers innervated by that motor unit in opposing directions. HD-sEMG has proven to be successful in capturing this signal propagation, and IZs can be determined by observing the phase reversal using differential signal analysis or amplification (133).

In this study, the first effort to assess neurogenic PFH via an intra-vaginal HD-sEMG probe in women with IC/BPS and localize the IZ nearest to the hypertonic region to allow for the targeted injection of BoNT using HD-sEMG signal decomposition is presented. This will provide a reliable tool for the characterization of pelvic floor dysfunction in IC/BPS patients, and possibly improve the efficacy of treatment by directing the injection of BoNT to the IZs of the hypertonic region.

Materials and Methods

Participants

Female subjects (n=7, mean age 44±13 yr., range (27-68)) with a prior diagnosis of IC/BPS were recruited via a voluntary sample from the Urology Clinic at Baylor College of Medicine in Houston, Texas. Inclusion criteria were females between the ages of 18 and 70, a diagnosis of IC/BPS, and an unpleasant sensation in the PFM in the absence of infection or an immediately identifiable cause. Subjects were excluded from participation if they were pregnant, breast feeding or were later found not to meet inclusion criteria. All subjects were informed of any associated risks and gave written informed consent. The institutional review

boards of the Baylor College of Medicine and the University of Houston approved the experimental protocol.

Study Protocol

Urinary and pain symptoms associated with IC/BPS was assessed with the interstitial cystitis symptom and problem index. Pain symptoms were assessed with the McGill pain questionnaire, pain quality assessment scale, and Numeric Pain Rating Scale. Participants were asked mark their baseline pain on a 0-10 numeric pain rating scale (0 is no pain, 10 is worst possible pain). Subjects were asked to consider their pain in the preceding week. Subjects were then situated in the dorsal lithotomy position, and digital pelvic exams were administered by the study urologist. Pain upon palpating the left and right sides of the obturator internus, pubococcygeus, and puborectalis was graded on a visual analog scale. Muscle tone was assessed binarily and noted as normal (-) or hypertonic (+).

A 64-channel (8x8) high-density surface electromyography (HD-sEMG) probe (length 175 mm, diameter 22.7 mm, inter-electrode distance 8.5 mm) as shown in Figure 3.2 was lubricated with conductive gel and introduced into the vaginal space. Figure 3.2 shows A) Recording electrode with 64-channel mapping overlaid and intra-vaginal HDsEMG probe; B) 64-channel mappings for each subject in the non-hypertonicity group (Subjects 1-3, 5-6) generated from session 1; C) 64-channel mappings from each subject in the hypertonicity group (subjects 4 and 7) from session 1. Red indicates increased muscle RMS amplitude at that location. Mappings in Figure 3.2 were interpolated by a factor of 4 for display purposes.

A fully soaked Velcro strap was affixed to the wrist as the ground, and a single reference electrode was placed to the subject's thigh. Subjects were instructed to relax, and resting EMG activity was simultaneously recorded for 60 seconds. All HD-sEMG recordings were sampled at 2048 Hz with a Refa 136-channel amplifier (TMSi, Enschede, Netherlands). Signal quality was verified in real-time via a display monitor. To evaluate the repeatability of HD-sEMG recording, a 5-10-minute rest period was given, and then same recording protocol was repeated by the same examiner to give session 2. Consistent probe depth and orientation was achieved by orienting the company trademark in the anterior direction. Care was taken by the physician to keep the probe in a fixed location, with no longitudinal movement or rotation of the probe during testing to maintain a fixed spatial reference by holding the probe during the recording session.

Signal processing

Resting HD-sEMG signals were bandpass filtered between 10 and 500 Hz with a second-order Butterworth bandpass filter. Time periods with movement artifacts or poor electrode contact were segmented out from further analysis. Power line contamination was removed with a 60 Hz second-order Butterworth notch filter. Root mean squared amplitude (RMS) was calculated for each channel in 0.5 second intervals. The resulting resting RMS values for each 0.5 second interval were then averaged to give a 64-channel RMS mapping. The average resting RMS of the 16 channels with the highest RMS amplitude were averaged and termed the “hypertonicity index” (HI), and were compared between groups,

and sessions, as shown in Figure 3.3(C). All offline processing was performed post-exam in MATLAB R2018 (Mathworks, Natick, MA).

Monopolar HD-sEMG recordings during rest were decomposed into constitutive MUAP spike trains using a blind source separation approach, as described in previous publications (127). The 64-channel MUAP profiles were then constructed using by averaging the HD-sEMG signals at the time of each decomposed MUAP's firing. The bipolar mappings of each 64-channel MUAP profile was obtained by subtracting the signal of each channel from that of its neighboring channel in a clockwise direction around the probe.

IZs were visually identified by observing the phase reversal from the bipolar mappings (130, 186, 192), as shown in Figure 3.1 and 3.2. The clock position in axial view, depth from the introitus, and MUAP propagation length were noted and visualized for each motor unit, as shown in Figures 3.4 and 3.5. MUAP propagation length was determined by the most distant channels with visible MUAP waveforms ($> 10 \mu\text{V}$) from the defined IZ.

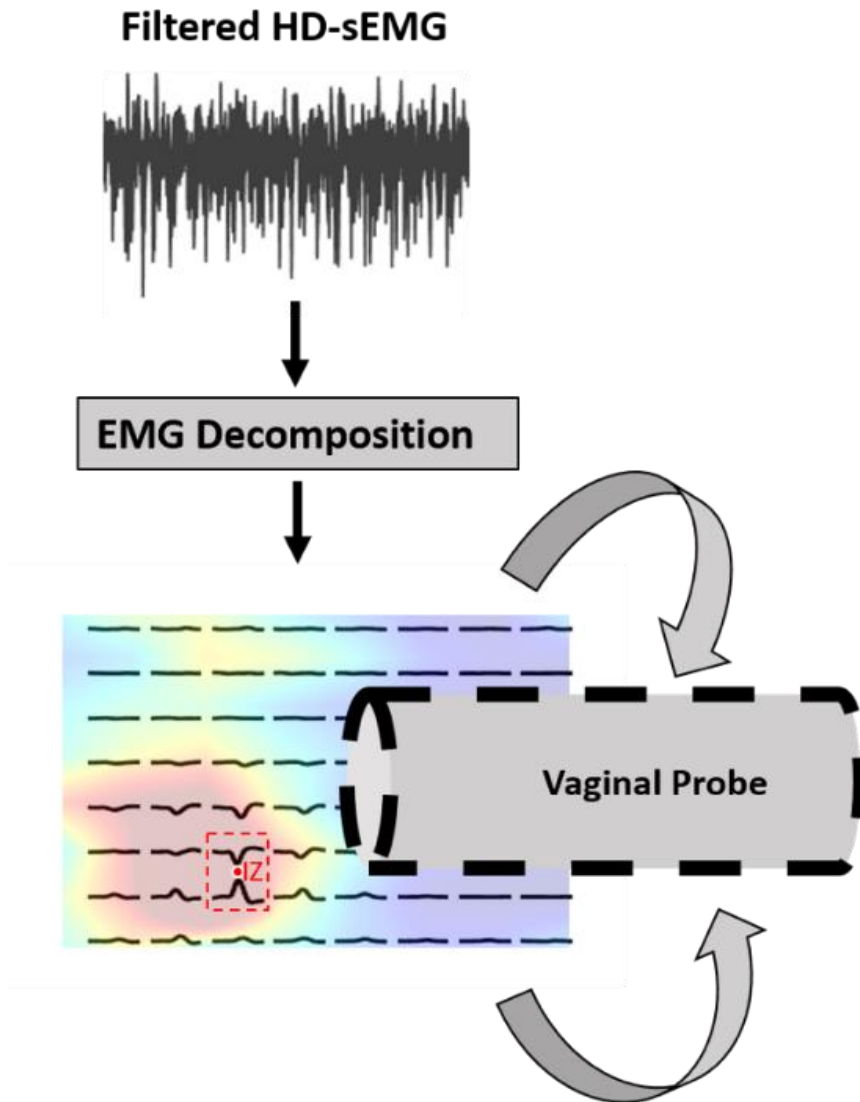


Figure 3.1 Top) Filtered HD-sEMG signals from one subject, Bottom) 64-channel motor unit action potential mapping overlaid on hypertonicity mapping result for one subject. Red box marks the IZ location. Figure reproduced from (193)

Statistical analysis

Subjects with confirmed PFH were grouped to the hypertonicity group and the remaining subjects were grouped to the non-hypertonicity group. The repeatability of the HD-sEMG assessment was evaluated by the correlation coefficient (CC) between the hypertonicity indexes in two consecutive sessions.

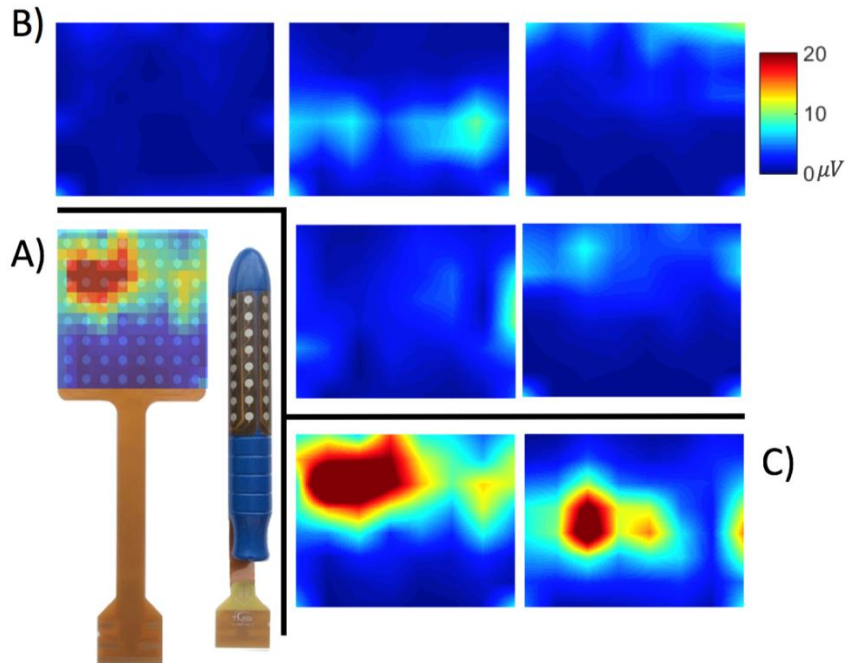


Figure 3.2 Summary of hypertonicity mapping results. Figure reproduced from (193)

Results

The average interstitial cystitis symptom and problem scores were 10 ± 1.8 (range: 8-14) and 9.4 ± 2.2 (7-13), respectively. The average self-reported baseline numerical pelvic pain score of pain felt in the preceding week for all subjects was 5.6 ± 1.7 (3-8). All seven subjects described their pain as “intense”, “cramping”, and reported a sensation of “heat” in the PFM muscles, as described in the pain quality assessment scale. 3 of the 7 subjects reported numbness or the sensation of electrical shocks in the PFM. PFM pain and muscle hypertonicity upon palpitation was assessed all subjects, and summarized in Table I. An averaged cumulative pain score, defined as the sum of pain felt in each muscle when palpated, of 16.3 ± 6.9 (7-27) was found. PFH was observed in two of the seven subjects. Average cumulative pain upon palpation for the women without PFH was 14.6 ± 7.4

and 20.5 ± 2.5 for women with PFH. The average baseline pain scores were 4.8 ± 1.3 and 7.5 ± 0.5 , for women without and with PFH, respectively.

Table 3-1: Digital VAS pain scores and hypertonicity assessment (+/-) for all subjects upon palpitation.

Sub	NPS	ROI	LOI	RPC	LPC	RPR	LPR	CP	HI
1	7	3 (-)	3 (-)	2 (-)	2 (-)	0 (-)	0 (-)	10	3.0 ± 1.0
2	5	5 (-)	9 (-)	6 (-)	7 (-)	0 (-)	0 (-)	27	5.8 ± 0.8
3	4	0 (-)	0 (-)	2 (-)	3 (-)	1 (-)	4 (-)	10	5.6 ± 0.3
4	8	3 (-)	2 (-)	6 (+)	5 (+)	4 (-)	3 (+)	23	15.1 ± 3.4
5	3	0 (-)	1 (-)	2 (-)	2 (-)	1 (-)	1 (-)	7	3.6 ± 1.8
6	5	0 (-)	4 (-)	4 (-)	5 (-)	3 (-)	3 (-)	19	4.7 ± 1.2
7	7	3 (-)	3 (-)	4 (-)	2 (-)	3 (+)	3 (-)	18	10.2 ± 3.2

HD-sEMG signals were successfully acquired from all subjects, and 64-channel high-density RMS mappings were calculated for the subjects without hypertonicity Figure 3.2(B) and with hypertonicity Figure 3.2(C). Figure 3.3 summarizes the findings for all subjects, where A) shows a bar chart displaying hypertonicity index for both sessions; B) Comparison of hypertonicity index between sessions; C) Bar-plot for both groups and sessions. A marked difference between groups was found in sessions 1 and 2. An apparent reduction in hypertonicity index was found between sessions 1 and 2 for the hypertonicity group, but not the non-hypertonic group.

Average hypertonicity indexes of 4.5 ± 1.2 (3.0-5.7) and 12.6 ± 3.5 (10.2-15.1) were obtained for subjects without hypertonicity and with hypertonicity respectively, as shown in Table 1 and Figure 3.3(A). Subjects with PFH demonstrated a higher hypertonicity index in both sessions 1 and 2. The proposed

hypertonicity index was repeatable with a correlation coefficient between sessions 1 and 2 of 0.95, as shown in Figure 3.3(B). The hypertonicity index represents the myoelectric output of the muscles nearest the 16 channels with the highest amplitude. In both subjects with hypertonicity, the RMS mapping “hotspot” appeared on the ipsilateral side with respect to the hypertonic muscle found on the digital muscle tone exam. Hypertonicity index was not associated with increased pelvic floor muscle pain upon palpation in each muscle. Subjects with PFH, however, reported higher average baseline pain (4.8 ± 1.3 for the non-hypertonicity group, 7.5 ± 0.5 for the hypertonicity group), and slightly higher cumulative pain upon palpation (14.6 ± 7.4 for the non-hypertonicity group and 20.5 ± 2.5 for the hypertonicity group) .

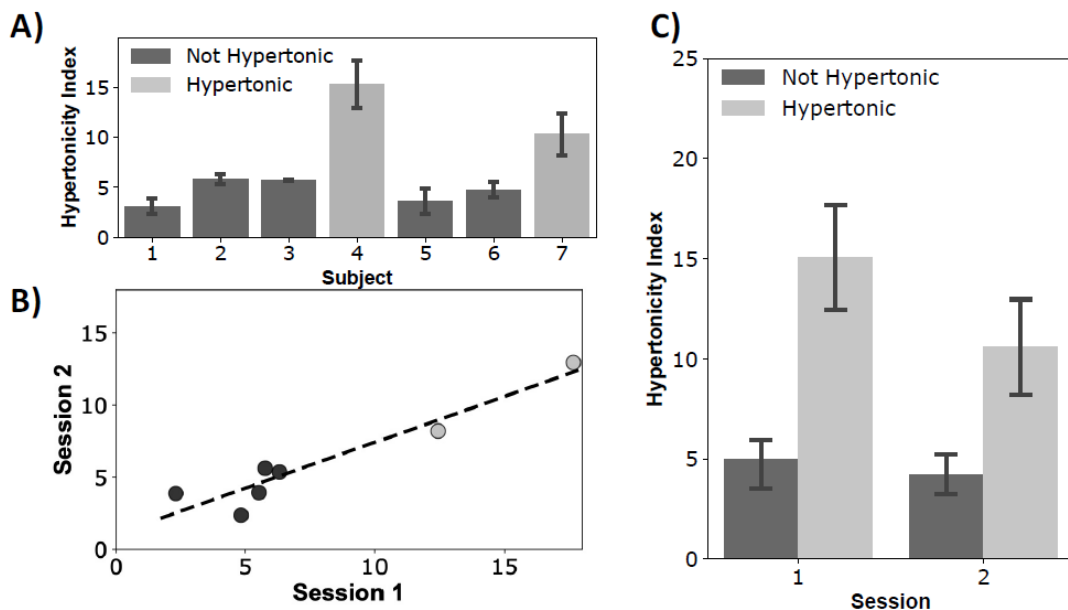


Figure 3.3 Summary of hypertonicity index and repeatability results. Figure reproduced from (193)

IZ locations were successfully localized from the decomposed HD-sEMG signals, as exemplified in Figures 3.1, and 3.4. The IZ detection technique is summarized in Figure 3.4, where IZ mapping in both expanded HD-sEMG grid view (A)&(B) and axial view (C)&(D) in IC/BPS subjects with PFH. Red dots mark IZ locations of hypertonic muscle; Blue dots mark IZ locations of non-hypertonic muscle. Values in axial view (C)&(D) indicate the corresponding IZ depth in cm from vaginal introitus. The black trace marks the propagation of the motor unit action potential. The IZ depth and orientation measures are made based on the vaginal HD-sEMG electrode configuration in (E) and (F). In subject 7, hypertonic zones were found near the right puborectalis (LPC) and right puborectalis (LPR), agreeing with our digital palpation findings. An axial depiction of decomposed motor units innervating the PFM was derived, as shown in Figures 3.4(C) and 3.4(D).

The linear relationship between either baseline pain, or cumulative pain, and average hypertonicity index was assessed using Spearman correlation as shown in Figure 3.5, and strong correlation was found for baseline pain and hypertonicity index ($R=0.67$). Cumulative pain upon palpation and hypertonicity index were found to be moderately correlated ($R=0.44$).

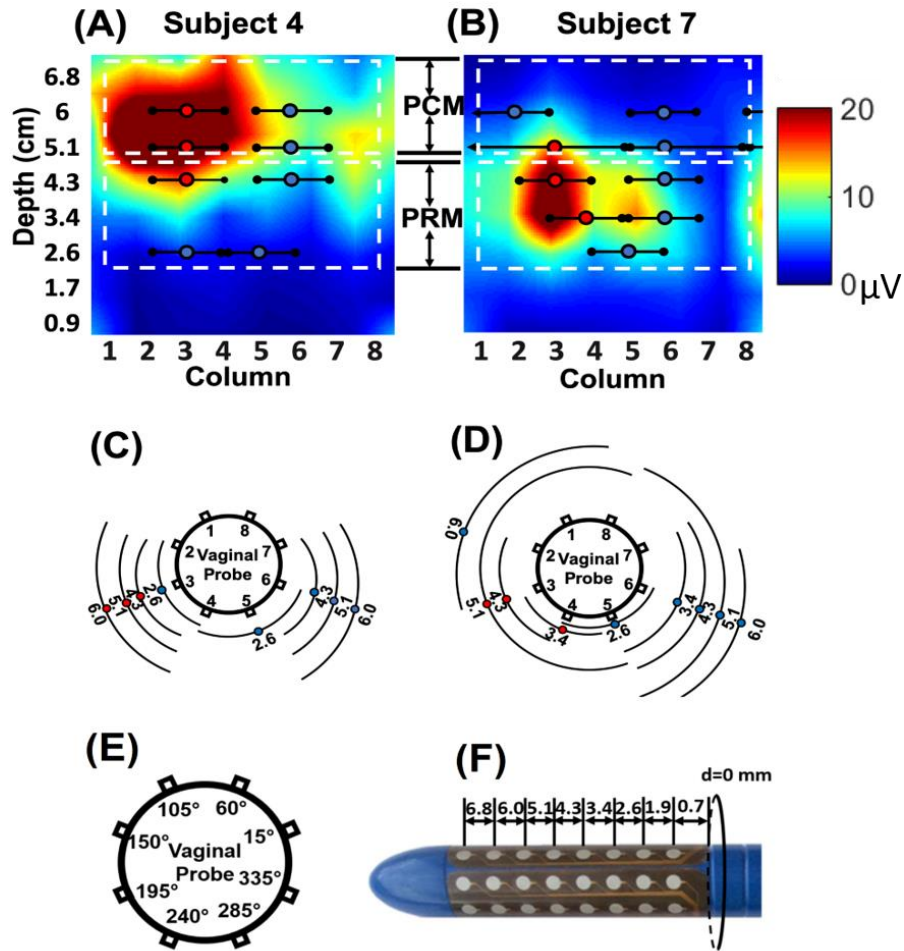


Figure 3.4 Summary of proposed IZ injection guidance technique. Figure reproduced from (193)

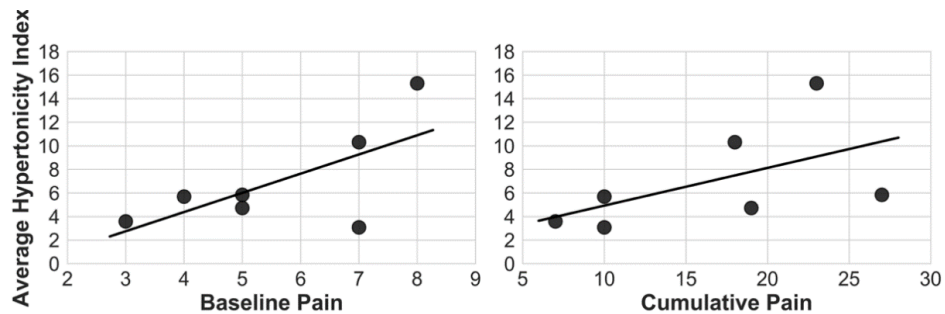


Figure 3.5 Left) Relationship between average hypertonicity index and baseline pain. Right) Relationship between average hypertonicity index and cumulative pain upon palpation. Figure reproduced from (193)

Discussion

This study presents the first effort to assess PFH and extract innervation information in female IC/BPS subjects using intra-vaginal HD-sEMG. The presented intra-vaginal probe can capture abundant myoelectric information from muscles located in the proximity of the vaginal wall, including puborectalis, pubococcygeus, and bulbospongiosus. In subjects with confirmed hypertonicity, the RMS mapping “hotspot” appeared on the ipsilateral side with respect to the digital muscle tone exam. A marked difference in the RMS mapping and defined hypertonicity index acquired at rest was found between IC/BPS subjects with and without hypertonicity, as shown in Figure 3.2(B) and Figure 3.2(C). An increase in hypertonicity index was found in the hypertonic group, when compared to the non-hypertonic group, as shown in Figure 3.3(C), indicating that the proposed HD-sEMG based technique can detect hypertonic muscles from resting EMG signals. A decrease in hypertonic index was found between sessions 1 and 2 for the hypertonic group, but not the non-hypertonic group. Our findings in the non-hypertonic group were similar to those reported in healthy subjects by Grape et al, with a mean hypertonicity index of 4.5 ± 1.2 being comparable to their resting EMG amplitude findings of 5.0 ± 1.1 μV in 17 healthy women (171).

Furthermore, the hypertonic zones visualized from the mapping match well with the hypertonic muscles defined by the digital pelvic exams. Our results suggest that HD-sEMG can be a promising tool to enhance the clinical diagnosis of PFH, including the localization of hypertonic muscles via RMS mapping and the objective estimation of severity.

A relationship between hypertonicity index and individual muscle pain scores upon palpation was not observed. This observation suggests that severe pelvic pain can exist in the absence of a myofascial component. This may be explained by the etiology of PFH, where noxious stimuli (pain) results in upregulation of the dorsal horn, causing central and peripheral sensitization. Viscerosomatic convergence can then lead to painful muscles, causing muscle spasms, instability and hyper contraction. In this case, the pain may exist without the associated muscle over activity. It should be mentioned that the patients with hypertonicity rated their baseline pelvic pain to be much higher than the patients with normal muscle tone, as shown in Figure 3.5. Furthermore, previous studies have estimated the prevalence of PFH in ICBPS patients to be as high as 87% (79). The low rate (28.5%) of PFH we observed is likely explained by the low sample size of our study, and care should be taken not to extrapolate this prevalence to the general population.

IZs are commonly identified using an evenly-spaced linear electrode array that is placed along the muscle fiber direction (192). Beretta Piccoli et al. employed visual signal inspection for signal phase inversion to localize IZs in 43 superficial muscles, and reported excellent or good results in 76% of the muscles using this method (192). Enck et al. were the first to assess external anal sphincter IZ distributions by employing visual identification of signal phase inversion in 52 healthy adults (137). If IZs are unable to be discerned directly from the surface interference pattern, a valid alternative is a decomposition based IZ detection scheme. Our previous work has demonstrated the feasibility of characterizing IZ

distribution in the pelvic muscles of healthy participants using pelvic HD-sEMG. Peng et al. employed HD-sEMG decomposition to generate an IZ distribution of the PFMs of healthy young women (133). Dias et al. applied a similar technique to study the IZ distribution of the EAS in young and elderly healthy women (118). HD-sEMG decomposition was performed in the present study to suppress signal crosstalk and generate a clean mapping for the estimation, and we successfully generated personalized IZ mappings for each subject. As shown in Figure 2.4(A), we were able to localize an IZ near the hypertonic zone for both subjects with hypertonicity from the decomposed surface interference pattern EMG data, suggesting the feasibility of an HD-sEMG guided injection protocol directed to the IZ. A marked inter-subject variation of the IZ maps was observed, as shown in Figures 3.4 (C) and (D), which coincides with previous observations of varied IZ distribution in limb muscles (136). This finding stresses the importance of a personalized injection strategy to maximize BoNT efficiency.

Future studies may explore whether the derived axial IZ mappings shown in Figure 3.4(C) and (D) can be used to optimize the treatment efficacy of BoNT for alleviating PFH. The efficacy of BoNT therapy can likely be potentiated by endplate targeted injections achieved by specifying the muscle(s) responsible for PFH, as well as the offending IZ. Lapatki *et al.* reported a 46% reduction in efficacy when BoNT was injected 1 cm away from the IZ, stressing the importance of an accurate injection guidance (164), however it has yet to be determined if these results can be generalized to the PFMs. Several studies have explored guided BoNT injections by employing ultrasound techniques to localize spastic muscles in

both limb and face muscles (194, 195). Ultrasound, however, is unable to quantify neuromuscular activity and is best used as a source of real-time feedback during BoNT injection, rather than a tool to localize the source of muscle spasticity. Morrissey *et al.* utilized intramuscular EMG (iEMG) to specify the muscular origins of PFH in women, and reported significant improvements in pain scores upon BoNT injection (155). However, iEMG does not provide an estimation of the global muscle activity of the PFM; rather, it is limited to the small uptake area of the intramuscular sensor. This limitation necessitates multiple needle insertions to assess the activity of the entire pelvic floor.

It is important to contrast myofascial trigger points and IZs. Myofascial trigger points are identified by a palpable band or nodule in the muscle that refer pain and elicit a twitch response when touched. A recent trial of BoNT injections into palpable myofascial trigger points in women with myofascial pain did not result in a significant improvement in myofascial pain when compared to placebo (157). However, the accuracy of manual needle placement has been proved surprisingly low, and in most cases more than half (57%) injections fell outside the target muscle (196). In addition, as BoNT acts at the neuromuscular junction, which is electromyographically indicated by the IZ, injection towards the IZs in hypertonic patients may produce better therapeutic outcomes than trigger point injections. In fact, the location of myofascial trigger points and IZ's have been shown to not overlap. Barbero *et al.* used a IZ detection technique to compare the locations of IZs to myofascial trigger point locations in the upper trapezius muscle, and found that trigger points were proximally located to the IZ, but did not overlap (spaced

10.4mm apart on average) (186). This finding suggests that BoNT injections targeted near trigger points may not reach the IZ.

In addition to personalizing injection therapies, the proposed hypertonicity mapping technique may help guide myofascial and/or Theile's massage towards hypertonic muscles. Weiss et. al used conventional surface EMG to show that women with myofascial pain demonstrated high resting EMG pre-treatment via manual therapy when compared to post-treatment sessions (190). We believe that augmenting the myofascial massage procedure presented in Weiss et al. to include patient-specific HD-sEMG guidance towards hypertonic muscles, rather than simply as a measure of global muscle activity may improve treatment outcomes.

Although HD-sEMG can reliably capture activities from multiple muscles, it is unlikely that vaginal EMG is successful in detecting signals from the obturator internus, or piriformis. Source imaging studies need to be completed to verify this assumption. Another limitation of this study is the lack of an objective measure of PFM tone, such as vaginal manometry. Therefore, we can only use the subjective findings of the digital exam to validate the proposed technique. However, our results suggest that the hypertonicity index can stand as an objective measure of PFH severity and may provide new perspectives in the understanding and diagnosis of PFH. Follow-up studies with a larger sample of hypertonic subjects are necessary to confirm these findings. The location of the probe electrodes with respect to the surrounding anatomy needs to be confirmed for our probe in a future study. Magnetic resonance images have been published with a similarly

dimensioned intravaginal probe in place, and it was able to clearly capture signals from both sides of the puborectalis, pubococcygeus, and iliococcygeus muscles (139).

Finally, a concurrent EMG-anatomical imaging study should take place to assess potential confounding factors introduced by anticipatory contraction of the PFM's prior to pelvic exam or intravaginal HD-sEMG. Following a fear-avoidance model of chronic pain, pelvic floor muscle contraction may occur in anticipation of a painful trigger, in this case, vaginal penetration with the EMG probe. This vaginismus would be predominantly exhibited in the IC/BPS group, but not the Control group. We believe this sequela would present in women with a history of sexual abuse or pelvic trauma, however, this information was not collected at the time of data acquisition. Even in the case of vaginismus driving the heightened intensity of RMS ratio mappings, the opportunities for treatment are the same. IZs could potentially be injected with BoNT to transiently relieve the vaginismus, allowing for the patient to undergo desensitization for potential triggers, ending the vicious pain cycle.

Conclusion

HD-sEMG provides novel perspectives for assessing the neuromuscular health of the PFM's. We have found that this intra-vaginal HD-sEMG probe was successful in assessing PFH in women with IC/BPS. The innervation information of the PFM, whether hypertonic or not, can be extracted to provide a personalized IZ mapping that may greatly benefit the clinical management of PFH.

Chapter 4 Assessment of PFM myofascial trigger points using HD-sEMG

Introduction

Myofascial trigger points (TrPs) are defined as a bundle of dense, hypercontracted muscle sarcomeres that can be palpated as a small localized nodule or band inside a muscle. TrPs can be latent, in that they do not refer pain when palpated, or active, in which they do refer pain upon palpation. There are multiple proposed etiologies surrounding the observance of TrPs. The first proposed theory is the “energy crisis theory (197).” In short, the energy crisis theory proposes that muscle trauma leads to the release of Calcium from the sarcoplasmic reticulum, causing muscle fiber shortening and the emergence of a tight band of muscle (197). This constant fiber contraction leads to a positive feedback loop in which metabolic activity is increased, and blood flow is decreased, leading to ischemia and an energy crisis (197). This energy crisis theory proposes that the TrPs are endogenous contractions, and electrically silent.

A later theory, referred to as the “expanded trigger point hypothesis” proposes that the physiology underlying TrPs centers around the equilibrium of Acetylcholine (ACh) in the postsynaptic membrane (89). Normally, an equilibrium exists facilitating the removal of ACh from Acetylcholine receptors (AChR)s via acetylcholinesterase (89). When injury occurs whether due to trauma or muscle overuse, muscle fibers begin to degenerate and release cytokines leading to increased muscle pain. Furthermore, the ischemic conditions lower the pH of the motor endplate, facilitating the release of calcitonin gene-related peptide. This

release results in a cascade of events in which Ach equilibrium is lost, and persistent muscle fiber contraction emerges, as is felt as a nodule or taut band of fibers upon palpation (89). The newly formed TrP then forms a positive feedback loop in which more cytokines are released, and more ischemia occurs, perpetuating the existence of the TrP.

Hubbard and Berkoff first measured spontaneous electrical activity via needle EMG from TrPs located inside the trapezius muscle, and remarked a significant increase in baseline needle EMG amplitude inside the active TrPs of tension headache and fibromyalgia sufferers (198). However, it is not clear if these observed spontaneous spikes were the result of mechanical abrasion of the endplate zone by the insertion of the needle electrode. Furthermore, Thomas and Shankar reported reduced blood flow inside the TrP, potentially suggesting an ischemic etiology of pain in active TrPs (199). The same group reported hyperechogenic in the regions near a TrP using 2D and 3D ultrasound (200). These studies demonstrated that the Trp is a densely contracted band of muscle that can be seen on ultrasound imaging.

To date, objective measures of TrPs in the PFM patients are lacking, which would otherwise help elucidate the contribution of pelvic floor dysfunctions to the pathophysiology of IC/BPS and provide objective characteristics of IC/BPS. Although previous studies suggest that TPs IZs, are well-defined distinct regions in the trapezius muscle (186), and injections at the IZ location showed a better treatment outcome than TrPs (164), the relation between TPs and IZs in IC/BPS patients with hypertonic PFM remain poorly investigated, leading to non-targeted

injection sites and dose. Recent advances in non-invasive high-density (HD) surface electromyography (EMG) technique have demonstrated itself as a promising tool to overcome these limitations. Clinical evidence has shown that spontaneous electrical activity is a characteristic behavior of TP, which can be captured by surface EMG electrode at rest (16), providing the basis to the detection of TPs based on objective measures

Materials and Methods

Materials and Methods were as described in Chapter 2 “Assessment of Pelvic Floor Overactivity in Women with IC/BPS and Healthy Controls”. The presence of palpable hypercontracted bands and nodules in the PFMs were noted during the pelvic exam. Cohens κ was calculated as

$$K = \frac{P_o - P_e}{1 - p_e}. \quad (2)$$

Where P_o is the observed agreement, P_e is agreement by chance. Cohens κ was chosen as it is a robust measure of agreement that accounts for agreement due to random guessing (201). Any κ value below 0.20 represents that the measures demonstrate no agreement (201). RMS Ratio and RMS ratio mappings were calculated as described in Chapter 2. Location of PFM TrPs felt during were overlaid on RMS ratio mappings, and agreement between the RMS ratio mapping and TrP location was accepted if the RMS ratio of at least one channel near the muscle of interest was greater than 40%, and a myofascial TrP was present in the muscle corresponding to that channel.

Results and Statistical Analysis

As shown in Figure 4.1 average intensity of RMS ratio mappings for women with CPP and TrPs was 0.156 ± 0.055 , and 0.139 ± 0.055 for those without TrPs. The average intensity of RMS ratio mappings for healthy controls with latent TrPs was 0.098 ± 0.042 , and 0.103 ± 0.034 for those without latent TrPs. Means were compared with Student's independent t-tests. There was no significant difference between women in either group with or without TrPs ($p > 0.5$, Student's t-test).

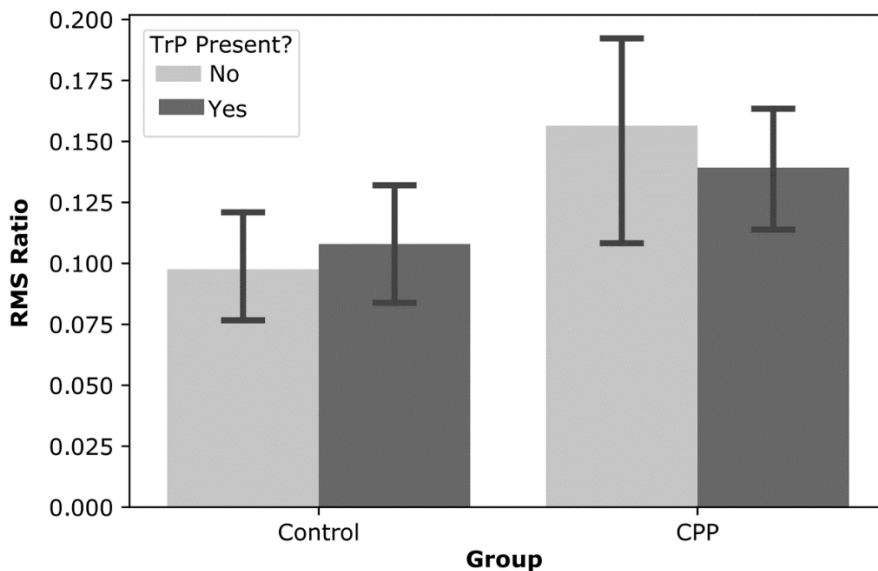


Figure 4.1 RMS ratios for participants with and without myofascial trigger points.

The agreement between TrP location and hypertonicity was poor, with Cohen's $\kappa = 0.08$. Figure 4.2 shows the RMS Ratio mappings for all subjects, with the Trigger point locations detected via digital palpation marked by a red box in women with CPP.

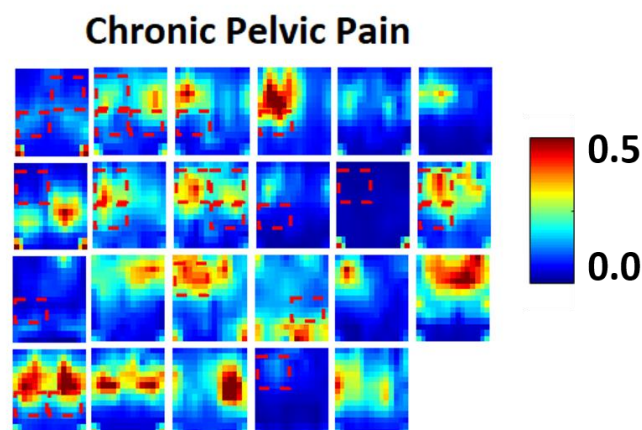


Figure 4.2 Location of myofascial trigger points (red box) overlaid on RMS mappings from Chronic Pelvic Pain Patients.

Discussion

This study is the first effort to employ HD-sEMG for detecting myofascial TrPs in the PFMs. In this study, we show that myofascial TrPs are not directly associated with significantly increased EMG activity. The proposed HD-sEMG technique could not detect myofascial trigger points that were identified during the digital pelvic exam. This may be because, based upon the “energy crisis” theory myofascial trigger points are electrically silent (83).

Recently, Lu et al. reported increased iEMG activity at trigger points that subsided with dry needling (202). These contrasting results suggest that trigger points may not produce a large enough electrical signature to be reliably detected with sEMG. Our study did not find a clear relationship between a muscle exhibiting a trigger point and an increase in resting RMS ratio.

A recent RCT comparing myofascial TrP targeted BoNT injections showed no significant improvement in pain symptoms over placebo. Our study provides a

possible explanation for this, in that by targeting myofascial TrPs, the BoNT may not be the most optimized injection strategy. By targeting TrPs, the BoNT may not be reaching the specific pelvic muscle that is in hyper-contraction. Barbero et al. showed that myofascial trigger points are located, on average, 10.4mm away from the IZ. Taken in combination with the results of Lapatki et al, who showed that injections distanced at least 10mm away from an IZ reduced injection efficiency by up to 46%, it is possible that trigger point targeted injections may in turn be compromising the optimal treatment efficiency of BoNT, as trigger points and IZs are distinct muscle features spaced on average 10.4mm apart (186).

Several studies have demonstrated that targeting BoNT towards hypertonic PFMs significantly improve treatment outcomes. Morrissey et al. examined the utility of intramuscular EMG guidance for localizing PFM overactivity, and the guidance of BoNT injections towards these overactive regions, and demonstrated significant reductions in patient reported outcomes, as well as PFM pressure at rest (155). Likewise, Adelwolo et al. studied outcomes of intra-PFM BoNT injections in women with a short, tightened PFM, and found that 79.3% of patients reported improvement in pain (156). Our current study thus supports the findings of Morrissey and Adelwolo, in that targeting BoNT injections towards hypertonic muscles is a preferable strategy in comparison to trigger point targeted injections.

Conclusions

This chapter aimed to develop a non-invasive technique for assessing and locating myofascial TrPs. The HD-sEMG technique was unable to localize myofascial TrPs alone. However, by combining information acquired from digital

palpation, potential considerations for future treatment, namely the preferable injection of hypertonic muscle instead of myofascial TrPs.

Chapter 5 Non-invasive and Quantitative Assessment of the Number of Functioning Motor Units in the Puborectalis Muscle

Introduction

Motor unit number estimation (MUNE) serve as a neurophysiological tool to quantify the number of functioning motor units in a target muscle, by calculating the ratio between the CMAP, representing the size of the whole muscle's neuromuscular capacity, and single motor unit potential (SMUP), representing the size of an individual motor unit (MU) (203). MUNE has been employed to aid in the diagnosis, and progression tracking of various neuromuscular diseases (204). Specifically, MUNE has been used to monitor the progression of motor neuron disorders like amyotrophic lateral sclerosis (ALS), spinal cord injury, polio, and the gradual loss of MUs that occurs with normal aging. Despite the promising performance of MUNE in distal and proximal limb muscles, no effort has been made to apply such techniques to the pelvic space in human subjects,(205) due to the complicated anatomy of the pelvis, poor accessibility to the nerve, and invasiveness of current MUNE techniques.

The aforementioned technical roadblocks have impeded the estimation of MU numbers in proximal muscles, and are especially prohibitive to pelvic floor muscle (PFM) applications (205). Furthermore, incremental, multi-point, and statistical MUNE techniques all require repetitive stimulation of the target nerve, and substantial tolerance from the operators and subjects. Such an arduous acquisition is not well suited to an intra-rectal stimulation system, as is required for a PFM application. Spike triggered-averaging (STA) (204) and decomposition

MUNE (206) require the painful placement of an intramuscular sensor to determine motor unit action potential (MUAP) spike times. Clearly, the application of MUNE to the pelvic space requires a non-invasive technique that minimizes patient discomfort.

High-density surface (HD-sEMG) signals can be decomposed into constitutive motor unit spike trains, providing the basis for a non-invasive evaluation of muscle function at the MU level. Peng *et. al* reported the successful decomposition of EMG signals acquired from the pelvic muscles of healthy women using a 64-channel HD-sEMG probe, suggesting the feasibility of estimating the SMUP size from intra-vaginal recordings (133). Our previous work has developed an HD-sEMG MUNE method in the biceps brachii muscle with marked repeatability (207). HD-sEMG MUNE provides a unique opportunity for PFM applications, by employing non-invasive recording techniques and avoiding repetitive stimulations. In this study, HD-sEMG MUNE was applied, for the first time, to pelvic muscles, in order to test the feasibility of using HD-sEMG MUNE as a non-invasive electrophysiological biomarker for assessing the number of functional motor units in the PFMs.

Material and Methods

Participants

Female subjects (n=5, mean age 48±19 years, range (19-71)) presenting with symptoms of pudendal nerve entrapment, who were scheduled for a pudendal nerve terminal motor latency test (PNTML) to test for motor impairment due to entrapment, were recruited via a voluntary sample from the outpatient Neurology

Clinic at Fort Bend Neurology. All patients gave informed consent. Study protocol was reviewed by the UH IRB.

Signal Acquisition

During a standard-of-care pudendal nerve terminal motor latency (PNTML) test, subjects were situated in the supine position on an examination table. A ground electrode (TMSi, Enschede, Netherlands) was affixed to the left wrist of the subject. A monopolar needle (26 Gauge, Ambu, Baltorpbakken, Denmark) was first inserted into the left bulbospongiosus muscle to record the intramuscular CMAP (iCMAP) and PNTML. A 64-channel intra-vaginal surface EMG probe was introduced into the vaginal space, and EMG activity was recorded at 2,048Hz with a Refa-136 bio-signal amplifier (TMSi Refa, Enschede, the Netherlands), as shown in Figure 5.1B.

A St. Mark's stimulating electrode was affixed to the examiner's right hand and attached to a constant current stimulator (Cadwell Central, Kennewick WA, USA). Rectangular stimuli with a pulse width of 0.2 msec were triggered manually by an experienced technician. The examiner located the left ischial spine via a digital rectal exam. The optimal stimulation site was confirmed by the largest potential evoked via 15-mA constant current test stimulation. Upon confirmation of proper electrode placement, a stimulation series increasing in amplitude was delivered to the pudendal nerve in 10-mA steps, until the supramaximal CMAP response was obtained, where further increases in stimulation amplitude no longer incited an increase in CMAP amplitude. The procedure was then repeated on the right side. Upon completion of the stimulation portion, the subject was instructed

to perform three contractions of the PFM with moderate, but consistent effort. High-density surface EMG signals during stimulation and voluntary contraction were recorded and stored for offline processing.

Signal Analysis

PNTML was estimated from the iCMAP recordings via an automated protocol, and the subject excluded from this pilot study with a latency exceeding 4 msec in at least one side, suggesting Wallerian degeneration (9, 208). Acquired HD-sEMG signals were analyzed with MATLAB R2018a (Mathworks Natick MA). Contraction periods were bandpass filtered with a 10 Hz to 500 Hz second-order Butterworth filter. A 60 Hz second-order Butterworth notch filter was then applied to remove power line artifacts. Contraction HD-sEMG was decomposed into motor unit action potential (MUAP) spike trains using a k-means clustering modified convolution kernel compensation (KmCKC) algorithm (176). Briefly, a time instant n_0 with several simultaneously active MUs was selected based on the global activity index. Then, firing instants generated by MUs which are simultaneously active at n_0 are collected. The K-mean clustering method was utilized to cluster these collected firing instants into groups corresponding to different MUs. The group with the largest number of firing instants is used to construct the initial MUAP pulse train via the linear minimum mean square error method. Finally, a modified multi-step iterative convolution kernel compensation (CKC) method (126) was employed to update the estimated MUAP pulse trains to improve the decomposition accuracy. MUAP pulse trains with a pulse-to-noise ratio greater than 30 were accepted (129). The resulting MUAP trains were used to spike

triggered average HD-sEMG signals to give a 64-channel MUAP template for each decomposed MU.

The active channels (Ch_{active}) of each SMUP template were grouped into “left side” and “right side” for each set of decomposed MUs. An average MUAP template was calculated for each group, to give an average SMUP for the left and right sides, as shown in Figure 5.1C. A_{SMUP} and A_{CMAP} were calculated for each channel as the maximum negative peak. MUNE was calculated as described in our previous study (207), with the exception that the left and right sided MUNE values were calculated separately, to account for the anatomy and bilateral innervation of PFM, and is expressed as

$$W_{SMUP} = \frac{A_{SMUP}^2}{\sum_1^{Ch_{active}} A_{SMUP}^2} \quad (3)$$

and

$$MUNE = \sum_1^{Ch_{active}} W_{SMUP} \frac{A_{CMAP}}{A_{SMUP}}, \quad (4)$$

where W_{SMUP} is the weighting, A_{SMUP} is the SMUP amplitude, and A_{CMAP} is the CMAP amplitude.

Results

The experimental flowchart is diagramed in Figure 5.1, where A) is a single channel recording during PFM contraction; B) shows the stimulation and recording configuration; C) shows an example average SMUP profile for a left sided recording; D) shows a single channel recording of a series of evoked potentials during increasing stimulation intensity; E) shows an example CMAP profile for a left sided recording; and F) shows an zoomed in view of the selected channels.,

with representative HD-sEMG recordings during voluntary vaginal contraction. HD-sEMG signals were successfully acquired and decomposed for all subjects.

On average, the PNTML was 1.38 ± 0.53 ms. 4 subjects showed a bilateral surface CMAP (sCMAP) response; 1 exhibited a unilateral sCMAP response. A total number of 9 qualified recordings were included. An average sCMAP response of 1.56 ± 0.97 mV was observed. The average SMUP size was 32.2 ± 26.4 μ V. The average MUNE was 64 ± 31 for each side. The average cumulative MUNE (sum of both sides) for participants with a bilateral response was 129 ± 62 .

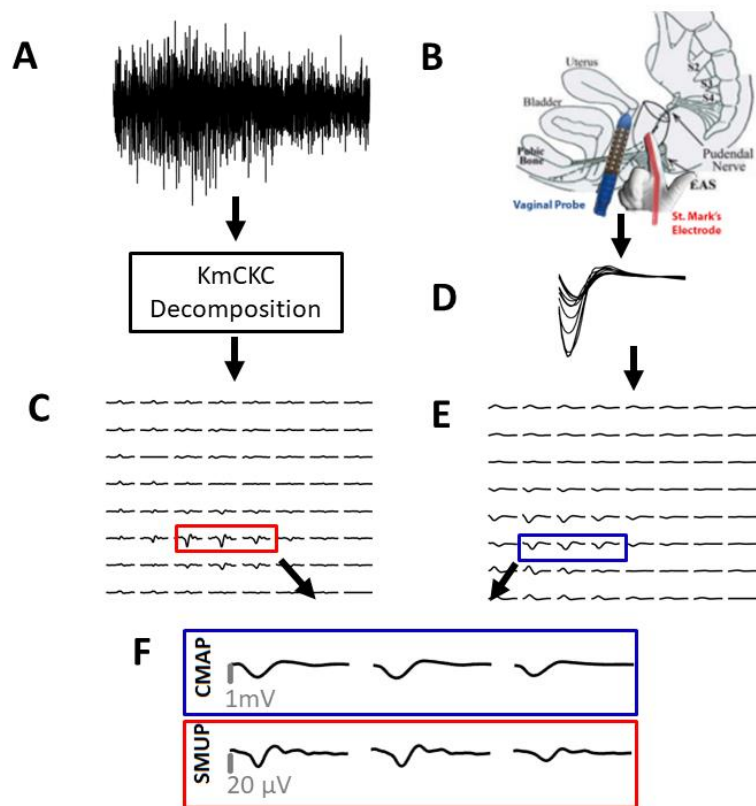


Figure 5.1 Procedural flowchart for PFM MUNE

Discussion

PNE causes widespread pain in the dermatome of the pudendal nerve and can later lead to axonal degeneration. This axonal degeneration has been studied in compression neuropathies of the limb muscles, but not in the pelvic space, likely due to the complicated and/or invasive nature of the currently available MUNE methods. In this study, we presented the first effort to quantitatively and non-invasively assess neurodegeneration in peripheral nerve dysfunction caused by PNE, by employing an HD-sEMG MUNE technique. For the first time, MUNE was successfully calculated bilaterally in 4 subjects, and unilaterally in 1 subject in the PFMs of women.

Motor Unit Number Estimation

Incremental MUNE was the first proposed by McComas *et.al.*, where the size of the SMUP is estimated by the subsequent increase in CMAP amplitude in response to incremental stimulation (203). Multiple point stimulation (MPS) MUNE method was proposed by delivering stimulation at multiple sites along the nerve to activate multiple motor units (203). MPS features improved repeatability compared to incremental MUNE. Both incremental and multiple point MUNE introduce systematic bias by sampling MUs near their voluntary threshold. Statistical MUNE was proposed to remove this bias by sampling motor units over a wide response range. By investigating the nerve over 4 stimulus intensities, an estimate of SMUP size is obtained at each intensity, reducing bias (209). Other approaches such as CMAP scan and Bayesian statistical MUNE have also been proposed (210, 211). Excellent performance has been reported for these approaches in the limb

muscles, yet the complex pelvic anatomy has largely prohibited their application to the PFM. Our group has proposed the first pelvic MUNE in a rat model using a statistical MUNE method (205); however, this method, as well as other aforementioned MUNE techniques, is not easily adaptable to humans as they require a large number of stimulation repetitions and therefore substantial patient discomfort. Moreover, incremental and MPS MUNE are only applicable to distal muscles, and the compact anatomy precludes the use of fixed stimulation electrodes and limits the suitable stimulation locations to the ischial spine. STA MUNE estimates the SMUP size by recording the response of a single motor unit to voluntary contraction with a concentric needle (43). From this, a concurrent surface EMG can be averaged with respect to spike times to estimate the SMUP size. While STA MUNE overcomes procedural complexity brought on by multiple stimulations, it requires the insertion of a needle, which is a significant drawback when dealing with the PFM.

HD-sEMG MUNE overcame the aforementioned technical challenges, by avoiding repetitive stimulations, or the use of invasive intramuscular sensors. It only requires 1-2 sets of stimulations to find the optimal stimulation site and maximal CMAP, and therefore can be conveniently completed in 10-20 minutes per visit (206, 207, 209). In our study, the average SMUP size for each side of the PFM was determined non-invasively from the spatiotemporal information acquired from the 64-channel grid using the KmCKC algorithm (133). We observed a significant decrease in MUNE on the affected side. Our results suggest that the number of motor units in the PFM is 129 ± 62 , yet no further validation provided as

there is currently no other studies which provide the true number of motor units or motoneurons that innervate the PFMs.

The presented HD-sEMG MUNE can be employed as a novel diagnostic tool for the clinical evaluation of neurogenic pelvic dysfunctions, including diabetic neuropathy, obstetric nerve injury and aging. By employing an intra-vaginal stimulation and intra-rectal HD-sEMG recording technique, the proposed technique can easily be adapted to assess external anal sphincter function. This configuration may be particularly useful in cases of idiopathic fecal incontinence with no visible sphincter injury; it may be clinically useful to assess the number of functioning MUs in the external anal sphincter for the direct assessment of muscle remodeling and peripheral nervous system health. The ability to assess neuromuscular health directly provides clinicians with a new perspective to supplement the functional evaluations provided by manometry and imaging. HD-sEMG MUNE can further the understanding of urinary and fecal incontinence pathophysiology and help individualize treatment plans to optimize therapeutic outcome.

Limitations

This study is limited to women who presented to the clinic with symptoms associated with pudendal nerve entrapment but had a normal PNTML. A follow-up study with healthy controls is required.

The relatively low sampling rate often caused the stimulation artifact to overwhelm the time of CMAP onset, rendering a surface-based conduction study impractical. To overcome this limitation, we employed concurrent needle

examination to assess latency. Further tests with higher sampling rates should be conducted to explore the ability of HD-sEMG to assess PNTML non-invasively. Finally, a longitudinal study should take place to characterize the ability of this PFM MUNE technique to study changes in motor unit numbers with motor neuron degeneration.

Conclusions

In this study HD-sEMG was used for the first time to non-invasively estimate the number of functioning motor units in the puborectalis of women. This technique may prove useful in assessing various disease states, such as entrapment neuropathy, ALS, and idiopathic fecal incontinence.

Chapter 6 Conclusions and Future Directions

Guidance of Physical Therapy

These findings have the potential to inform the treatment of CPP and PFM tenderness. Treatment for pelvic floor pain is largely dependent on the attributed conditions underlying the pain. Commonly, first line treatment includes behavioral modification, stress reduction, and education about CPP and pelvic muscle pain, followed by myofascial physical therapy approaches as 2nd line, and pain management via oral analgesics as 3rd line treatment (212). If patients do not respond to conservative care, lidocaine or BOTOX may injections may be indicated as 4th line treatment (100). The current gold-standard for the management of pelvic floor pain is myofascial therapy. A recent landmark RCT of 81 women with IC/BPS and concomitant pelvic floor tenderness showed a 59% global response assessment rate to a 10-week MPT protocol (142). Despite being proven to be an effective treatment for pelvic floor pain in women with IC/BPS, 41% of women still did not respond to treatment, possibly due to heterogeneous symptom etiology. Myofascial therapy treats the muscle directly via manual manipulation of hyper contracted muscles and trigger points, release of connective tissue restrictions, and retraining of weak PFMs where necessary (142). Complementary to myofascial therapy, movement pattern training aims to correct postural dysfunction and aberrant movement patterns that are associated with pelvic floor pain (101). Pelvic floor pain is intrinsically a multifactorial dysfunction that can be attributed to postural issues (101), myofascial trigger points, peripheral sensitization, and

abnormal muscle tone (213). Women with pain originating from impaired relaxation and pelvic floor overactivity may respond better to muscle-focused treatment protocols, like myofascial therapy. Conversely, women with pelvic floor pain arising from poor posture and impaired muscle coordination may respond better to a comprehensive treatment strategy, including movement pattern training. Physical therapy, while effective, requires a substantial time commitment. The HD-sEMG techniques described in this dissertation, in combination with conventional EMG recorded from the Hip and Trunk muscles may aid in differentiating myofascial pain from pain related to abnormal movement or muscle coordination. In addition to the intravaginal HD-sEMG probe, bipolar sEMG signals were collected from the left and right rectus abdominus, adductor brevis, gluteus maximus, and gluteus medius. The two patients were able to activate all muscles groups listed above. EMG signals from this developed PFM-Hip-Trunk network were processed using intermuscular coherence and non-negative matrix factorization to create the PFM-Hip-Trunk network for two CPP patients, as shown in Figure 6.1 where the left panel shows the PFM-Trunk-Hip muscle networks of the two CPP patients where red lines show inter-muscle interactions between PFMs and hip/trunk muscles, blue lines show inter-muscle interactions between PFM pairs, and black lines show inter-muscle interactions between hip/trunk muscle pairs. Right panel shows the PFM EMG RMS mapping of the two CPP patients, where the red color indicates muscle regions with high overactivity severity. **Glu. Max:** Gluteus Maximus; **Glu. Med:** Gluteus Medius; **Add. Brev:** Adductor Brevis; **Rect. Ab:** Rectus Abdominis.

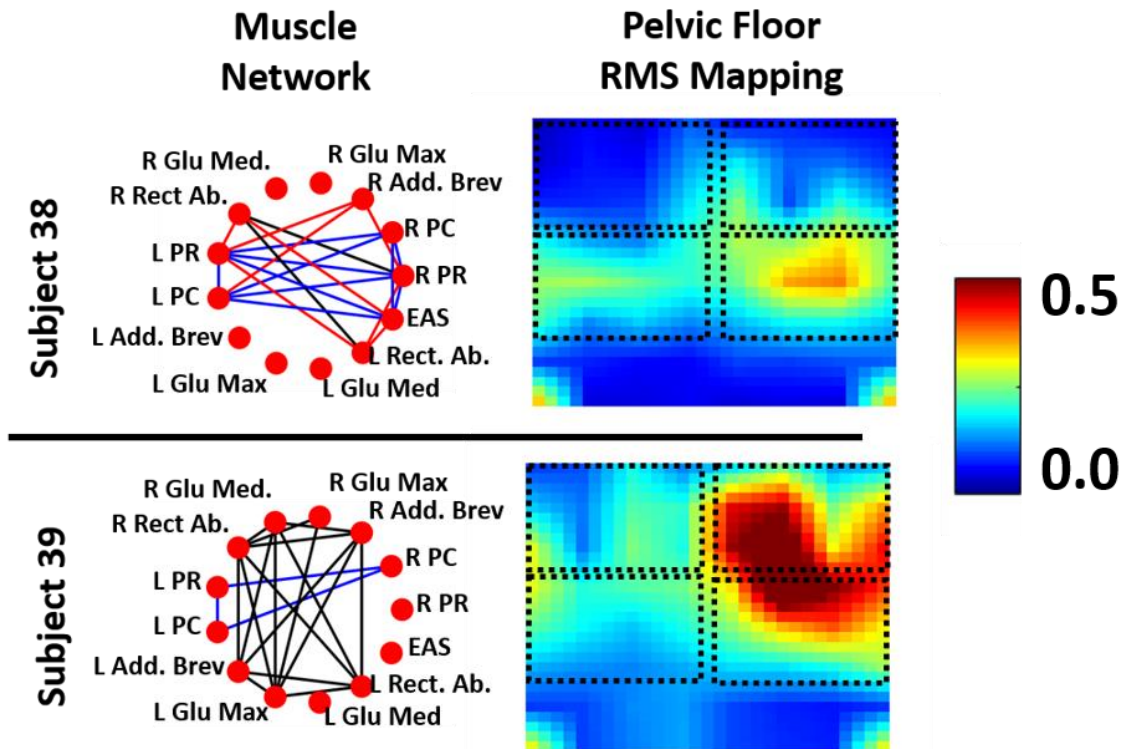


Figure 6.1 Pilot results from two women with CPP and PFM tenderness.

Patient #38 exhibited pelvic muscle pain with palpation but very mild overactivity. Interestingly, her PFM-Hip-Trunk muscle network analysis results showed strong interactions between the right hip adductor, left and right abdominus rectus, and the left puborectalis, left pubococcygeus and external anal sphincter muscles (highlighted in red). This finding may indicate that the major pathologic contributor for this CPP patient (Patient #38) is like to be the abnormality of her hip/trunk muscles. Patient #39 exhibited pelvic muscle pain with palpation with concurrent unilateral PFM overactivity. Her PFM-Hip-Trunk muscle network analysis showed no connectivity between any PFMs and hip/trunk muscles, i.e., the Hip-Trunk (black) and PFM muscle networks (blue) were self-contained, while her RMS ratio results show severe overactivity of her PFMs. This finding may

indicate that the major pathologic contributor for this CPP patient (Patient #39) is likely to be myofascial pain and overactivity. These pilot results suggest that Patient #38 may benefit from a combination of movement pattern training to address muscle coordination of the hip and trunk (primary) and myofascial therapy (secondary), whereas Patient #39 would benefit solely from myofascial therapy. The proposed network analyses may help to better understand the etiology and mechanisms of CPP and provide further phenotyping information to optimize conservative care.

Injection therapy

When conservative care and oral analgesics fail, PFM BoNT injections may be recommended. Current injection strategies are guided by a standardized injection template at 5 o'clock and 7 o'clock of the vaginal introitus, highly constrained needle EMG, or digital palpation for muscle tone. The findings of this thesis may improve injection strategies in two ways. First, as shown in Chapter 4 "Assessment of PFM myofascial trigger points using HD-sEMG", there is poor agreement between the location of myofascial TrP's and muscle hypertonicity. Clinicians who injection BoNT towards myofascial TrPs may in fact be compromising the efficacy of the BoNT. Instead BoNT should be injected towards the muscle IZ to maximize potency.

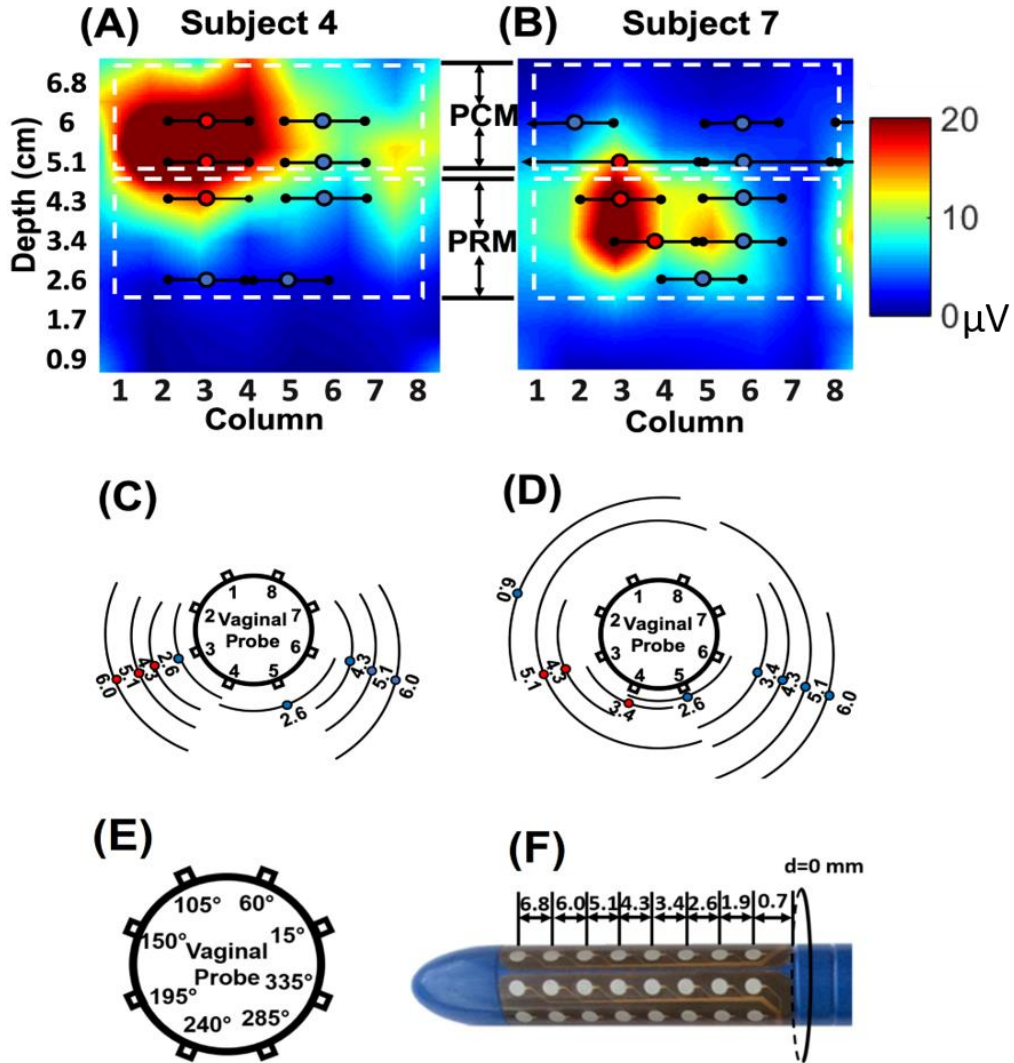


Figure 6.2 Summary of proposed IZ injection guidance technique. Figure reproduced from (193)

Figure 6.2 (reprinted from Chapter 3) A-D shows IZ distributions and for two subjects, which may be used to guide BoNT injections towards a more personalized treatment protocol. In these two example subjects, a standard 5 o'clock and 7 o'clock would not optimally reach the IZ in Subject 7, and this Subject would likely benefit from a personalized IZ injection strategy. Subject 4, on the other hand, appears to have a more "standard" IZ map, and would likely respond well to the standard 5 o'clock and 7 o'clock template. Secondly, the hypertonicity

mapping can be used to inform injection dosages, and increased units can be targeted to the IZs that fall inside hypertonicity “hotspots” on the RMS mapping.

Summary

This dissertation aimed to develop 1) a high-density surface EMG based diagnostic tool for PFM hypertonicity and 2) develop a patient specific PFM IZ mapping technique, and all aims have been explored, as described in Chapters 2-4. Additionally, effort was made in Chapter 5 to establish the first PFM specific MUNE technique. High-density surface EMG was able to detect PFM overactivity in patients with IC/BPS, and a localize these regions of overactivity to expected areas on the HD-sEMG probe nearest to the overactive muscle. Additionally, HD-sEMG was able to reliably detect PFM overactivity in a group of 15 women with IC/BPS, and demonstrated a significant increase in the ratio between resting PFM EMG and the maximum EMG amplitude reached during contraction. HD-sEMG was able to detect PFM IZs based on decomposed MUAP spike trains for all subjects, and a patient specific IZ map was developed for every subject., providing clinicians with a potential target for injecting neurotoxin towards the NMJ. HD-sEMG was unable to reliably detect myofascial TrP's, and poor agreement was present between the location of TrPs felt during palpation and the hypertonic zones present on HD-sEMG, suggesting that TrP targeted BoNT injections may in fact be sacrificing the effectiveness of BoNT in some patients by not guiding the injections towards the hypertonic muscle.

References

1. Cohen D, Gonzalez J, Goldstein I. "The role of pelvic floor muscles in male sexual dysfunction and pelvic pain". *Sexual medicine reviews*. 2016;4(1):53-62.
2. Schmidt MH, Schmidt HS. "The ischiocavernosus and bulbospongiosus muscles in mammalian penile rigidity". *Sleep*. 1993;16(2):171-83.
3. Stein TA, DeLancey JO. "Structure of the perineal membrane in females: gross and microscopic anatomy". *Obstetrics and gynecology*. 2008;111(3):686.
4. Petros PE, Woodman PJ. "The integral theory of continence". *International Urogynecology Journal*. 2008;19(1):35-40.
5. Peng Y, Miller BD, Boone TB, Zhang Y. "Modern theories of pelvic floor support". *Current urology reports*. 2018;19(1):9.
6. Lawson J. "Pelvic anatomy. I. Pelvic floor muscles". *Annals of the Royal College of surgeons of England*. 1974;54(5):244.
7. Dias N, Peng Y, Khavari R, Nakib NA, Sweet RM, Timm GW, Erdman AG, Boone TB, Zhang Y. "Pelvic floor dynamics during high-impact athletic activities: A computational modeling study". *Clinical Biomechanics*. 2017;41:20-7.
8. George SE, Clinton SC, Borello - France DF. "Physical therapy management of female chronic pelvic pain: Anatomic considerations". *Clinical Anatomy*. 2013;26(1):77-88.
9. Popeney C, Ansell V, Renney K. "Pudendal entrapment as an etiology of chronic perineal pain: diagnosis and treatment". *Neurourology and Urodynamics: Official Journal of the International Continence Society*. 2007;26(6):820-7.
10. Grigorescu BA, Lazarou G, Olson TR, Downie SA, Powers K, Greston WM, Mikhail MS. "Innervation of the levator ani muscles: description of the nerve

branches to the pubococcygeus, iliococcygeus, and puborectalis muscles".

International Urogynecology Journal. 2008;19(1):107-16.

11. Snooks S, Swash M. "The innervation of the muscles of continence". *Annals of the Royal College of Surgeons of England*. 1986;68(1):45.
12. Wallner C, van Wissen J, Maas CP, Dabhoiwala NF, DeRuiter MC, Lamers WH. "The contribution of the levator ani nerve and the pudendal nerve to the innervation of the levator ani muscles; a study in human fetuses". *European urology*. 2008;54(5):1136-44.
13. Bø K. "Urinary incontinence, pelvic floor dysfunction, exercise and sport". *Sports medicine*. 2004;34(7):451-64.
14. DeLancey JO. "Structural support of the urethra as it relates to stress urinary incontinence: the hammock hypothesis". *American journal of obstetrics and gynecology*. 1994;170(6):1713-23.
15. DeLancey JO. "Fascial and muscular abnormalities in women with urethral hypermobility and anterior vaginal wall prolapse". *American journal of obstetrics and gynecology*. 2002;187(1):93-8.
16. Luber KM. "The definition, prevalence, and risk factors for stress urinary incontinence". *Reviews in urology*. 2004;6(Suppl 3):S3.
17. Madill SJ, Harvey M-A, McLean L. "Women with stress urinary incontinence demonstrate motor control differences during coughing". *Journal of Electromyography and Kinesiology*. 2010;20(5):804-12.
18. Goode PS, Burgio KL, Halli AD, Jones RW, Richter HE, Redden DT, Baker PS, Allman RM. "Prevalence and correlates of fecal incontinence in community - dwelling older adults". *Journal of the American Geriatrics Society*. 2005;53(4):629-35.

19. Lewicky-Gaupp C, Hamilton Q, Ashton-Miller J, Huebner M, DeLancey JO, Fenner DE. "Anal sphincter structure and function relationships in aging and fecal incontinence". *American journal of obstetrics and gynecology*. 2009;200(5):559. e1-. e5.
20. Knowles A, Knowles C, Scott S, Lunniss P. "Effects of age and gender on three-dimensional endoanal ultrasonography measurements: development of normal ranges". *Techniques in coloproctology*. 2008;12(4):323-9.
21. Fox JC, Fletcher JG, Zinsmeister AR, Seide B, Riederer SJ, Bharucha AE. "Effect of aging on anorectal and pelvic floor functions in females". *Diseases of the colon & rectum*. 2006;49(11):1726-35.
22. Frudinger A, Halligan S, Bartram CI, Price AB, Kamm MA, Winter R. "Female Anal Sphincter: Age-related Differences in Asymptomatic Volunteers with High-Frequency Endoanal US 1". *Radiology*. 2002;224(2):417-23.
23. Handa VL, Harris TA, Ostergard DR. "Protecting the pelvic floor: obstetric management to prevent incontinence and pelvic organ prolapse". *Obstetrics & Gynecology*. 1996;88(3):470-8.
24. Rao SS. "Pathophysiology of adult fecal incontinence". *Gastroenterology*. 2004;126:S14-S22.
25. Bharucha AE, Dunivan G, Goode PS, Lukacz ES, Markland AD, Matthews CA, Mott L, Rogers RG, Zinsmeister AR, Whitehead WE. "Epidemiology, pathophysiology, and classification of fecal incontinence: state of the science summary for the National Institute of Diabetes and Digestive and Kidney Diseases (NIDDK) workshop". *The American journal of gastroenterology*. 2015;110(1):127.

26. Snooks S, Swash M, Henry M, Setchell M. "Risk factors in childbirth causing damage to the pelvic floor innervation". *International journal of colorectal disease*. 1986;1(1):20-4.
27. Bharucha AE, Daube J, Litchy W, Traue J, Edge J, Enck P, Zinsmeister AR. "Anal sphincteric neurogenic injury in asymptomatic nulliparous women and fecal incontinence". *American Journal of Physiology-Gastrointestinal and Liver Physiology*. 2012;303(2):G256-G62.
28. Pretlove S, Thompson P, Toozs - Hobson P, Radley S, Khan K. "Does the mode of delivery predispose women to anal incontinence in the first year postpartum? A comparative systematic review". *BJOG: An International Journal of Obstetrics & Gynaecology*. 2008;115(4):421-34.
29. Borello-France D, Burgio KL, Richter HE, Zyczynski H, FitzGerald MP, Whitehead W, Fine P, Nygaard I, Handa VL, Visco AG. "Fecal and urinary incontinence in primiparous women". *Obstetrics & Gynecology*. 2006;108(4):863-72.
30. Rosenblatt P, Schumacher J, Lucente V, McNevin S, Rafferty J, Mellgren A. "A preliminary evaluation of the TOPAS system for the treatment of fecal incontinence in women". *Female pelvic medicine & reconstructive surgery*. 2014;20(3):155-62.
31. Klass M, Baudry S, Duchateau J. "Voluntary activation during maximal contraction with advancing age: a brief review". *European journal of applied physiology*. 2007;100(5):543-51.
32. Smith AE, Ridding MC, Higgins RD, Wittert GA, Pitcher JB. "Age-related changes in short-latency motor cortex inhibition". *Experimental brain research*. 2009;198(4):489-500.

33. Scaglioni G, Ferri A, Minetti AE, Martin A, Van Hoecke J, Capodaglio P, Sartorio A, Narici MV. "Plantar flexor activation capacity and H reflex in older adults: adaptations to strength training". *Journal of Applied Physiology*. 2002;92(6):2292-302.
34. Kossev AR, Schrader C, Däuper J, Dengler R, Rollnik JD. "Increased intracortical inhibition in middle-aged humans; a study using paired-pulse transcranial magnetic stimulation". *Neuroscience letters*. 2002;333(2):83-6.
35. Kido A, Tanaka N, Stein RB. "Spinal excitation and inhibition decrease as humans age". *Canadian journal of physiology and pharmacology*. 2004;82(4):238-48.
36. Klass M, Baudry S, Duchateau J. "Age-related decline in rate of torque development is accompanied by lower maximal motor unit discharge frequency during fast contractions". *Journal of Applied Physiology*. 2008;104(3):739-46.
37. Christie A, Kamen G. "Doublet discharges in motoneurons of young and older adults". *Journal of neurophysiology*. 2006;95(5):2787-95.
38. Kamen G, Sison SV, Du C, Patten C. "Motor unit discharge behavior in older adults during maximal-effort contractions". *Journal of Applied Physiology*. 1995;79(6):1908-13.
39. Nelson RM, Soderberg GL, Urbscheit NL. "Comparison of skeletal muscle motor unit discharge characteristics in young and aged humans". *Archives of gerontology and geriatrics*. 1983;2(3):255-64.
40. Doherty TJ, Brown WF. "The estimated numbers and relative sizes of thenar motor units as selected by multiple point stimulation in young and older adults". *Muscle & nerve*. 1993;16(4):355-66.

41. Power GA, Dalton BH, Behm DG, Vandervoort AA, Doherty TJ, Rice CL. "Motor unit number estimates in masters runners: use it or lose it". *Med Sci Sports Exerc.* 2010;42(9):1644-50.
42. McNeil CJ, Doherty TJ, Stashuk DW, Rice CL. "Motor unit number estimates in the tibialis anterior muscle of young, old, and very old men". *Muscle & nerve.* 2005;31(4):461-7.
43. Brown WF, Strong MJ, Snow R. "Methods for estimating numbers of motor units in biceps - brachialis muscles and losses of motor units with aging". *Muscle & nerve.* 1988;11(5):423-32.
44. Delmonico MJ, Harris TB, Visser M, Park SW, Conroy MB, Velasquez-Mieyer P, Boudreau R, Manini TM, Nevitt M, Newman AB. "Longitudinal study of muscle strength, quality, and adipose tissue infiltration". *The American journal of clinical nutrition.* 2009;90(6):1579-85.
45. Vandervoort AA, McCOMAS AJ. "Contractile changes in opposing muscles of the human ankle joint with aging". *Journal of Applied Physiology.* 1986;61(1):361-7.
46. Payne AM, Jimenez-Moreno R, Wang Z-M, Messi ML, Delbono O. "Role of Ca²⁺, membrane excitability, and Ca²⁺ stores in failing muscle contraction with aging". *Experimental gerontology.* 2009;44(4):261-73.
47. Hibner M, Desai N, Robertson LJ, Nour M. "Pudendal neuralgia". *Journal of minimally invasive gynecology.* 2010;17(2):148-53.
48. Labat JJ, Riant T, Robert R, Amarenco G, Lefaucheur JP, Rigaud J. "Diagnostic criteria for pudendal neuralgia by pudendal nerve entrapment (Nantes criteria)". *Neurourology and Urodynamics: Official Journal of the International Continence Society.* 2008;27(4):306-10.

49. Benson JT, Griffis K. "Pudendal neuralgia, a severe pain syndrome". *American journal of obstetrics and gynecology*. 2005;192(5):1663-8.
50. Brown R, Pedowitz R, Rydevik B, Woo S, Hargens A, Massie J, Kwan M, Garfin SR. "Effects of acute graded strain on efferent conduction properties in the rabbit tibial nerve". *Clinical orthopaedics and related research*. 1993(296):288-94.
51. Lien K-C, Morgan DM, Delancey JO, Ashton-Miller JA. "Pudendal nerve stretch during vaginal birth: a 3D computer simulation". *American journal of obstetrics and gynecology*. 2005;192(5):1669-76.
52. Lubowski D, Swash M, Nicholls R, Henry M. "Increase in pudendal nerve terminal motor latency with defaecation straining". *British Journal of Surgery*. 1988;75(11):1095-7.
53. Ahangari A. "Prevalence of chronic pelvic pain among women: an updated review". *Pain Physician*. 2014;17(2):E141-E7.
54. Nickel JC, Teichman JM, Gregoire M, Clark J, Downey J. "Prevalence, diagnosis, characterization, and treatment of prostatitis, interstitial cystitis, and epididymitis in outpatient urological practice: the Canadian PIE Study". *Urology*. 2005;66(5):935-40.
55. Marszalek M, Wehrberger C, Temml C, Ponholzer A, Berger I, Madersbacher S. "Chronic pelvic pain and lower urinary tract symptoms in both sexes: analysis of 2749 participants of an urban health screening project". *European Urology*. 2009;55(2):499-508.
56. Clemens JQ, Meenan RT, ROSETTI MCOK, Brown SO, Gao SY, Calhoun EA. "Prevalence of interstitial cystitis symptoms in a managed care population". *The Journal of urology*. 2005;174(2):576-80.

57. Mathias SD, Kuppermann M, Liberman RF, Lipschutz RC, Steege JF. "Chronic pelvic pain: prevalence, health-related quality of life, and economic correlates". *Obstetrics & Gynecology*. 1996;87(3):321-7.
58. Zondervan KT, Yudkin PL, Vessey MP, Jenkinson CP, Dawes MG, Barlow DH, Kennedy SH. "The community prevalence of chronic pelvic pain in women and associated illness behaviour". *Br J Gen Pract*. 2001;51(468):541-7.
59. FitzGerald MP, Koch D, Senka J. "Visceral and cutaneous sensory testing in patients with painful bladder syndrome". *Neurourology and Urodynamics: Official Journal of the International Continence Society*. 2005;24(7):627-32.
60. Hanno P, Dmochowski R. "Status of international consensus on interstitial cystitis/bladder pain syndrome/painful bladder syndrome: 2008 snapshot". *Neurourology and Urodynamics: Official Journal of the International Continence Society*. 2009;28(4):274-86.
61. Lai HH, Pickersgill NA, Vetter JM. "Hunner lesion phenotype in interstitial cystitis/bladder pain syndrome: a systematic review and meta-analysis". *The Journal of urology*. 2020;204(3):518-23.
62. Berkley KJ. "A life of pelvic pain". *Physiology & behavior*. 2005;86(3):272-80.
63. Dmitrieva N, Johnson OL, Berkley KJ. "Bladder inflammation and hypogastric neurectomy influence uterine motility in the rat". *Neuroscience letters*. 2001;313(1-2):49-52.
64. Butrick CW. "Interstitial Cystitis/Bladder Pain Syndrome". *Controversies in Female Pelvic Reconstruction, An Issue of Urologic Clinics-E-Book*. 2012;39(3):377.
65. Stovner LJ, Ægidius K, Linde M. "Endometriosis and headache". *Current pain and headache reports*. 2011;15(5):415-9.

66. Giudice LC. "Endometriosis". *New England Journal of Medicine*. 2010;362(25):2389-98.
67. Wagtmans M, Verspaget H, Lamers C, Van Hogezaand R. "Crohn's disease in the elderly: a comparison with young adults". *Journal of clinical gastroenterology*. 1998;27(2):129-33.
68. Malykhina AP, Qin C, Greenwood - van Meerveld B, Foreman R, Lupu F, Akbarali H. "Hyperexcitability of convergent colon and bladder dorsal root ganglion neurons after colonic inflammation: mechanism for pelvic organ cross - talk". *Neurogastroenterology & Motility*. 2006;18(10):936-48.
69. Goldstein AT, Pukall CF, Brown C, Bergeron S, Stein A, Kellogg-Spadt S. "Vulvodynia: assessment and treatment". *The journal of sexual medicine*. 2016;13(4):572-90.
70. Ventolini G. "Vulvar pain: anatomic and recent pathophysiologic considerations". *Clinical Anatomy*. 2013;26(1):130-3.
71. Sadownik LA. "Etiology, diagnosis, and clinical management of vulvodynia". *International journal of women's health*. 2014;6:437.
72. Kahn BS, Tatro C, Parsons CL, Willems JJ. "Prevalence of interstitial cystitis in vulvodynia patients detected by bladder potassium sensitivity". *The Journal of Sexual Medicine*. 2010;7(2):996-1002.
73. Payne S. "Sex, gender, and irritable bowel syndrome: making the connections". *Gender medicine*. 2004;1(1):18-28.
74. Sambrook P, Taylor TK, Ellis A. The Musculoskeletal System E-Book: Systems of the Body Series: Elsevier Health Sciences; 2014.
75. Katner T, Kasarskis E. "Muscle Tone"2014.

76. Trompetto C, Marinelli L, Mori L, Pelosin E, Currà A, Molfetta L, Abbruzzese G. "Pathophysiology of spasticity: implications for neurorehabilitation". *BioMed research international*. 2014;2014.
77. Wilson LR, Gracies J-M, Burke D, Gandevia SC. "Evidence for fusimotor drive in stroke patients based on muscle spindle thixotropy". *Neuroscience letters*. 1999;264(1-3):109-12.
78. Pluess M, Conrad A, Wilhelm FH. "Muscle tension in generalized anxiety disorder: a critical review of the literature". *Journal of anxiety disorders*. 2009;23(1):1-11.
79. Peters KM, Carrico DJ, Kalinowski SE, Ibrahim IA, Diokno AC. "Prevalence of pelvic floor dysfunction in patients with interstitial cystitis". *Urology*. 2007;70(1):16-8.
80. Reissing ED, Brown C, Lord M, Binik Y, Khalife S. "Pelvic floor muscle functioning in women with vulvar vestibulitis syndrome". *Journal of Psychosomatic Obstetrics & Gynecology*. 2005;26(2):107-13.
81. Verne GN, Price DD. "Irritable bowel syndrome as a common precipitant of central sensitization". *Current rheumatology reports*. 2002;4(4):322-8.
82. Hoffman D. "Understanding multisymptom presentations in chronic pelvic pain: the inter-relationships between the viscera and myofascial pelvic floor dysfunction". *Current pain and headache reports*. 2011;15(5):343.
83. Bo K, Frawley HC, Haylen BT, Abramov Y, Almeida FG, Berghmans B, Bortolini M, Dumoulin C, Gomes M, McClurg D. "An International Urogynecological Association (IUGA)/International Continence Society (ICS) joint report on the terminology for the conservative and nonpharmacological management of female pelvic floor dysfunction". *International urogynecology journal*. 2017;28(2):191-213.

84. Gajdosik RL. "Passive extensibility of skeletal muscle: review of the literature with clinical implications". *Clinical biomechanics*. 2001;16(2):87-101.
85. Thibault-Gagnon S, Morin M. "Active and passive components of pelvic floor muscle tone in women with provoked vestibulodynia: a perspective based on a review of the literature". *The Journal of Sexual Medicine*. 2015;12(11):2178-89.
86. Baranowski AP, Abrams P, Berger RE, Buffington CT, Williams ACdC, Hanno P, Loeser JD, Nickel JC, Wesselmann U. Urogenital pain—time to accept a new approach to phenotyping and, as a consequence, management. Citeseer; 2008.
87. Johansson H, Sojka P. "Pathophysiological mechanisms involved in genesis and spread of muscular tension in occupational muscle pain and in chronic musculoskeletal pain syndromes: a hypothesis". *Medical hypotheses*. 1991;35(3):196-203.
88. Knutson GA. "The role of the γ -motor system in increasing muscle tone and muscle pain syndromes: a review of the Johansson/Sojka hypothesis". *Journal of manipulative and physiological therapeutics*. 2000;23(8):564-72.
89. Gerwin RD, Dommerholt J, Shah JP. "An expansion of Simons' integrated hypothesis of trigger point formation". *Current pain and headache reports*. 2004;8(6):468-75.
90. Smith LJ, Macefield VG, Birznieks I, Burton AR. "Effects of tonic muscle pain on fusimotor control of human muscle spindles during isometric ankle dorsiflexion". *Journal of neurophysiology*. 2019;121(4):1143-9.
91. Paras ML, Murad MH, Chen LP, Goranson EN, Sattler AL, Colbenson KM, Elamin MB, Seime RJ, Prokop LJ, Zirakzadeh A. "Sexual abuse and lifetime diagnosis of somatic disorders: a systematic review and meta-analysis". *Jama*. 2009;302(5):550-61.

92. Heim C, Newport DJ, Heit S, Graham YP, Wilcox M, Bonsall R, Miller AH, Nemeroff CB. "Pituitary-adrenal and autonomic responses to stress in women after sexual and physical abuse in childhood". *Jama*. 2000;284(5):592-7.
93. McEuen JG, Beck SG, Bale TL. "Failure to mount adaptive responses to stress results in dysregulation and cell death in the midbrain raphe". *Journal of Neuroscience*. 2008;28(33):8169-77.
94. Watts G, Nettle D. "The role of anxiety in vaginismus: a case-control study". *The journal of sexual medicine*. 2010;7(1):143-8.
95. Pacik PT, Geletta S. "Vaginismus treatment: clinical trials follow up 241 patients". *Sexual medicine*. 2017;5(2):e114-e23.
96. Gupta P, Gaines N, Sirls LT, Peters KM. "A multidisciplinary approach to the evaluation and management of interstitial cystitis/bladder pain syndrome: an ideal model of care". *Translational andrology and urology*. 2015;4(6):611.
97. Alappattu MJ, Bishop MD. "Psychological factors in chronic pelvic pain in women: relevance and application of the fear-avoidance model of pain". *Physical therapy*. 2011;91(10):1542-50.
98. Butrick CW. "Pelvic floor hypertonic disorders: identification and management". *Obstetrics and Gynecology Clinics*. 2009;36(3):707-22.
99. Tu FF, Holt J, Gonzales J, Fitzgerald CM. "Physical therapy evaluation of patients with chronic pelvic pain: a controlled study". *American journal of obstetrics and gynecology*. 2008;198(3):272. e1-. e7.
100. Prather H, Spitznagle TM, Dugan SA. "Recognizing and treating pelvic pain and pelvic floor dysfunction". *Physical Medicine and Rehabilitation Clinics of North America*. 2007;18(3):477-96.

101. Haugstad GK, Haugstad TS, Kirste UM, Leganger S, Wojniusz S, Klemmetsen I, Malt UF. "Posture, movement patterns, and body awareness in women with chronic pelvic pain". *Journal of psychosomatic research*. 2006;61(5):637-44.
102. Haugstad GK, Haugstad TS, Kirste UM, Leganger S, Wojniusz S, Klemmetsen I, Malt UF. "Continuing improvement of chronic pelvic pain in women after short-term Mensendieck somatocognitive therapy: results of a 1-year follow-up study". *American Journal of Obstetrics and Gynecology*. 2008;199(6):615. e1-. e8.
103. Sedighimehr N, Manshadi FD, Shokouhi N, Baghban AA. "Pelvic musculoskeletal dysfunctions in women with and without chronic pelvic pain". *Journal of bodywork and movement therapies*. 2018;22(1):92-6.
104. Abbott JA, Jarvis SK, Lyons SD, Thomson A, Vancaille TG. "Botulinum toxin type A for chronic pain and pelvic floor spasm in women: a randomized controlled trial". *Obstetrics & Gynecology*. 2006;108(4):915-23.
105. Harris - Hayes M, Spitznagle T, Probst D, Foster SN, Prather H. "A narrative review of musculoskeletal impairments associated with nonspecific chronic pelvic pain". *PM&R*. 2019;11:S73-S82.
106. Bansal N, Sachdeva M, Jain P, Ranjan P, Arora A. "Anorectal manometry: current techniques and indications". *JIMSA*. 2013;26:169-70.
107. Ackerman AL, Lee UJ, Jellison FC, Tan N, Patel M, Raman SS, Rodriguez LV. "MRI suggests increased tonicity of the levator ani in women with interstitial cystitis/bladder pain syndrome". *International urogynecology journal*. 2016;27(1):77-83.
108. Nesbitt - Hawes E, Dietz H, Abbott J. "Four - dimensional ultrasound guidance for pelvic floor Botulinum toxin - A injection in chronic pelvic pain: a novel technique". *Ultrasound in Obstetrics & Gynecology*. 2018;51(3):396-400.

109. Naess I, Bø K. "Can maximal voluntary pelvic floor muscle contraction reduce vaginal resting pressure and resting EMG activity?". *International urogynecology journal*. 2018;29(11):1623-7.
110. Nesbitt-Hawes E, Won H, Jarvis S, Lyons S, Vancaillie T, Abbott J. "Improvement in pelvic pain with botulinum toxin type A—single vs. repeat injections". *Toxicon*. 2013;63:83-7.
111. Keshwani N, McLean L. "State of the art review: intravaginal probes for recording electromyography from the pelvic floor muscles". *Neurourology and urodynamics*. 2015;34(2):104-12.
112. Hetrick DC, Glazer H, Liu YW, Turner JA, Frest M, Berger RE. "Pelvic floor electromyography in men with chronic pelvic pain syndrome: a case - control study". *Neurourology and Urodynamics: Official Journal of the International Continence Society*. 2006;25(1):46-9.
113. Loving S, Thomsen T, Jaszczak P, Nordling J. "Pelvic floor muscle dysfunctions are prevalent in female chronic pelvic pain: A cross - sectional population - based study". *European Journal of Pain*. 2014;18(9):1259-70.
114. Engman M, Lindehammar H, Wijma B. "Surface electromyography diagnostics in women with partial vaginismus with or without vulvar vestibulitis and in asymptomatic women". *Journal of Psychosomatic Obstetrics & Gynecology*. 2004;25(3-4):281-94.
115. Lodish H, Zipursky SL. "Molecular cell biology". *Biochem Mol Biol Educ*. 2001;29:126-33.
116. Christensen E. "Topography of terminal motor innervation in striated muscles from stillborn infants". *American Journal of Physical Medicine & Rehabilitation*. 1959;38(2):65-78.

117. Pierce LM, Reyes M, Thor KB, Dolber PC, Bremer RE, Kuehl TJ, Coates KW. "Innervation of the levator ani muscles in the female squirrel monkey". *American journal of obstetrics and gynecology*. 2003;188(5):1141-7.
118. Dias N, Li X, Zhang C, Zhang Y. "Innervation asymmetry of the external anal sphincter in aging characterized from high - density intra - rectal surface EMG recordings". *Neurourology and urodynamics*. 2018;37(8):2544-50.
119. Stålberg EV, Sanders DB. "Jitter recordings with concentric needle electrodes". *Muscle & Nerve: Official Journal of the American Association of Electrodiagnostic Medicine*. 2009;40(3):331-9.
120. Hilton - Brown P, Stålberg E, Trontelj J, Mihelin M. "Causes of the increased fiber density in muscular dystrophies studied with single fiber EMG during electrical stimulation". *Muscle & Nerve: Official Journal of the American Association of Electrodiagnostic Medicine*. 1985;8(5):383-8.
121. Nandedkar SD, Dumitru D, King JC. "Concentric needle electrode duration measurement and uptake area". *Muscle & Nerve: Official Journal of the American Association of Electrodiagnostic Medicine*. 1997;20(10):1225-8.
122. Keenan KG, Farina D, Merletti R, Enoka RM. "Amplitude cancellation reduces the size of motor unit potentials averaged from the surface EMG". *Journal of Applied Physiology*. 2006;100(6):1928-37.
123. Pullman SL, Goodin DS, Marquinez AI, Tabbal S, Rubin M. "Clinical utility of surface EMG: report of the therapeutics and technology assessment subcommittee of the American Academy of Neurology". *Neurology*. 2000;55(2):171-7.

124. Arendt-Nielsen L, Zwarts M. "Measurement of muscle fiber conduction velocity in humans: techniques and applications". *Journal of clinical neurophysiology: official publication of the American Electroencephalographic Society*. 1989;6(2):173-90.
125. Mambrito B, De Luca CJ. "A technique for the detection, decomposition and analysis of the EMG signal". *Electroencephalography and clinical neurophysiology*. 1984;58(2):175-88.
126. Holobar A, Zazula D. "Multichannel blind source separation using convolution kernel compensation". *IEEE Transactions on Signal Processing*. 2007;55(9):4487-96.
127. Ning Y, Zhu X, Zhu S, Zhang Y. "Surface EMG Decomposition Based on K-means Clustering and Convolution Kernel Compensation". *IEEE journal of biomedical and health informatics*. 2014;19(2):471-7.
128. Kay SM. Fundamentals of statistical signal processing: Prentice Hall PTR; 1993.
129. Holobar A, Minetto MA, Farina D. "Accurate identification of motor unit discharge patterns from high-density surface EMG and validation with a novel signal-based performance metric". *Journal of neural engineering*. 2014;11(1):016008.
130. Zhang C, Dias N, He J, Zhou P, Li S, Zhang Y. "Global Innervation Zone Identification with High-Density Surface Electromyography". *IEEE Transactions on Biomedical Engineering*. 2019.
131. Masuda T, Miyano H, Sadoyama T. "The position of innervation zones in the biceps brachii investigated by surface electromyography". *IEEE Transactions on Biomedical Engineering*. 1985(1):36-42.
132. Afsharipour B, Sandhu MS, Rasool G, Suresh NL, Rymer WZ, editors. Using surface electromyography to detect changes in innervation zones pattern after human cervical spinal cord injury. Engineering in Medicine and Biology Society (EMBC), 2016 IEEE 38th Annual International Conference of the; 2016: IEEE.

133. Peng Y, He J, Khavari R, Boone TB, Zhang Y. "Functional mapping of the pelvic floor and sphincter muscles from high-density surface EMG recordings". *International urogynecology journal*. 2016;27(11):1689-96.
134. Enck P, Hinrichsen H, Wietek B, Becker HD. "Functional asymmetry of pelvic floor innervation and its role in the pathogenesis of fecal incontinence". *Digestion*. 2004;69(2):102-11.
135. McComas A, Quartly C, Griggs R. "Early and late losses of motor units after poliomyelitis". *Brain: a journal of neurology*. 1997;120(8):1415-21.
136. Saitou K, Masuda T, Michikami D, Kojima R, Okada M. "Innervation zones of the upper and lower limb muscles estimated by using multichannel surface EMG". *Journal of human ergology*. 2000;29(1-2):35-52.
137. Enck P, Franz H, Azpiroz F, Fernandez-Fraga X, Hinrichsen H, Kaske-Bretag K, Bottin A, Martina S, Merletti R. "Innervation zones of the external anal sphincter in healthy male and female subjects". *Digestion*. 2004;69(2):123-30.
138. Cescon C, Bottin A, Fraga XLF, Azpiroz F, Merletti R. "Detection of individual motor units of the puborectalis muscle by non-invasive EMG electrode arrays". *Journal of Electromyography and Kinesiology*. 2008;18(3):382-9.
139. Voorham - van der Zalm PJ, Voorham JC, van den Bos TW, Ouwkerk TJ, Putter H, Wasser MN, Webb A, DeRuiter MC, Pelger RC. "Reliability and differentiation of pelvic floor muscle electromyography measurements in healthy volunteers using a new device: the Multiple Array Probe Leiden (MAPLe)". *Neurourology and urodynamics*. 2013;32(4):341-8.
140. Zijta F, Froeling M, Van Der Paardt M, Lakeman M, Bipat S, van Swijndregt AM, Strijkers G, Nederveen A, Stoker J. "Feasibility of diffusion tensor imaging (DTI)

- with fibre tractography of the normal female pelvic floor". *European radiology*. 2011;21(6):1243-9.
141. Engeler DS, Baranowski AP, Dinis-Oliveira P, Elneil S, Hughes J, Messelink EJ, van Ophoven A, Williams AC. "The 2013 EAU guidelines on chronic pelvic pain: is management of chronic pelvic pain a habit, a philosophy, or a science? 10 years of development". *European urology*. 2013;64(3):431-9.
142. FitzGerald M, Payne C, Lukacz E, Yang C, Peters K, Chai T, Nickel J, Hanno P, Kreder K, Burks D. "Randomized multicenter clinical trial of myofascial physical therapy in women with interstitial cystitis/painful bladder syndrome and pelvic floor tenderness". *The Journal of urology*. 2012;187(6):2113-8.
143. Prendergast SA, Weiss JM. "Screening for musculoskeletal causes of pelvic pain". *Clinical obstetrics and gynecology*. 2003;46(4):773-82.
144. Filippiadis DK, Velonakis G, Mazioti A, Alexopoulou E, Malagari A, Brountzos E, Kelekis N, Kelekis A. "CT-guided percutaneous infiltration for the treatment of Alcock's neuralgia". *Pain Physician*. 2011;14(2):211-5.
145. Porta M. "A comparative trial of botulinum toxin type A and methylprednisolone for the treatment of myofascial pain syndrome and pain from chronic muscle spasm". *Pain*. 2000;85(1-2):101-5.
146. Aredo JV, Heyrana KJ, Karp BI, Shah JP, Stratton P, editors. Relating chronic pelvic pain and endometriosis to signs of sensitization and myofascial pain and dysfunction. Seminars in reproductive medicine; 2017: Thieme Medical Publishers.
147. Raj PP. "Botulinum toxin therapy in pain management". *Anesthesiology Clinics of North America*. 2003;21(4):715-31.

148. Maria G, Cadeddu F, Brisinda D, Brandara F, Brisinda G. "Management of bladder, prostatic and pelvic floor disorders with botulinum neurotoxin". *Current medicinal chemistry*. 2005;12(3):247-65.
149. Aoki KR. "Evidence for antinociceptive activity of botulinum toxin type A in pain management". *Headache: The Journal of Head and Face Pain*. 2003;43:9-15.
150. Aoki K. "Review of a proposed mechanism for the antinociceptive action of botulinum toxin type A". *Neurotoxicology*. 2005;26(5):785-93.
151. Fortuna R, Vaz MA, Youssef AR, Longino D, Herzog W. "Changes in contractile properties of muscles receiving repeat injections of botulinum toxin (Botox)". *Journal of biomechanics*. 2011;44(1):39-44.
152. Mancini F, Sandrini G, Moglia A, Nappi G, Pacchetti C. "A randomised, double-blind, dose-ranging study to evaluate efficacy and safety of three doses of botulinum toxin type A (Botox) for the treatment of spastic foot". *Neurological Sciences*. 2005;26(1):26-31.
153. Graham HK, Aoki KR, Autti-Rämö I, Boyd RN, Delgado MR, Gaebler-Spira DJ, Gormley Jr ME, Guyer BM, Heinen F, Holton AF. "Recommendations for the use of botulinum toxin type A in the management of cerebral palsy". *Gait & posture*. 2000;11(1):67-79.
154. Greene P, Fahn S, Diamond B. "Development of resistance to botulinum toxin type A in patients with torticollis". *Movement Disorders*. 1994;9(2):213-7.
155. Morrissey D, El-Khawand D, Ginzburg N, Wehbe S, O'Hare III P, Whitmore K. "Botulinum toxin A injections into pelvic floor muscles under electromyographic guidance for women with refractory high-tone pelvic floor dysfunction: a 6-month prospective pilot study". *Female pelvic medicine & reconstructive surgery*. 2015;21(5):277-82.

156. Adelowo A, Hacker MR, Shapiro A, Modest AM, Elkadry E. "Botulinum toxin type A (BOTOX) for refractory myofascial pelvic pain". *Female pelvic medicine & reconstructive surgery*. 2013;19(5):288.
157. Dessie SG, Von Bargaen E, Hacker MR, Haviland MJ, Elkadry E. "A randomized, double-blind, placebo-controlled trial of onabotulinumtoxin A trigger point injections for myofascial pelvic pain". *American journal of obstetrics and gynecology*. 2019;221(5):517. e1-. e9.
158. Zhang Y, Smith CP. "Botulinum toxin to treat pelvic pain". *Toxicon*. 2018;147:129-33.
159. Jarvis SK, Abbott JA, Lenart MB, Steensma A, Vancaillie TG. "Pilot study of botulinum toxin type A in the treatment of chronic pelvic pain associated with spasm of the levator ani muscles". *Australian and New Zealand journal of obstetrics and gynaecology*. 2004;44(1):46-50.
160. El-Enen MA, Abou-Farha M, El-Abd A, El-Tatawy H, Tawfik A, El-Abd S, Rashed M, El-Sharaby M. "Intraprostatic injection of botulinum toxin-A in patients with refractory chronic pelvic pain syndrome: The transurethral vs. transrectal approach". *Arab journal of urology*. 2015;13(2):94-9.
161. Nash DL, editor. *The practical management of spasticity in children and adults*. Mayo Clinic Proceedings; 1991: Elsevier.
162. O'Brien CF. "Injection techniques for botulinum toxin using electromyography and electrical stimulation". *Muscle & Nerve: Official Journal of the American Association of Electrodiagnostic Medicine*. 1997;20(S6):176-80.
163. Grigoriu A-I, Dinomais M, Rémy-Néris O, Brochard S. "Impact of injection-guiding techniques on the effectiveness of botulinum toxin for the treatment of focal spasticity and dystonia: a systematic review". *Archives of physical medicine and rehabilitation*. 2015;96(11):2067-78. e1.

164. Lapatki B, Van Dijk J, Van de Warrenburg B, Zwarts M. "Botulinum toxin has an increased effect when targeted toward the muscle's endplate zone: a high-density surface EMG guided study". *Clinical Neurophysiology*. 2011;122(8):1611-6.
165. Guzmán-Venegas RA, Araneda OF, Silvestre RA. "Differences between motor point and innervation zone locations in the biceps brachii. An exploratory consideration for the treatment of spasticity with botulinum toxin". *Journal of Electromyography and Kinesiology*. 2014;24(6):923-7.
166. Butrick CW. "Pathophysiology of pelvic floor hypertonic disorders". *Obstetrics and Gynecology Clinics*. 2009;36(3):699-705.
167. Zhou JY, Wang D. "An update on botulinum toxin A injections of trigger points for myofascial pain". *Current pain and headache reports*. 2014;18(1):386.
168. Marcelissen T, Jacobs R, Van Kerrebroeck P, De Wachter S. "Sacral neuromodulation as a treatment for chronic pelvic pain". *The Journal of urology*. 2011;186(2):387-93.
169. Ho KY, Tan KH. "Botulinum toxin A for myofascial trigger point injection: a qualitative systematic review". *European journal of pain*. 2007;11(5):519-27.
170. Kumar A, Rao SS. "Diagnostic testing in fecal incontinence". *Current gastroenterology reports*. 2003;5(5):406-13.
171. Grape HH, Dederig Å, Jonasson AF. "Retest reliability of surface electromyography on the pelvic floor muscles". *Neurourology and Urodynamics: Official Journal of the International Continence Society*. 2009;28(5):395-9.
172. Hanno PM, Erickson D, Moldwin R, Faraday MM. "Diagnosis and treatment of interstitial cystitis/bladder pain syndrome: AUA guideline amendment". *The Journal of urology*. 2015;193(5):1545-53.

173. Dietz H, Jarvis S, Vancaillie T. "The assessment of levator muscle strength: a validation of three ultrasound techniques". *International Urogynecology Journal*. 2002;13(3):156-9.
174. Meister MR, Sutcliffe S, Ghetti C, Chu CM, Spitznagle T, Warren DK, Lowder JL. "Development of a standardized, reproducible screening examination for assessment of pelvic floor myofascial pain". *American journal of obstetrics and gynecology*. 2019;220(3):255. e1-. e9.
175. Spitznagle TM, Robinson CM. "Myofascial pelvic pain". *Obstetrics and Gynecology Clinics*. 2014;41(3):409-32.
176. Ning Y, Zhu X, Zhu S, Zhang Y. "Surface EMG decomposition based on K-means clustering and convolution kernel compensation". *IEEE journal of biomedical and health informatics*. 2015;19(2):471-7.
177. Dias N, Zhang C, Spitznagle T, Lai HH, Zhang Y. "High-Density Surface Electromyography Assessment of Pelvic Floor Dysfunction in Women with Interstitial Cystitis/Bladder Pain Syndrome". *The Journal of Urology*. 2020:10.1097/JU. 0000000000001237.
178. Bartko JJ. "The intraclass correlation coefficient as a measure of reliability". *Psychological reports*. 1966;19(1):3-11.
179. Virtanen P, Gommers R, Oliphant TE, Haberland M, Reddy T, Cournapeau D, Burovski E, Peterson P, Weckesser W, Bright J. "SciPy 1.0: fundamental algorithms for scientific computing in Python". *Nature methods*. 2020;17(3):261-72.
180. Portney LG, Watkins MP. Foundations of clinical research: applications to practice: Pearson/Prentice Hall Upper Saddle River, NJ; 2009.
181. Kavvadias T, Pelikan S, Roth P, Baessler K, Schuessler B. "Pelvic floor muscle tenderness in asymptomatic, nulliparous women: topographical distribution and

- reliability of a visual analogue scale". *International urogynecology journal*. 2013;24(2):281-6.
182. Navarro Brazález B, Torres Lacomba M, de la Villa P, Sánchez Sánchez B, Prieto Gómez V, Asúnsolo del Barco Á, McLean L. "The evaluation of pelvic floor muscle strength in women with pelvic floor dysfunction: a reliability and correlation study". *Neurourology and urodynamics*. 2018;37(1):269-77.
183. Auchincloss CC, McLean L. "The reliability of surface EMG recorded from the pelvic floor muscles". *Journal of neuroscience methods*. 2009;182(1):85-96.
184. Conwit RA, Stashuk D, Suzuki H, Lynch N, Schrager M, Metter EJ. "Fatigue effects on motor unit activity during submaximal contractions". *Archives of physical medicine and rehabilitation*. 2000;81(9):1211-6.
185. Tucker K, Butler J, Graven-Nielsen T, Riek S, Hodges P. "Motor unit recruitment strategies are altered during deep-tissue pain". *Journal of Neuroscience*. 2009;29(35):10820-6.
186. Barbero M, Cescon C, Tettamanti A, Leggero V, Macmillan F, Coutts F, Gatti R. "Myofascial trigger points and innervation zone locations in upper trapezius muscles". *BMC musculoskeletal disorders*. 2013;14(1):179.
187. He J, Yi X, Luo Z. "A simulation study on the depth information of motor units". *Biomedical Engineering Letters*. 2016;6(2):80-6.
188. Zhang Y, Wang D, Timm GW. "A three-dimensional muscle activity imaging technique for assessing pelvic muscle function". *Inverse Problems*. 2010;26(11):115018.
189. Liu Y, Zhang C, Dias N, Chen Y-t, Li S, Zhou P, Zhang Y. "Transcutaneous innervation zone imaging from high-density surface electromyography recordings". *Journal of Neural Engineering*. 2020.

190. Weiss JM. "Pelvic floor myofascial trigger points: manual therapy for interstitial cystitis and the urgency-frequency syndrome". *The Journal of urology*. 2001;166(6):2226-31.
191. Thomson AJ, Jarvis SK, Lenart M, Abbott JA, Vancaillie TG. "The use of botulinum toxin type A (BOTOX®) as treatment for intractable chronic pelvic pain associated with spasm of the levator ani muscles". *BJOG: An International Journal of Obstetrics & Gynaecology*. 2005;112(2):247-9.
192. Beretta Piccoli M, Rainoldi A, Heitz C, Wüthrich M, Boccia G, Tomasoni E, Spirolazzi C, Egloff M, Barbero M. "Innervation zone locations in 43 superficial muscles: toward a standardization of electrode positioning". *Muscle & nerve*. 2014;49(3):413-21.
193. Dias N, Zhang C, Smith CP, Lai HH, Zhang Y. "High-density surface electromyographic assessment of pelvic floor hypertonicity in IC/BPS patients: a pilot study". *International Urogynecology Journal*. 2020:1-8.
194. Yang EJ, Rha D-w, Yoo JK, Park ES. "Accuracy of manual needle placement for gastrocnemius muscle in children with cerebral palsy checked against ultrasonography". *Archives of physical medicine and rehabilitation*. 2009;90(5):741-4.
195. Walter U, Dressler D. "Ultrasound-guided botulinum toxin injections in neurology: technique, indications and future perspectives". *Expert review of neurotherapeutics*. 2014;14(8):923-36.
196. Schnitzler A, Roche N, Denormandie P, Lautridou C, Parratte B, Genet F. "Manual needle placement: accuracy of botulinum toxin A injections". *Muscle & nerve*. 2012;46(4):531-4.
197. Simons DG. "Clinical and etiological update of myofascial pain from trigger points". *Journal of musculoskeletal pain*. 1996;4(1-2):93-122.

198. Hubbard DR, Berkoff GM. "Myofascial trigger points show spontaneous needle EMG activity". *Spine*. 1993;18(13):1803-7.
199. Thomas K, Shankar H. "Targeting myofascial taut bands by ultrasound". *Current pain and headache reports*. 2013;17(7):349.
200. Shankar H, Reddy S. "Two-and three-dimensional ultrasound imaging to facilitate detection and targeting of taut bands in myofascial pain syndrome". *Pain medicine*. 2012;13(7):971-5.
201. McHugh ML. "Interrater reliability: the kappa statistic". *Biochemia medica: Biochemia medica*. 2012;22(3):276-82.
202. Lu Z, Briley A, Zhou P, Li S. "Are there trigger points in the spastic muscles? Electromyographical evidence of dry needling effects on spastic finger flexors in chronic stroke". *Frontiers in Neurology*. 2020;11.
203. McComas A, Fawcett PRW, Campbell M, Sica R. "Electrophysiological estimation of the number of motor units within a human muscle". *Journal of Neurology, Neurosurgery & Psychiatry*. 1971;34(2):121-31.
204. Shefner JM. "Motor unit number estimation in human neurological diseases and animal models". *Clinical neurophysiology*. 2001;112(6):955-64.
205. Zhang C, Munoz A, Lai HH, Boone T, Zhang Y. "Non - invasive electromyographic estimation of motor unit number in the external anal sphincter of the rat". *Neurourology and urodynamics*. 2018;37(1):115-22.
206. Boe SG, Stashuk DW, Doherty TJ. "Motor unit number estimation by decomposition - enhanced spike - triggered averaging: Control data, test - retest reliability, and contractile level effects". *Muscle & Nerve: Official Journal of the American Association of Electrodiagnostic Medicine*. 2004;29(5):693-9.

207. Peng Y, He J, Yao B, Li S, Zhou P, Zhang Y. "Motor unit number estimation based on high-density surface electromyography decomposition". *Clinical Neurophysiology*. 2016;127(9):3059-65.
208. Ramsden CE, McDaniel MC, Harmon RL, Renney KM, Faure A. "Pudendal nerve entrapment as source of intractable perineal pain". *American journal of physical medicine & rehabilitation*. 2003;82(6):479-84.
209. Daube JR. "Estimating the number of motor units in a muscle". *Journal of clinical neurophysiology: official publication of the American Electroencephalographic Society*. 1995;12(6):585-94.
210. Bostock H. "Estimating motor unit numbers from a CMAP scan". *Muscle & nerve*. 2016;53(6):889-96.
211. Henderson RD, Ridall PG, Hutchinson NM, Pettitt AN, McCombe PA. "Bayesian statistical MUNE method". *Muscle & Nerve: Official Journal of the American Association of Electrodiagnostic Medicine*. 2007;36(2):206-13.
212. Hanno PM, Burks DA, Clemens JQ, Dmochowski RR, Erickson D, FitzGerald MP, Forrest JB, Gordon B, Gray M, Mayer RD. "AUA guideline for the diagnosis and treatment of interstitial cystitis/bladder pain syndrome". *The Journal of urology*. 2011;185(6):2162-70.
213. Butrick CW. "Interstitial cystitis and chronic pelvic pain: new insights in neuropathology, diagnosis, and treatment". *Clinical obstetrics and gynecology*. 2003;46(4):811-23.

Appendix 1. Publication list.

- **Dias, N.**, Spitznagle, T, Lai, H., and Zhang, Y. (In preparation) Assessment of Myofascial Trigger points in Women With Chronic Pelvic Pain.
- **Dias, N.**, Spitznagle, T, Lai, H., and Zhang, Y. (In preparation) Test-Retest Reliability and Classification Ability of Intra-Vaginal High-Density Surface EMG in Women With IC/BPS
- **Dias, N.**, Zhang, C., Smith, C.P., Lai, H., and Zhang, Y. (2020) High-Density Surface Electromyographic Assessment of Pelvic Floor Hypertonicity in IC/BPS Patients: A Pilot Study. *International Urogynecology Journal*. In Press.
- **Dias, N.**, Zhang, C., Spitznagle, T., Lai, H. H., & Zhang, Y. (2020). High-Density Surface Electromyography Assessment of Pelvic Floor Dysfunction in Women with Interstitial Cystitis/Bladder Pain Syndrome. *The Journal of Urology*, 10-1097.
- Liu, Y., Zhang, C., **Dias, N.**, Chen, Y. T., Li, S., Zhou, P., & Zhang, Y. (2020). Transcutaneous innervation zone imaging from high-density surface electromyography recordings. *Journal of Neural Engineering*.
- Ning, Y., **Dias, N.**, Li, X., Jie, J., Li, J., & Zhang, Y. (2019). Improve computational efficiency and estimation accuracy of multi-channel surface EMG decomposition via dimensionality reduction. *Computers in Biology and Medicine*, 103372.
- **Dias, N.**, Zhang, C., Li, X., Neshatian, L., Orejuela, F. J., & Zhang, Y. (2019). Neural control properties of the external anal sphincter in young and elderly women. *Neurourology and urodynamics*.
- Li, X., Zhang, C., **Dias, N.**, Liu, J., Hu, F., Yang, S., & Zhang, Y. (2019). Effects of delivery mode and age on motor unit properties of the external anal sphincter in women. *International urogynecology journal*, 30(6), 945-950.
- Zhang, C., **Dias, N.**, He, J., Zhou, P., Li, S., & Zhang, Y. (2019). Global Innervation Zone Identification with High-Density Surface Electromyography. *IEEE Transactions on Biomedical Engineering*.
- **Dias, N.**, Li, X., Zhang, C., & Zhang, Y. (2018). Innervation asymmetry of the external anal sphincter in aging characterized from high-density intra-rectal surface EMG recordings. *Neurourology and urodynamics*, 37(8), 2544-2550.
- **Dias, N.**, Peng, Y., Khavari, R., Nakib, N. A., Sweet, R. M., Timm, G. W., & Zhang, Y. (2017). Pelvic floor dynamics during high-impact athletic

activities: a computational modeling study. *Clinical Biomechanics*, 41, 20-27.

Appendix 2. Conference Proceedings list.

- Dias, N., Smith, C.P., Lai H., & Zhang, Y. (2020, February). High-Density Surface EMG assessment of pelvic floor hypertonicity in IC/BPS patients. SUFU winter meeting, 2020, Scottsdale, AZ. In NEUROUROLOGY AND URODYNAMICS (Vol. 39, pp. S6-S6). 111 RIVER ST, HOBOKEN 07030-5774, NJ USA: WILEY. **Best Clinical Essay Winner**
- Dias, N., Zhang, C., Li, X., & Zhang, Y. (2019, February). Aging related alterations of neural control properties of the external anal sphincter. SUFU winter meeting, 2019, Miami, FL. In NEUROUROLOGY AND URODYNAMICS (Vol. 38, pp. S141-S141). 111 RIVER ST, HOBOKEN 07030-5774, NJ USA: WILEY.
- Dias, N., Zhang, C., Li, X., & Zhang, Y. (2019, February). Aging related alterations of neural control properties of the external anal sphincter. SUFU winter meeting, 2019, Miami, FL. In NEUROUROLOGY AND URODYNAMICS (Vol. 38, pp. S141-S141). 111 RIVER ST, HOBOKEN 07030-5774, NJ USA: WILEY.
- Dias, N., Zhang, C., Li, X., & Zhang, Y. (2018, December). Aging related alterations of motor unit firing rate in the bulbospongiosus muscle using high density surface electromyography. SPR Annual Meeting, 2018, New Orleans, LA.
- Dias, N., Zhang, C., Li, X., He, J., & Zhang, Y. (2018, August). Innervation Symmetry of the external anal sphincter in patients with fecal incontinence: A High-Density surface electromyography study. ICS Annual Meeting, 2018, Philadelphia, PA.
- Dias, N., Li, X., Zhang, C., He, J., and Zhang, Y. (2018, February) Assessment of Innervation Symmetry of External Anal Sphincter in Young and Elderly Females using High-density Surface Electromyography Recordings. SUFU winter meeting, 2018, Austin, TX.
- Dias, N., Popeney, C., He, J., and Zhang, Y. (2018, February) Noninvasive Motor Unit Number Estimation of the Puborectalis Muscle in Females. SUFU winter meeting, 2018, Austin, TX.
- Dias, N., Zhang, C., He, J., Li, X., and Zhang, Y. (2017, December) Assessment of Aging Related Changes in the Innervation of the External Anal Sphincter Based on Motor Unit Action Potential Quantitative Analysis. The 2nd Annual Meeting of the Society for Pelvic Research, 2017, Reno, NV. **Best Podium Winner**
- Zhang, C., Dias, N., He, J., Li, X., and Zhang, Y. (2017, December) Investigation of Motor Unit Firing Patterns of Bulbospongiosus Muscle in Type II Diabetic Female Patients. The 2nd Annual Meeting of the Society for Pelvic Research, 2017, Reno, NV.

- Dias, N., Peng, Y., He, J., Popeney, C., and Zhang, Y. (2017, May) Motor Unit Number Estimation Of The Puborectalis Muscle. American Urological Association's 2017 Annual Meeting, 2017, Boston, MA.
- Dias, N., Peng, Y., Neshatian, L., Quigley, E.M.M., and Zhang, Y. (2016, September) Effects of Puborectalis Muscle Contractions on the Resulting Anorectal Angles: A Computational Modelling Study. International Continence Society (ICS) Conference. Tokyo, Japan. 2016.
- Dias N., Y. Peng, B.J. Miles, R. Khavari, V. MacDonnell, T. Boone and Zhang, Y. (2016, May) A Finite Element Model of the Male Pelvis from Magnetic Resonance Images. American Urological Association's 2016 Annual Meeting, San Diego, CA. 2016.